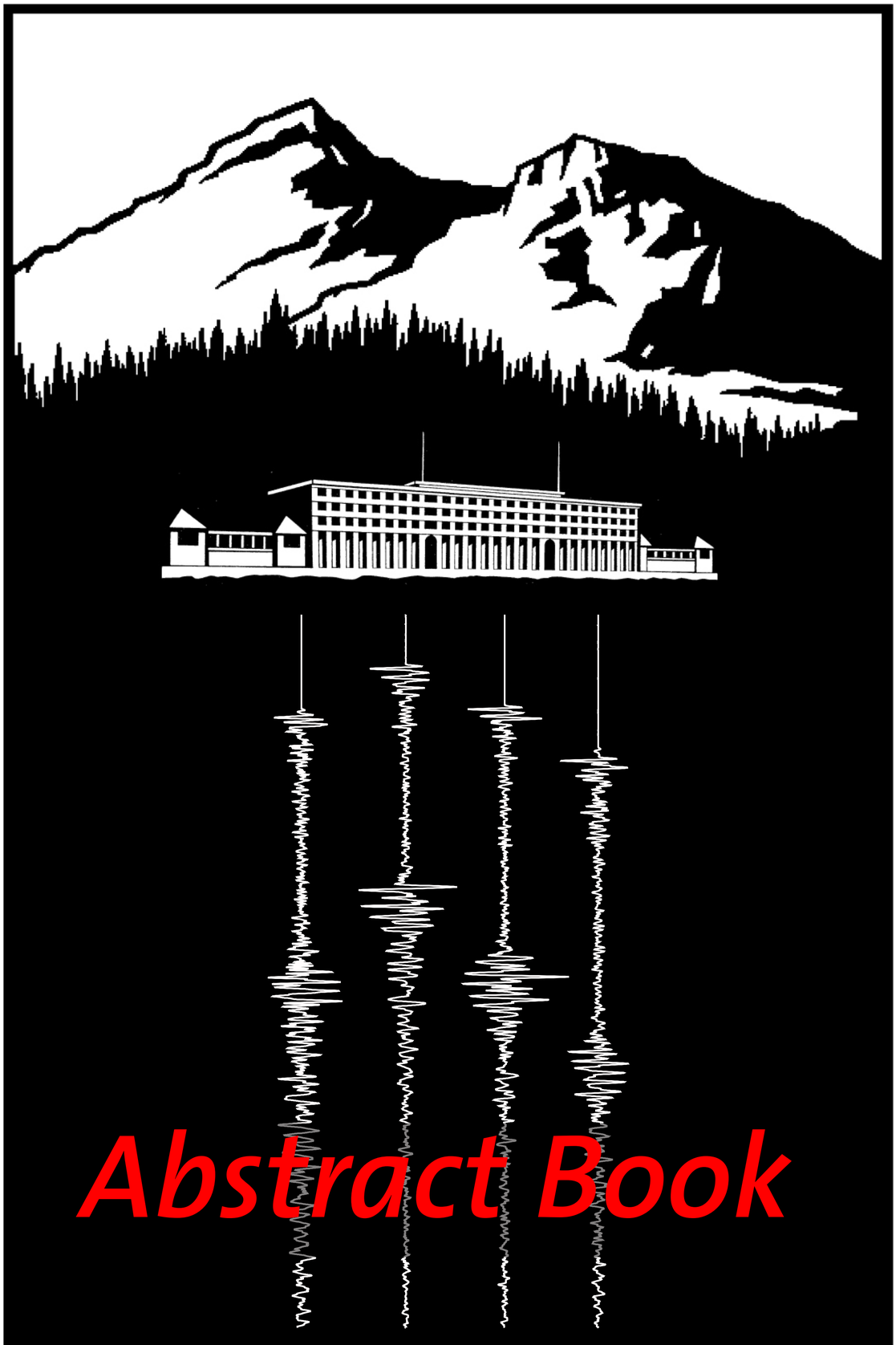

Abstract Book

14 - 17 March 2017

DAVOS

SCHATZALP

2nd Induced Seismicity Workshop

Contents

Abstracts Talks

Sessions 1 and 2

Case Studies

Hiding in Plain Sight? Evidence for Possible Induced Earthquakes in California in the Early 20th Century

Susan E. Hough[1], Victor Tsai[2], Robert Walker[3], Morgan Page[1], Fred Aminzadeh[3]

1 U.S. Geological Survey, Pasadena, California, hough@usgs.gov; **2** California Institute of Technology, Pasadena, California; **3** University of Southern California, Los Angeles, California.

Several recent studies have presented evidence that significant induced earthquakes occurred in a number of regions in the United States during the 20th century related to either production or early wastewater injection (e.g., Hough and Page, BSSA, 2015; Frohlich et al., SRL, 2016). We consider whether the M_w6.4 Long Beach and M_w7.3 1952 Kern County earthquakes might have been induced by production in the Huntington Beach and Wheeler Ridge oil fields, respectively.

The Long Beach earthquake occurred within nine months of the start of directional drilling that first exploited offshore tideland reserves at depths of ≈1200 m; the well location was within ≈3 km of the event epicenter (Hough and Page, 2016). The Kern County earthquake occurred 111 days following the first exploitation of deep Eocene production horizons within the Wheeler Ridge field at depths reaching 3 km, within ≈1 km of the White Wolf fault (WWF); the epicenter of this earthquake is poorly constrained but within no more than a few km of the well.

While production in the Wheeler Ridge field would have reduced pore pressure, inhibiting failure on the WWF assuming a Coulomb failure criteria, we present a model based on analytical solutions with model parameters constrained from detailed industry data, whereby direct pore pressure effects were blocked by a normal fault that created an impermeable barrier close to the WWF, allowing the normal stress change associated with production to dominate, thereby promoting failure by unclamping the fault. Our proposed triggering mechanism is consistent with the observation that significant earthquakes are only rarely induced by production in proximity to major faults. Our results also suggest that significant induced earthquakes in southern California during the early 20th century might have been associated with industry practices that are no longer employed (i.e., production without water re-injection). The occurrence of significant earthquakes during the earthquake 20th century therefore does not necessarily imply a high likely of induced earthquakes at the present time.

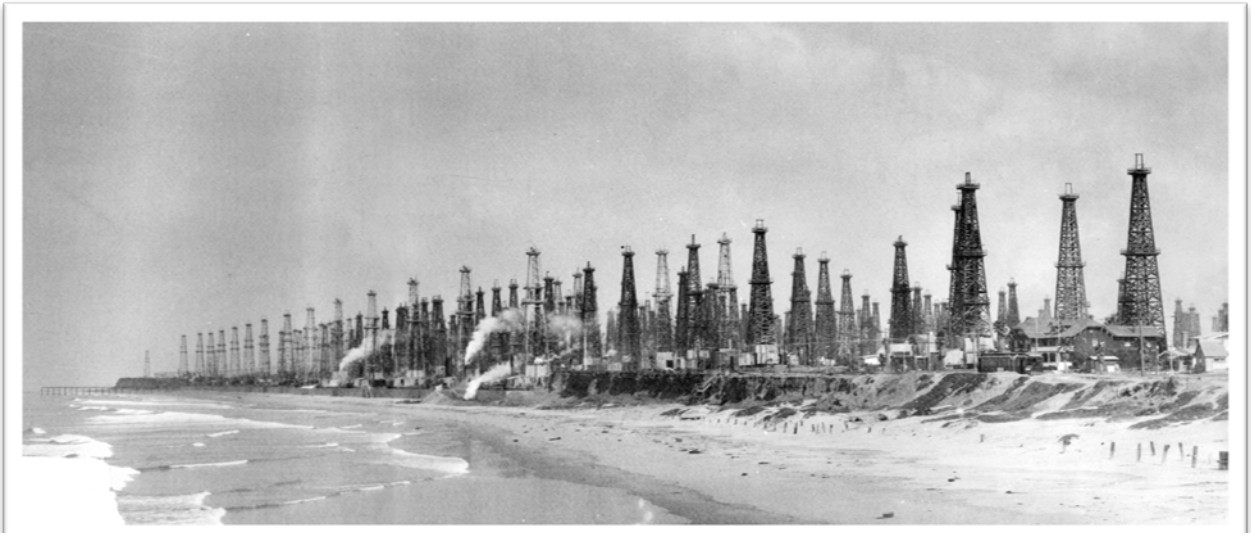

Fig. 1 Photograph of oil derricks in the Huntington Beach oil field in 1926, near the epicenter of the 11 March 1933 M6.4 Long Beach earthquake (photo courtesy of Orange County archives.) Directional drilling into offshore tideland reserves began in the field nine months before the earthquake, at a well located approximately 3 km from the preferred epicenter of the 1933 earthquake.

The Evolving Earthquake Hazard near Cushing, Oklahoma

William L. Ellsworth[1], Martin Schoenball[1], Matthew Weingarten[1], Robert Skoumal[2], David R. Shelly[2]

1 Department of Geophysics, Stanford University, Stanford, CA, USA (wellsworth@stanford.edu); **2** U. S. Geological Survey, Menlo Park, CA, USA

The dramatic rise in seismicity in Oklahoma since 2009 is an unintended consequence of disposal of wastewater by injection into the permeable Arbuckle Formation. This formation water is co-produced along with oil, separated at the surface and transported to disposal wells where it is injected just above crystalline basement. Earthquakes spread across north-central Oklahoma in the wake of the development of these unconventional oil fields, driven by a regionally extensive pore pressure increases cause by the disposal operations. The excess pressure at the top of basement is estimated to be about 1 MPa. High-resolution hypocenters show that the induced earthquakes principally activate previously unknown strike slip faults in the basement that are well oriented for failure in the contemporary stress field.

Here, we focus on the evolution of and potential for future earthquakes in the vicinity of the city of Cushing, Ok. Cushing (population 8,000) is known as the "Pipeline Crossroads of the World" for the role it plays as a transshipment point for the U.S. oil market. It is where the benchmark West Texas Crude enters the market, and is home to the largest above ground oil storage tank farm in the world with a capacity of over 10 million m^3. Because of their key role in the economy, the petroleum facilities in Cushing have been designated as Critical National Infrastructure.

Earthquakes near Cushing were unknown before October 2014, when M 4.0 and 4.2 events struck 3 km south of the town near the main tank farm but causing only nonstructural damage. The next year, three more events, M 4.0 – 4.3 ruptured along a previously unknown ENE trending strike slip fault located 3 km west of the city center, again with only minor effects. This was not the case on November 7, 2016 when a M 5.0 earthquake rupture an additional 5 km of the same fault structure, causing extensive damage to 50 unreinforced masonry buildings (URM) in the downtown and to over 100 houses. Accelerations exceeded 0.5 g and velocities 10 cm/s.

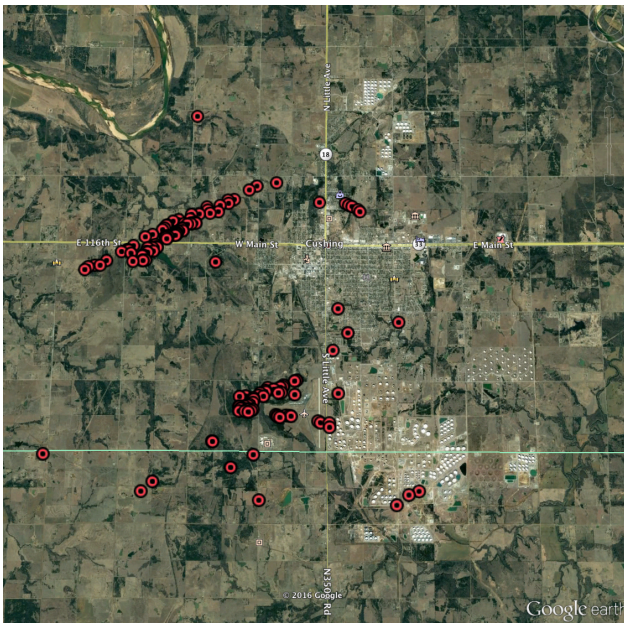

Fig 1. Google Earth image of Cushing (upper center) and oil storage facilities (above and below). Red symbols show seismicity from 3/2013-3/2016. The patchwork grid of roads and land boundaries are 1 mile on a side.

We are using the fault structures illuminated by microearthquakes, knowledge of the local stress field, finite fault models of the largest events, pore pressure modeling and calibrated ground motion prediction equations to inform time-dependent estimates of the evolving earthquake hazard.

Using underground experiments to improve the understanding of induced seismicity

Domenico Giardini[1]

1 ETH Zurich, domenico.giardini@erdw.ethz.ch

Most countries are defining a strategy for their future electricity supply focusing on the need to reduce carbon emissions while securing a sustainable balance between baseload supply and stochastic renewable sources such as solar and wind. In the Swiss Energy Strategy, deep geothermal energy is identified as a source of baseload electricity capable of reaching by 2050 up to 7-10% of the national electricity supply.

The exploitation of deep geothermal energy exploitation in the swiss geological environment, devoid of active vulcanism and high temperature gradients, requires the ability to engineer reservoirs at 4-6 km depth at 180-200 °C, capable to sustain stable water circulation of 200-250 l/sec over decades, while reducing the costs and the risk of induced seismicity.

To address these challenges, Switzerland has designed, in cooperation with other international partners, a R&D roadmap integrating

- ✓ A new National Geodata Infrastructure operated by SwissTopo, mapping geology, geothermal resources and faults at depth
- ✓ An integrated R&D agenda covering resource and reservoir exploration, assessment and characterization; fractures and reservoir creation; reservoir modeling and validation; induced seismicity; monitoring; well completion; chemical interactions and transformations.
- ✓ Two main classes of national experimental facilities: (i) a distributed infrastructure of rock deformation labs to handle large samples at conditions found in 4-6 km depth; (ii) a Deep UnderGround Laboratory infrastructure, at depth of 500-2‘000 m, to conduct 10-100m scale injection and stimulation experiments
- ✓ A masterplan to install up to 3 deep EGS reservoirs engineered in basement rock, conducted as demonstration projects with industry, with a target of 5-20 MWel installed

The rational for the experimental infrastructure is to perform stimulation experiments under a fully controlled environment at increasing depths, validate protocols and procedures before deployment in deep EGS, provide a testing ground integrating experimental, modeling and monitoring technologies, develop and test innovative methodologies for reservoir engineering, and increase public confidence in geo-energy technologies.

We report the first results of the pilot underground project, comprising two large scale in-situ experiment at different scale which address questions associated with the validation of stimulation procedures and sustainable utilization of heat exchangers in the deep underground. Stimulation concepts are tested in-situ while hydro-seismo-mechanical key parameters are monitored at a high spatial resolution. The addressed questions are: Which stimulation concepts are appropriate for enhancing the permeability by orders of magnitudes while minimizing induced seismicity , 2) What are the relationships between the hydro-mechanical response, the stimulation concept, permeability creation, effective porosity and induced seismicity, 3) How can micro-seismicity be minimized, 4) What are the heat exchanger properties of the reservoir.

The first experiment is conducted in the deep underground Grimsel testing facility operated by NAGRA; the first stimulation and injection campaign has been been successfully concluded, aiming at controlling induced micro-seismicity in a hydro-shear stimulation mode.

Kinematic inversion of pre-existing faults by wastewater injection-related induced seismicity: the Val d'Agri oil field case study (Italy)

Mauro Buttinelli[1], Luigi Improta[1], Samer Bagh[1], Claudio Chiarabba[2]

1 Istituto Nazionale di Geofisica e Vulcanologia, Department of Seismology and Tectonophysics, Rome, Italy, mauro.buttinelli@ingv.it **2** Istituto Nazionale di Geofisica e Vulcanologia, National Earthquake Centre, Rome, Italy

Since 2006 wastewater has been injected below the Val d'Agri Quaternary basin, which hosts the largest on-land oilfield in Europe.

Disposal activities induced micro-seismicity soon after the starting of the operations in the proximity of a high-rate injection well, which is located in a marginal and non-productive portion of the oil field.

In this area we had the rare opportunity to revise a massive set of 2D/3D seismic and deep borehole data in order to investigate the relationship between the spatial distribution of the induced earthquakes and the geometry of the active faults that bound the basin, which have been defined as responsible of the 1857 M7 earthquake.

Below the injection site we identified a very complex structural setting due to the overprint of several tectonic phases. At the level of the injection reservoir we were able to model a blind Pliocene thrusts and back-thrusts system inherited by the Apennines compression, with no apparent relation with such large normal faults bounding the basin.

The whole induced seismicity observed in the timespan between 2006 and 2014 is mostly confined within the injection reservoir, which is constituted by the fractured limestones of the Apulian platform. The Induced events aligns coherently with a NE-dipping back-thrust of the compressional system that is favorably oriented within the current extensional stress field.

Earthquakes spread upwards from the back-thrust deep portion activating a 2.5-km wide patch. Focal mechanisms show a predominant extensional kinematic testifying to an on-going kinematic inversion of the back-thrust. A minor strike-slip compound suggests a control exerted by a high angle transverse fault also developed within the compressional system, possibly at the intersection between the two fault sets.

The physical mechanism proposed to explain the observed induced microseismic events is the reactivation with extensional kinematics of small faults and fractures (100-200 m length) belonging to a high permeability zone of the fault delineated by the alignment of microseismicity, due to the increase of fluid pressure in the reservoir.

We stress that where wastewater disposal is active, understanding the complex interaction between injection-linked seismicity and pre-existing faults is a strong requisite for safe oilfield exploitation.

Geothermal induced seismicity: What links source mechanics and event magnitudes to faulting regime and injection rates?

Patricia Martínez-Garzón[1], Grzegorz Kwiatek[1], Marco Bohnhoff[1,2], Stephan Bentz[1], Georg Dresen[1,3]

1 Helmholtz Centre Potsdam, GFZ German Research Centre for Geosciences, Germany patricia@gfz-potsdam.de; **2** Free University of Berlin, Germany; **3** University of Potsdam, Germany

Stimulation and production of hydrocarbon and geothermal reservoirs as well as wastewater injection have resulted in a significant increase of induced seismicity rates over the last few years. Improving estimates of associated seismic hazard requires advanced understanding of the physical processes governing induced seismicity, which can be better achieved by carefully processing large datasets. To this end, we investigate source-type processes (shear/tensile/compaction) and earthquake rupture geometries with respect to the local stress field using induced seismicity from The Geysers (TG) and Salton Sea geothermal reservoirs in California. Analysis of 869 well-constrained full moment tensors (M_W 0.8-3.5) at TG reveals significant non-double-couple (NDC) components (>25%) for about 65% of the events and remarkably diversity in the faulting mechanisms. Volumetric deformation is clearly governed by injection rates with larger NDC components observed near the injection wells and during high injection periods. The overall volumetric deformation from the calculated moment tensors increases with time, possibly reflecting a reservoir pore pressure increase after several years of fluid injection with no significant production nearby (Figure 1a). Interestingly, the events with significant compensated linear vector dipole appear to peak after the start of injection operations in each of the wells and decrease with time, suggesting their link with the initial enhanced damage very close to the wells (Figure 1b). The obtained source mechanisms and fault orientations are magnitude-dependent and vary significantly between faulting regimes. Normal faulting events (M_W < 2) reveal substantial NDC components indicating dilatancy, and they occur on varying fault orientations. In contrast, strike-slip events dominantly reveal a double-couple source, comparatively larger magnitudes (mostly M_W > 2) and to a large extent occur on optimally oriented faults with respect to the local stress field. NDC components indicating closure of cracks and pore spaces in the source region are mostly found for reverse faulting events with M_W > 2.5. Our findings from TG are generally consistent with preliminary source-type results from a reduced subset of well-recorded seismicity at the Salton Sea geothermal reservoir. The combined results imply that source processes and magnitudes of geothermal-induced seismic events are strongly affected by and systematically related to the hydraulic operations and the reservoir stress state.

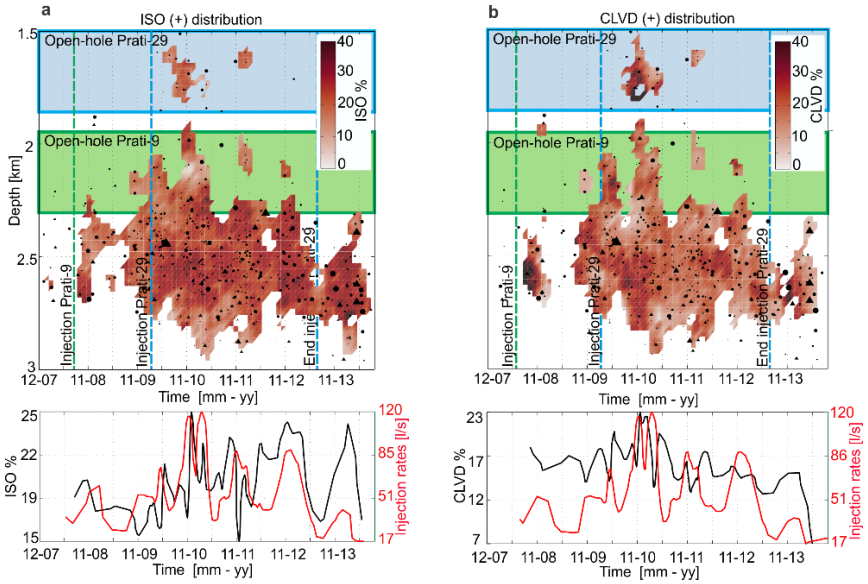

Fig. 1 (a) Top: depth-time mapping of the isotropic components of the analyzed seismicity at The Geysers geothermal field. Bottom: Average isotropic (ISO) components of the seismicity and injection rates of the two wells nearby as a function of time. (b) Same that (a) for CLVD.

Soft stimulation and induced seismicity

Ernst HUENGES[1] and the DESTRESS-team

1 GFZ Potsdam, huenges@gfz-potsdam.de

Enhanced geothermal systems (EGS) allow a widespread use of the enormous untapped geothermal energy potential. EGS measures are generally intended to improve productivity (or injectivity) of a geothermal reservoir by increasing the overall transmissivity of the reservoir rocks. Soft stimulation[1] approaches are under development to enhance the reservoir performance with a treatment affecting only a minimized environmental hazard such as induced seismicity. Scientific progress was made on topics such as fluid-rock interaction, the improved determination of the stress field and on the analysis of induced seismicity. Concepts of hydraulic treatments including mitigation of triggered or induced seismic events were proposed as an outcome of the GEISER-project[2]. This goal can be achieved by various methods that are dependent on the geological system, comprising the rocks, the rock structures, the tectonic situation as well as the stress field. Hydraulic treatments, as the high fluid pressures applied and the large fluid volumes injected in, sometimes induce seismic events that can, in some cases, be felt at the surface and jeopardize the public acceptance of a project. Hydraulic, thermal, and chemical treatments are options to address requirements for different geological environments respectively different settings of geothermal wells. These issues will be addressed by the DESTRESS[3] project. The project aims to demonstrate a concept-based approach to develop an EGS that takes the site-specific geological requirements into account. DESTRESS has three overall objectives: i) increase transmissivity of the reservoir, ii) maintain productivity of the system and iii) minimise the level of induced seismicity. Previous modeling studies of Zang et al. (2013) and Yoon et al (2014) and experiments on rock samples (Min et al. 2016) and in the Äspo mine (Zang et al. 2016) show that same increase of transmissivity can be reached with both treatments: (1) varying the injection rates combined with less seismicity compared to (2) constant rates. DESTRESS aims to reduce given seismicity concerns by good practice.

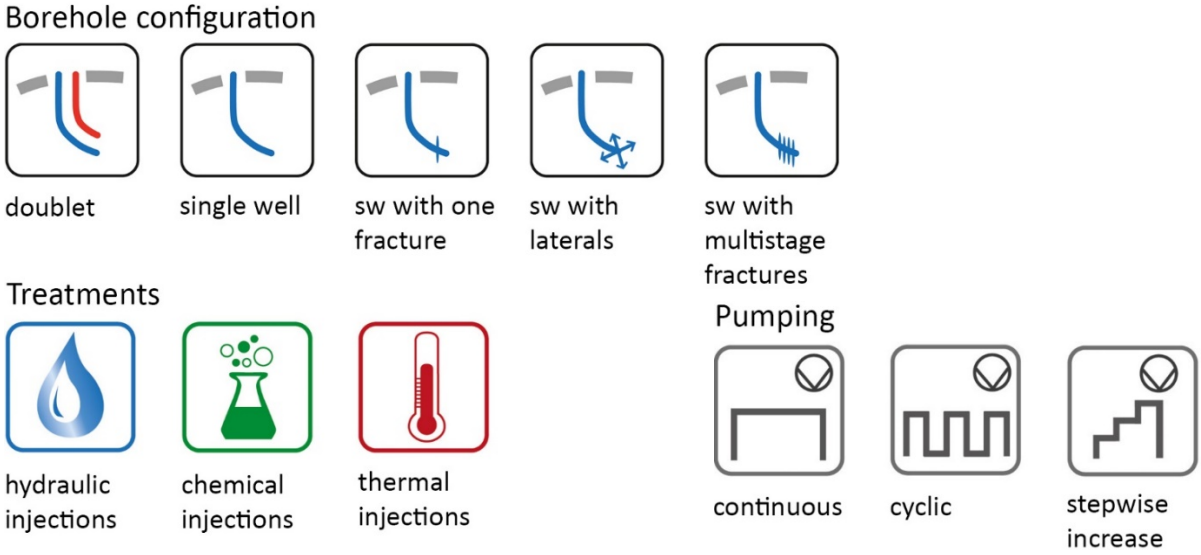

Fig. 1 Variety of aspects for soft stimulation, borehole configurations, treatments and pumping regime

[1] Soft Stimulation is a collective term for geothermal reservoir stimulation techniques that aim to achieve enhanced reservoir performance while minimizing environmental impacts including induced seismicity. Soft stimulation includes techniques such as cyclic/fatigue stimulation, multi-stage stimulation, chemical stimulation and thermal stimulation.

2 http://www.geiser-fp7.

3 www.destress-h2020.eu

Induced Seismicity in Switzerland: An update and outlook

Stefan Wiemer for the induced seismicity working group at the Swiss Seismological Service

[1] ETH Zurich, Swiss Seismological Service, stefan@sed.ethz.ch;

Research into induced seismicity in Switzerland has been greatly accelerated in response to the failed 'deep heat mining' project in Basel in 2006. Seismicity in the reservoir area is continuing until today. The fact that in an urban area, a few relatively small earthquakes with magnitudes of up to M_l = 3.4 could stop an ambitious and well accepted project was a wakeup call also for scientists. Since then, understanding induced seismicity and its direct and indirect effects has been a priority for many researchers in Switzerland. The subsequent failure of the ambitious deep hydrothermal project in St. Gallen in 2013, which caused a magnitude M_l =3.5 event while fighting a gas kick during reservoir testing, highlighted again the need for better techniques for induced seismicity risk assessment and mitigation. To enable the upcoming next generation of deep geothermal project in Switzerland, we are promoting a data-driven adaptive forecasting approach, implemented such that a pre-defined risk-based safety target can be ensured throughout all phases of a project.

To allow a classification of projects, we have developed a pre-screening test, the Geothermal Risk of Induced seismicity Diagnosis (GRID). GRID estimates based on a set of criteria to what extent induced seismicity is of concern for a specific project. A framework for tailor-made risk governance measures is then suggested, including hazard and risk assessment, social site characterization, seismic monitoring, insurance, structural retrofitting, traffic light systems, information and outreach, and public and stakeholder engagement. Because the existing tools to assess and control anthropogenic seismicity risk are clearly insufficient, we are currently developing and validating an adaptive traffic light system, in which the risk threshold is dynamically and quantitatively assessed, providing an objective and statistically robust mitigation strategy. This allows for a fair and transparent regulatory process where operators and regulators agree on an acceptable level of risk to adhere to. At the heart of any risk assessment are predictive models of the future behavior, and much effort was invested by our research team to improve and validate these models. We have developed also an induced seismicity test bench to test and rank forecast models; this test bench can be used for model development, model selection, and ensemble model building. The improve seismic data as input for forecasting, we are developing improved and automated processing workflows to monitor and analyze induced seismicity in near real-time.

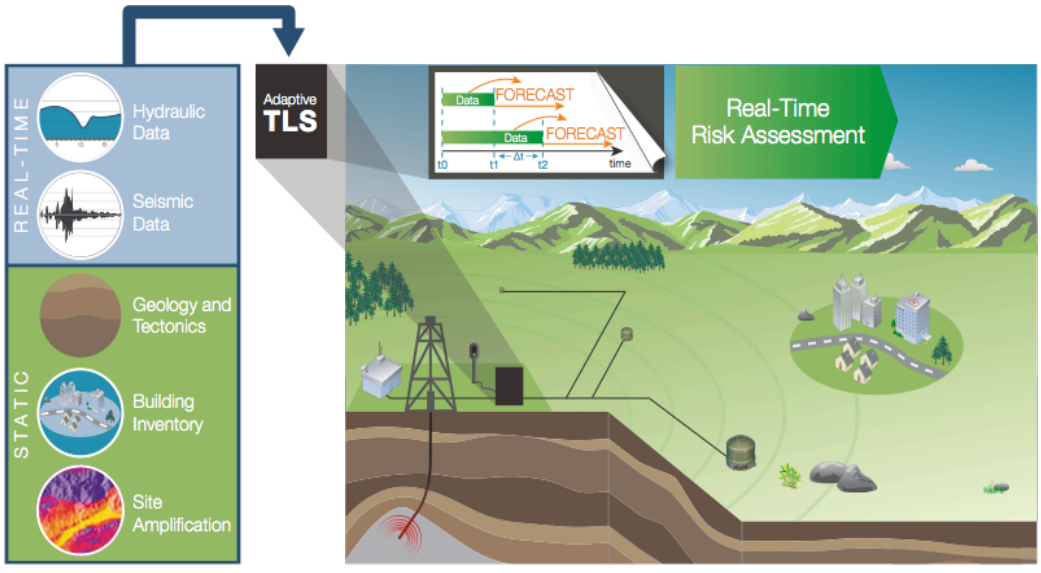

Fig. 1 Illustration of the workflow for a data-driven, adaptive traffic light system for real-time risk mitigation of induced seismicity.

The Challenge of Managing Extraction Induced Seismicity in Groningen, The Netherlands

Annemarie G. Muntendam-Bos[1]

1 Dutch State Supervision of Mines, The Netherlands, a.g.muntendam-bos@minez.nl

The Groningen gas field is located in the northeast of The Netherlands. The field, containing 2800 bcm of high-caloric gas, was first discovered in 1964 and gas extraction commenced in 1968. Induced seismicity in the Groningen region was first registered in December 1991. Till 2003 the seismic activity rate was low, reasonably constant and located at the center of the field. Between 2003 and 2013 seismic activity increased exponentially. While the rate increased, the magnitudes of the events increased as well. The first magnitude 3 event was recorded in 2003 followed by the first magnitude 3.5 event in 2006. The largest event to date (M=3.6) was recorded on August 12, 2012 at the town of Huizinge. The event caused significant non-structural damage throughout the region. In an area devout of any known natural seismicity, the shaking and damage resulted in a great deal of public turmoil.

A State Supervision of Mines (SSM) investigation[1] following the Huizinge earthquake showed an increased risk of larger magnitude events to occur due to the gas extraction. Subsequently, on advice of SSM, the Dutch Minister of Economic Affairs has gradually reduced production offtake in five steps from 53 bcm in 2013 to 24 bcm/a in its latest decision on October 1st 2016. Since, each six months SSM has analyzed the seismic response to both the change in production offtake as well as the changes in spatial distribution of the offtake.

In the initial reduction step in January 2014, production in five wells surrounding the most active, center region of the Groningen gas field was reduced by 80%. In order to minimize the reduction of the full field production, the Minister allowed an increase in production at the other wells. In response, especially production in the southwestern clusters was increased. As a result the seismic activity in the center of the field was significantly reduced. However, the increase in production in the southwestern clusters resulted in an increase in seismic activity in this area. Associated with the increase in activity, was an increase in local public commotion. The problem seemed to shift from the center to the southwest of the field. In January 2015 the authorization of the increase in production was therefore revoked. In all three subsequent steps, the further limitations on production offtake were distributed evenly over all producing clusters. At the same time further research indicated the importance of the seasonal fluctuations in production on the seismic activity. Hence, since March 2015 the seasonal fluctuation in the production rates has been minimized. In response, the seismic activity has diminished to a rate of approximately one M≥1.5 event per month.

Along with the decrease in seismic activity, the public commotion has declined. Currently, public displeasure is focused mainly on the process of damage handling and compensation. However, each event felt still draws the interest of both public and press. As some clustering of events in both time and space is still observed, managing both the seismicity as well as the public perception still provides a continuing challenge.

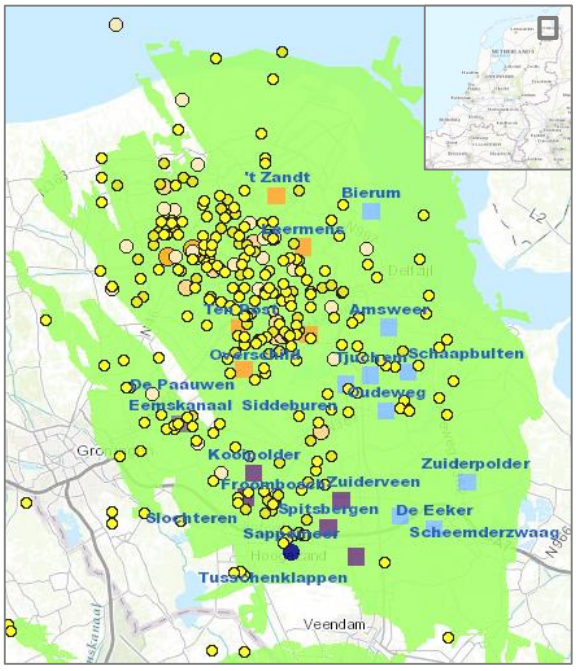

Fig. 1 The Groningen gas field. The colored dots show all seismic events of M≥1.5. Both color and size scale with magnitude The squares and blue dots indicate the production clusters.

[1] Muntendam-Bos, A.G. and J.A. de Waal (2013) Reassessment of the probability of higher magnitude earthquakes in the Groningen gas field. SSM Technical Report.

Continued Reservoir Triggered Seismicity at Koyna, India

Harsh K Gupta[1]

1 National Geophysical Research Institute, India, harshg123@gmail.com

''Globally there are over 120 sites where artificial water reservoir triggered earthquakes are known to have occurred. Koyna, near the west coast of India is the most prominent site where triggered earthquakes are occurring since the impoundment of the Koyna Dam in 1962. These include the M 6.3 December 10, 1967 earthquake, 22 M≥5.0, and thousands of smaller earthquakes. The entire earthquake activity is limited to an area of about 30 km x 20 km, with most focal depths being within 6 km. There is no other earthquake source within 50 km of the Koyna Dam. The triggered earthquakes in the Koyna region are governed by the rate of loading, highest reservoir levels reached and duration of retention of high water levels. Magnitude ≥ 5 earthquakes usually occur when the previous water level maximum is exceeded. However, the role water reservoir in triggering earthquakes is not well understood. An ICDP Workshop held in March 2011 found Koyna to be the most suitable site to investigate reservoir- triggered seismicity (RTS) through deep drilling. Studies carried out in the preparatory phase since 2011 include airborne magnetic and gravity-gradient surveys, MT surveys, drilling of 9 boreholes going to depths of ~ 1500 m and logging, heat flow measurements, seismological investigations including the deployment of six borehole seismometers, and LiDAR. Significant results include absence of sediments below the basalt cover, the thickness of the basalt column and its relation with the surface elevation, and almost flat topography of the basement. The Second ICDP Workshop held during 16- 18 May 2014, reviewed the progress made and detailed planning of putting the borehole observatory was discussed. The location of the first Pilot Borehole has been finalized and the drilling shall start shortly."

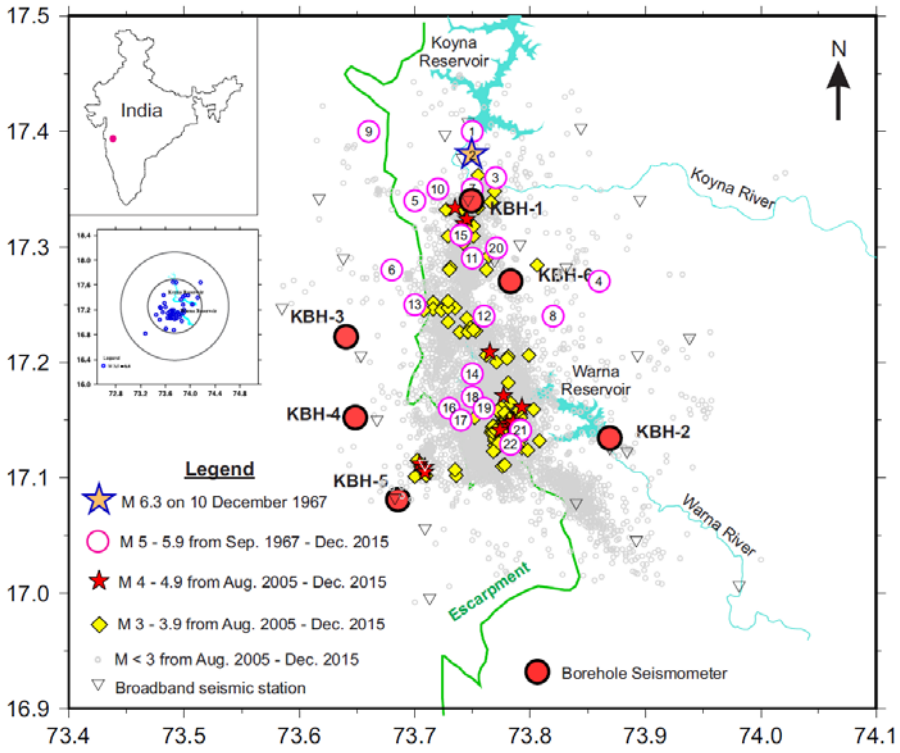

Fig. 1 Map of the Koyna–Warna region showing the locations of the 1967 main shock, M ≥ 5 earthquakes since September 1967 and M <5 earthquakes during August 2005–December 2015. Numbers inside pink circles show the chronological order of occurrence of the M ≥ 5 events. The network of surface and borehole seismic stations is also shown. The green curve indicates the WGE (Western Ghat Escarpment). (I) The location of Koyna on the outline map of India. (II) The distribution of earthquakes of M ≥ 3.7 during 1967–2015 (USGS) in the vicinity of the Koyna–Warna region and an outer circle of 100 km radius that shows there is almost no seismic activity outside the Koyna–Warna region.

On the variety of post-deformation phenomena in abandoned mining districts: Insights from seismic source analysis.

Jannes Kinscher[1], Isabelle Contrucci[1], Pascal Dominique[2], Emmanuelle Klein[1], Pascal Bigarré[1]

1 INERIS, L'Institut national de l'environnement industriel et des risqué, Nancy, France, Jannes-L.Kinscher@ineris.fr

2 BRGM, Bureau de recherché géologiques et minières, Orleans, France

Post-deformation in abandoned mining districts can be accompanied by significant surface subsidence and collapses, as well as ground shaking that bear serious risks for proximate urban areas. The origin of these phenomena can be related to a wide range of complexly interacting factors, often linked to the flooding evolution of the mine after groundwater pumping is stopped. Here, we present different case studies of seismic monitoring highlighting the variety of these post-mining deformations and the challenge of appropriate risk assessment in this context.

For more than 20 years, INERIS has been performing near-real time seismic monitoring to survey hazardous deformation in post-mining districts, with a main focus on the Lorraine region, in NE France, where hundreds of buildings have been damaged after several mine shutdowns in the 90s. As a complement to operational data analysis, several monitoring experiments have been performed (including controlled mine flooding and solution mining) to simulate and understand the cause and nature of these collapsing events. In the results, we found that the reactivation of pre-existing fault structures plays a fundamental role in the readjustment of stress due to external stimulations (i.e. flooding, seismic waves, partial collapses). Also aseismic processes as stress memory effects and slow surface subsidence are involved which underlines the necessity of multi-disciplinary monitoring approach in this context.

During monitoring in the Provence region at Gardanne (in SE France), we experience the high degree of complexity in which an abandoned, flooded mine can interact with its local tectonic setting. In this case, excessive and long term excavation has led to the formation of very efficient "anthropogenic" aquifer which, especially in wet periods, enable water migration into deeper levels below the mine workings. The modification of the hydrogeological system seems to be the today's cause of significant seismic swarming activity, including local magnitudes close to 2 that have been several times felt by the nearby living population. Further analysis shows that swarming activity is related to the reactivation of minor fault segments being favourably oriented with respect to the local tectonic stress field. However, it remains still unknown if the meteorologically controlled variations of the mine water level, might potentially trigger larger local tectonic events, as recorded in the past (Mw 4.3, 1984), or if swarming represents simply episodes of small transient creep.

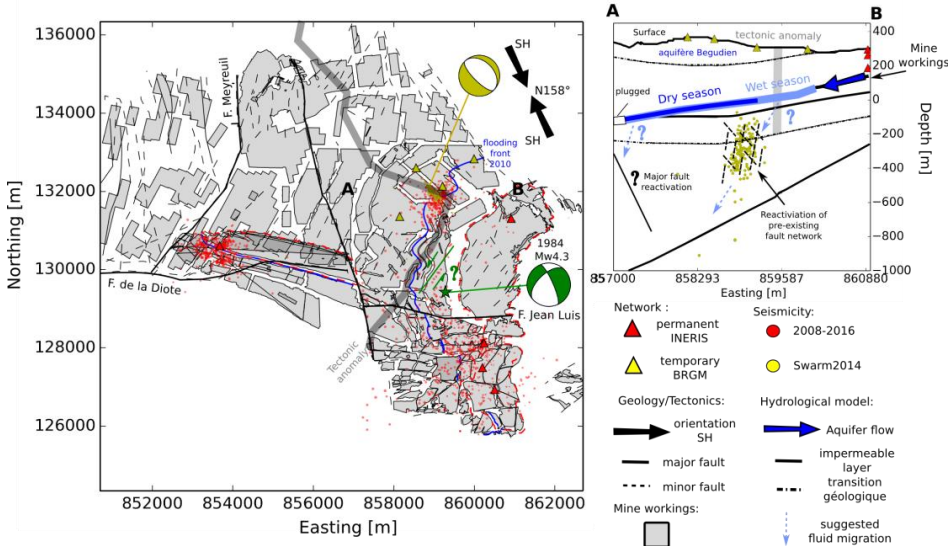

Fig. 1 Complex interactions of the abandoned, flooded coal mine at Gardanne with the local tectonic environment. Mine workings formed an important aquifer that triggers seismic swarming (see text) linked to the reactivation of preexisting fault structures (yellow beachball). Potential triggering of larger tectonic events as recorded in the past (green beachball) cannot be excluded.

Abstracts Talks

Sessions 3 and 4

Understanding and Modeling of Induced Seismicity

Application of Large-Scale Earthquake Simulations to Seismicity Induced by fluid injection

James Dieterich[1], Keith Richards-Dinger[1], Kayla Kroll[1,2]

1 University of California, Riverside, **2** Lawrence Livermore National Laboratory

Simulations that couple physics-based models of seismicity with reservoir models provide an experimental capability to investigate a variety of topics related to induced seismicity. These include 1) investigation of fundamental interactions controlling induced seismicity; 2) characterization of the relationships among injection parameters, reservoir characteristics and seismicity; 3) development of best-practices protocols for injection projects; and 4) probabilistic hazard evaluation of the potential for inducing earthquakes. We have linked the multi-cycle fault system earthquake simulator, RSQSim to reservoir models that give changes of effective stress due to fluid injection. RSQSim is a computationally efficient 3D boundary-element code that incorporates rate- and state-dependent fault friction to simulate long sequences of earthquakes (up to 10^6 events) in geometrically complicated, fully interacting fault systems. Space-time patterns and rates of induced seismicity are highly sensitive to both the amplitude and heterogeneity of pre-injection fault stresses. Over a range of subcritical initial stresses, the maximum magnitude of earthquakes induced by fluid injection scales by injection volume. However, if the pre-injection stress is near-critical over a region sufficient to generate a large earthquake, then small localized perturbations of effective stress can induce a large earthquake and maximum earthquake magnitude becomes independent of injection volume. Following shut-in of fluid injection seismicity may continue for several years, a phenomenon that complicates mitigation efforts to reduce the chances of large induced earthquakes. Continuing seismicity following shut-in may arise in part due to the delay in the arrival of the pressure decrease signal at progressively distant location from the injection site. In addition, a significant component of seismicity following shut-in occurs as a consequence of time-dependent earthquake nucleation that is inherent to rate- and state-dependent friction — in this case the continuing earthquakes are aftershocks to both the prior induced earthquakes and the regional perturbation of effective stresses from the injection episode. Simulations of different shut-in (and reduced injection rate) scenarios will be presented.

Two physics-based models for estimation of magnitudes of fluid-injection-induced earthquakes

Martin Galis[1], Jean-Paul Ampuero[2], P. Martin Mai[1], Frédéric Cappa[3]

[1] KAUST – King Abdullah University of Science and Technology, Saudi Arabia, martin.galis@kaust.edu.sa;
[2] California Institute of Technology, USA; [3] Geoazur, University Côte d'Azur, France

In this study, we focus on integrating fracture mechanics into estimates of magnitude of fluid-injection-induced earthquakes. For our analysis we assume that a fault crosses a reservoir with ongoing injection. Consequently, pore-pressure perturbation inside the reservoir may be large enough to trigger an earthquake. We use fracture mechanics and friction law to estimate the magnitude of a triggered earthquake. Our work is based on estimating whether on a given fault and for a given pore-pressure perturbation a rupture will stop spontaneously (arrested rupture) or will runaway. We derived two models. The first, more complex model is based on pore pressure evolution obtained by solving the diffusivity equation for a cylindrical reservoir with no-flow boundaries. This semi-analytical model allows us to investigate the size of arrested ruptures, as well as temporal aspects of their occurrence. This model can be used to investigate the roles of various parameters on the entire reservoir-fault system. The second model is an approximation to the first one, based on a point-load approximation of the pressure perturbation on the fault, allowing derivation of a complete analytical formula relating the magnitude of the largest arrested rupture, $M_{max\text{-}arr}$, to injection and slip-weakening friction parameters. Although it only provides information about the largest arrested rupture before transition to runaway ruptures, it provides the desired physical insight into which parameters control the behavior of the entire system. Similarly as the M_{max} relation by McGarr (2014), we find that $M_{max\text{-}arr}$ scales with cumulative injected fluid volume (V) as a power law. However, we find a slope 3/2 whereas McGarr's model (2014) predicts linear scaling with slope of 1. Comparison with observed data in different contexts and various scales (see figure) shows that while for the dataset used by McGarr (2014) the difference between the two models is relatively small, inclusion of datasets over a broader range of injected fluid volumes suggests better agreement with our model. This agreement may indicate that most of the recorded earthquakes happened in the 'spontaneously arrested rupture' regime. This is, in fact, expected, because with gradually increasing pore-pressure perturbation, arrested ruptures should occur before runaway ruptures. At the same time, should this conjecture be true, the gap between McGarr's and our estimates for larger injected volumes may indicate that even larger earthquakes may happen than what has been recorded to date.

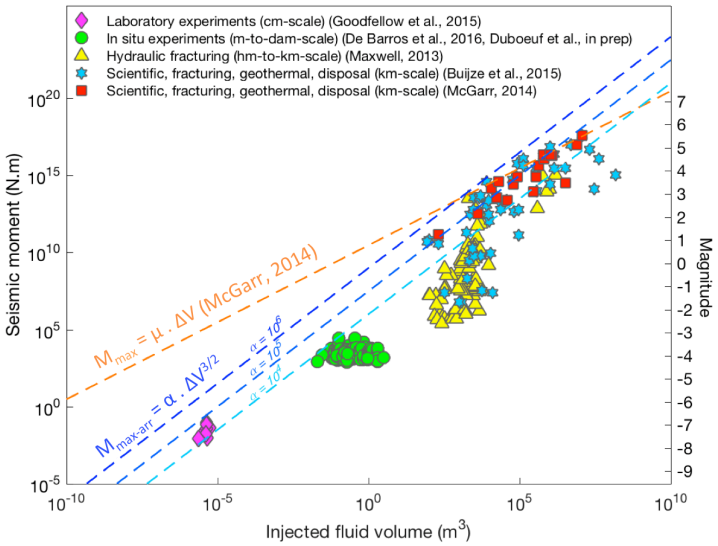

Fig. 1 Comparison of our $M_{max\text{-}arr}$ estimate with M_{max} by McGarr, (2014), and various observations in different contexts and various scales (from laboratory and in-situ experiments to kilometer-scale injections).

Applying numerical reservoir modelling concepts to the forecasting of induced seismicity

David Dempsey[1], Jenny Suckale[2]

1 University of Auckland, New Zealand, d.dempsey@auckland.ac.nz; **2** Stanford University, California, USA

In the geothermal sector, reservoir modelling involves three stages: (i) matching the pre-exploitation state (usually the temperature field), (ii) matching the production history (pressure decline and well enthalpy), and (iii) making a projection about the reservoir response due to future operations. Each step can be subject to rigorous uncertainty quantification such that the final product – a projection of the future – can be formulated as a probability distribution to serve as a basis for risk assessment.

Taking as an example the Groningen gas field in the Netherlands, a similar workflow is followed to construct a forecast for future induced seismicity (see Fig. 1). We use a forward model that computes rupture nucleation and propagation on ensembles of 1D faults with heterogeneous stress, and which outputs, for a given stressing history (pressure, shear, normal stress changes), a synthetic earthquake catalogue. This has average properties, e.g., a time-varying seismicity rate, which reflect the fault parameterization (e.g., initial proximity to failure), the stressing history and the earthquake physics. Using this model, a workflow is followed that is analogous to the three reservoir modelling steps described above.

For the first step, it is assumed that pre-exploitation seismicity is negligible compared to the induced seismicity rate and so the tectonic stressing is set to zero.

In the second step, as both the observed and modelled earthquakes are contaminated by randomness, it is not meaningful to compare events. Instead, we use Bayesian methods to infer an underlying, time-varying earthquake rate from the observations and then compare this to the rate predicted by the model. This provides a measure of model quality that, in addition to establishing the parameters of the best seismicity model, identifies the larger set of models that are comparable to, if not quite as good as, the best model.

In the third step, each of these models is projected out to some future time for a prescribed stressing scenario (corresponding to ongoing field operations). Each of these future outcomes is assigned a likelihood based on the model's goodness of fit with the available earthquake data. The ensemble of future predictions then forms a probabilistic description of both the future seismicity rate and, by extension, Mmax.

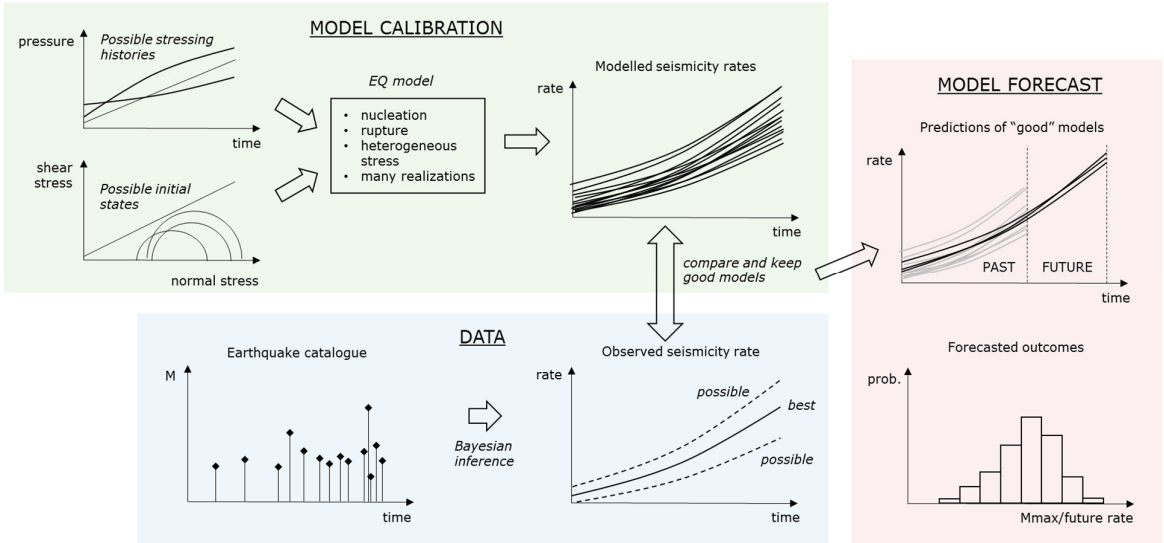

Fig. 1 Schematic depiction of workflow: uncertain model inputs; giving many model outputs; which are filtered against observations; the final set of predictions (forecast) is from "good" models that remain.

Comparing strategies for stimulating and relieving an EGS reservoir with 3D Monte Carlo simulations

Dimitrios Karvounis[1], Stefan Wiemer[1]

1 Swiss Seismological Service - ETH Zurich, Switzerland, karvounis@sed.ethz.ch;

Deep geothermal technologies like Enhanced Geothermal Systems (EGS) will assist non volcanic countries like Switzerland both in decentralizing energy and in meeting the climate goals. A crucial step for the development of a successful EGS project is the stimulation of the reservoir that will allow the production of commercially interesting flow rates of hot water. Typically, the stimulation of an EGS reservoir is performed by injecting large rates of fluid inside a fractured reservoir. Some of the fractures hydro-shear because of this injection and in general, their permeability is increased. The efficiency and the commercial interest of the EGS project depend strongly on the interconnectivity between the hydrosheared fractures and the wells. An important constraint in stimulating an EGS reservoir is the induced seismicity hazard, which needs to be under control at all times.

Hybrid models that combine deterministic and stochastic modeling can simulate stochastic sequences of induced seismicity and can return forecasts of induced seismicity by integrating over the space of uncertainty. Here, we present a three dimensional hybrid model that couples a stochastic geomechanical model with the in-house EGS simulator that is called HFR-Sim and employs discrete fracture modeling for flow and heat transport. This hybrid can process several observations from the field, including catalogs of observed seismicity, and can construct possible fracture networks that are based on the observations. Once one or more geological models have been located, then a Monte Carlo simulation can be performed. Long term forecasts of some of the characteristics of induced seismicity as well as of the expected thermal revenue from the resulting fracture networks can be obtained. Different strategies for stimulating or for mitigating any induced seismicity hazard can be compared with each other and EGS operators can be assisted in their decision making.

Poroelastic and Earthquake Nucleation Effects in Induced Seismicity

Paul Segall[1]

1 Geophysics Department, Stanford University, USA, segall@stanford.edu

Induced seismicity is understood to result from a decrease in effective normal stress, leading to a focus on the spatiotemporal distribution of pore-pressure caused by injection. Yet, the association of earthquakes with fluid *production*, and *decreasing* pore-pressure requires that poroelastic effects must dominate in some settings. In addition, laboratory experiments show that time to failure depends on stress history, suggesting that the space-time evolution of seismicity depends on fault friction as well as hydraulic properties.

Analytical models show that poroelastic coupling may increase or decrease the seismicity rate during injection, depending on the location and orientation of faults relative to the injector. If injection induced stresses inhibit slip, abrupt shut-in can lead to locally sharp increases in seismicity (Segall and Lu, 2015, JGR). The largest induced earthquakes occur on faults that extend into the basement, due to the limited area of ruptures restricted to sedimentary strata. The potential for induced earthquakes on basement faults depends on whether faults are hydraulically connected to the injection horizons, as well as the fault zone permeability. If faults are hydraulically isolated from injection horizons, poroelastic stressing can still increase the Coulomb stress, destabilizing faults even in the absence of direct pore-pressure diffusion (Chang and Segall, 2016, JGR). Analytical models also show that the time to reach a critical seismicity rate scales with distance-squared, although the inferred diffusivity is likely to be biased by frictional effects.

The maximum magnitude induced event often occurs post-injection, which presents a clear problem for `stop light' systems. Dynamic rupture models under spatially variable stresses indicate that under high background shear stress earthquake magnitudes are limited only by the sizes of available faults and heterogeneity of stress. In this limit, induced earthquakes would be expected to follow power law distributions, larger events occur only in proportion to the seismicity rate. Under lower ambient stresses ruptures are limited by the time varying volume of perturbed crust. This limit leads to a roll-over in frequency magnitude distribution for larger events, with a corner magnitude that increases with time; larger events occurring post shut-in are thus not unexpected. Observations from Basel support a temporal change in frequency magnitude statistics between co-injection and post-injection periods. The challenge for the future will be to incorporate poroelastic effects and slow tectonic loading into proper elastodynamic rupture models.

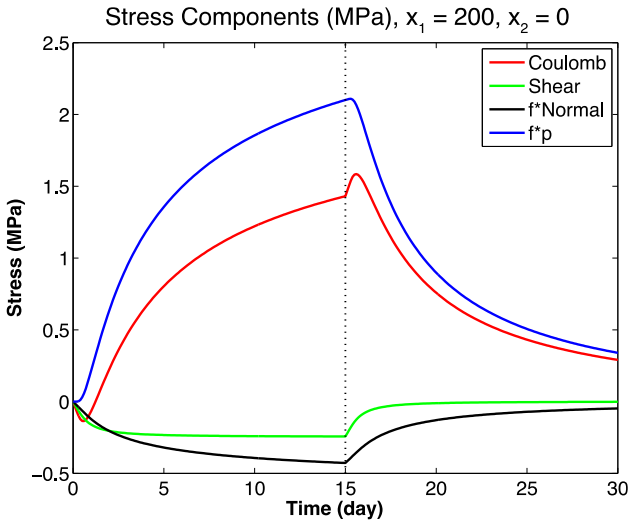

Fig. 1 Stress components acting on normal fault as a function of time. Friction coefficient: f. Vertical dashed line marks shut-in.

Injection induced stress rotations and their effect on induced seismicity

Moritz Ziegler[1,2], Oliver Heidbach[1], Arno Zang[1,2]

1 Helmholtz Centre Potsdam, German Research Centre for Geosciences, Telegrafenberg, 14473 Potsdam, Germany;
2 University of Potsdam, Institute of Earth and Environmental Science, Karl-Liebknecht-Str. 24-25, 14476 Potsdam-Golm, Germany

Engineering of a subsurface reservoir involves often injection of fluids in order to maintain the reservoir pressure or to enhance the permeabililty by hydraulic fracturing. In connection with the hot-dry-rock project in the geothermal reservoir The Geysers (California) significant rotations of the principal stress axis of about 20° have been observed by the analysis of focal mechanism solutions (Martinez-Garzón et al., 2013). By applying geomechanical modelling those stress rotations are attributed to injection of fluid in The Geysers (Jeanne et al., 2015) and at Groß Schönebeck (Yoon et al., 2015). Since the optimal orientation of faults for (re)activation depends on the prevailing stress field changes in the stress field are a key factor for the assessment of induced seismicity. Furthermore this stress rotation can be used as a proxy for the ratio between the relatively well-known induced stress changes and the background tectonic stress field which is in most cases not quantified.

In order to assess the influence of different reservoir parameters and borehole engineering procedures we set up a generic fully coupled 3D thermo-hydro-geomechanical model to simulate stress rotations due to injection of fluid into a reservoir. We perform different model runs testing various parameters such as e.g. reservoir permeability, porosity, initial stress field, temperature difference, and the amount of injected fluid. Thereby we quantify the parameter's impact on the stress rotation in terms of affected volume, time, and maximum rotation. This generic approach leads to a better understanding of the critical parameters for stress rotation, its mechanisms, and triggers. Furthermore we discuss the importance of inherent reservoir on the stress rotation structures such as anisotropies in reservoir properties or injection cycles. The results can be used as a first order assessment of the expected stress rotations in a reservoir. In particular we analyse the relative contribution of the thermally induced stress changes and the ones that are induced by pore pressure diffusion as well as their link to the occurrence of induced seismicity. Our model results show that for the injection of cold fluids the fully coupled process is essential. Furthermore, the results indicate that thermally induced stress changes have locally a large impact on the stress change and might be the cause for the nucleus of induced events.

Jeanne, Pierre, Rutqvist, Jonny, Dobson, Patrick F, Garcia, Julio, Walters, Mark, Hartline, Craig, & Borgia, Andrea. 2015. Geomechanical simulation of the stress tensor rotation caused by injection of cold water in a deep geothermal reservoir. Journal of Geophysical Research: Solid Earth, 120(12), 8422–8438.
Martinez-Garzón, Patricia, Bohnhoff, Marco, Kwiatek, Grzegorz, & Dresen, Georg. 2013. Stress tensor changes related to fluid injection at The Geysers geothermal field, California. Geophysical Research Letters, 40(11), 2596–2601.
Yoon, Jeoung Seok, Zimmermann, Günter, & Zang, Arno. 2015. Numerical Investigation on Stress Shadowing in Fluid Injection-Induced Fracture Propagation in Naturally Fractured Geothermal Reservoirs. Rock Mechanics and Rock Engineering, dec.

Potential Sources of Seismicity during the Propagation of a Height Contained Hydraulic Fracture

Brice Lecampion[1]

1 EPFL, Geo-Energy Lab-Gaznat chair on Geo-Energy, Lausanne, Switzerland, brice.lecampion@epfl.ch

Hydraulic fractures are tensile (opening mode) fractures propagating in rock under in-situ compressive stresses as a result of the injection of fluid under high pressure. Due to the volume control nature of the injection, their propagation is inherently stable [1]. However, micro-earthquakes are typically recorded during hydraulic fracturing both in the lab and in the field. Dynamic shear instabilities around the propagating hydraulic fracture triggered by stress and pore-pressure changes are the likely causes of these micro-earthquakes. Micro-seismic monitoring is often the method of choice for "imaging" these fractures in-situ [2]. The magnitudes M_w of the recorded micro-seismic events are typically in the range [-3, -1]. Although rare, larger seismic events (M_w up to ~4) have also been triggered in some cases due to the re-activation of near-by faults either via induced stresses perturbation or pore-pressure diffusion [3, 4, 5].

In this talk, we will briefly review the different mechanisms at play during the propagation of a hydraulic fracture. We will notably perform an energy budget of the complete process. From a modeling perspective, we then discuss the possible causes of micro-seismicity associated with the propagation of a height contained hydraulic fracture (PKN geometry [6]) depending on the in-situ stress regime, namely i) pure stress perturbation, ii) pure pore-pressure perturbation or iii) a combination of both on randomly distributed defects at different scales.

References

[1] E. Detournay. Mechanics of hydraulic fractures. Annual Review of Fluid Mechanics, 48:311–339, 2016.

[2] C. L. Cipolla, S. C. Maxwell, M. G. Mack, et al. Engineering guide to the application of microseismic interpretations. In SPE Hydraulic Fracturing Technology Conference. Society of Petroleum Engineers, 2012.

[3] X. Bao and D. W. Eaton. Fault activation by hydraulic fracturing in western Canada. Science, page 2583, 2016.

[4] A. Holland. Earthquakes triggered by hydraulic fracturing in south-central Oklahoma. Bulletin of the Seismological Society of America, 103(3):1784–1792, 2013.

[5] H. Clarke, L. Eisner, P. Styles, and P. Turner. Felt seismicity associated with shale gas hydraulic fracturing: The first documented example in Europe. Geophysical Research Letters, 41(23):8308–8314, 2014.

[6] Y. Kovalyshen and E. Detournay. A Reexamination of the Classical PKN Model of Hydraulic Fracture. Transport in Porous Media, 81(2):317–339, may 2009.

Rates of Induced-Earthquake Activation in Western Canada and Implications for Hazard

Hadi Ghofrani[1], Gail M. Atkinson[1]

1 Western University, Canada, hghofra@uwo.ca

"Hydraulic fracturing plays a significant role in triggering seismicity in the Western Canada Sedimentary Basin (WCSB; Atkinson et al., 2016; Bao and Eaton, 2016). Since 2010, most of the regional earthquakes of **M**≥3 in WCSB are highly correlated in time and space with horizontally-fractured wells .We develop a statistical model of the likelihood that horizontally-fractured wells in the WCSB will trigger earthquakes of moment magnitude (**M**) ≥3 using the concept of cellular seismicity. Our aim is to facilitate the forecasting of induced-seismicity potential for future HF operations, for use in hazard analyses. This differs from an exercise aimed at identifying individual wells that initiated past sequences. For future operations, we are interested in the probability that a significant sequence of events may be triggered (i.e. the activation probability). The rate of seismicity in a probabilistic seismic hazard analysis (PSHA) for induced seismicity is the product of the activation probability and the conditional earthquake rate (conditioned on activation). Thus changing the activation probability is equivalent to changing the seismicity rate parameter (Gutenberg–Richter *a*-value), which significantly impacts the expected ground motions (Atkinson et al., 2015).

We use statistical metrics to estimate the regionally-averaged probability that hydraulic fracture operations will be associated with **M**≥3 seismicity within a 10 km-grid cell; this provides an estimate of the prior probability of inducing seismicity by commencing operations in a small area. For the geological setting and operational parameters in the WCSB, the likelihood that hydraulic fracture operations in an area of 10 km radius will be associated with **M**≥3 earthquakes is 0.010 to 0.026, at the 95th percentile confidence limit. This is the likelihood averaged over the entire region. In some areas the rate is significantly higher than average, while in others it is lower. Monte Carlo simulations confirm that the observed correlations are extremely unlikely (<<1%) to have been obtained by chance. Proximity to a disposal well, and proximity to the Swan Hills Formation, which has been suggested as a proxy for basement faulting, appear to increase the likelihood that hydraulic fracturing will trigger seismicity."

The Static Behaviour of Induced Seismicity

Arnaud Mignan[1]

1 ETH Zurich, Institute of Geophysics, Switzerland, arnaud.mignan@sed.ethz.ch

The standard paradigm to describe seismicity induced by fluid injection is to apply non-linear diffusion dynamics in a poroelastic medium. I show that the spatio-temporal behaviour and rate evolution of induced seismicity can, instead, be expressed by geometric operations on a static stress field produced by volume change at depth (Fig. 1a). I obtain laws similar in form to the ones derived from poroelasticity while requiring a lower description length (Fig. 1b). Although fluid flow is known to occur in the ground, it is not pertinent to the geometrical description of the spatio-temporal patterns of induced seismicity. The proposed model is equivalent to the one for tectonic foreshocks developed in the Non-Critical Precursory Accelerating Seismicity Theory (N-C PAST). This study hence verifies the explanatory power of this theory outside of its original scope and provides an alternative physical approach to poroelasticity for the modelling of induced seismicity. The applicability of the proposed geometrical approach is illustrated for several EGS experiments, including problematic cases where the stress field may be spatially heterogeneous. The usability of the approach in time-dependent risk analysis (considering various injection profiles and mitigation strategies) is also discussed.

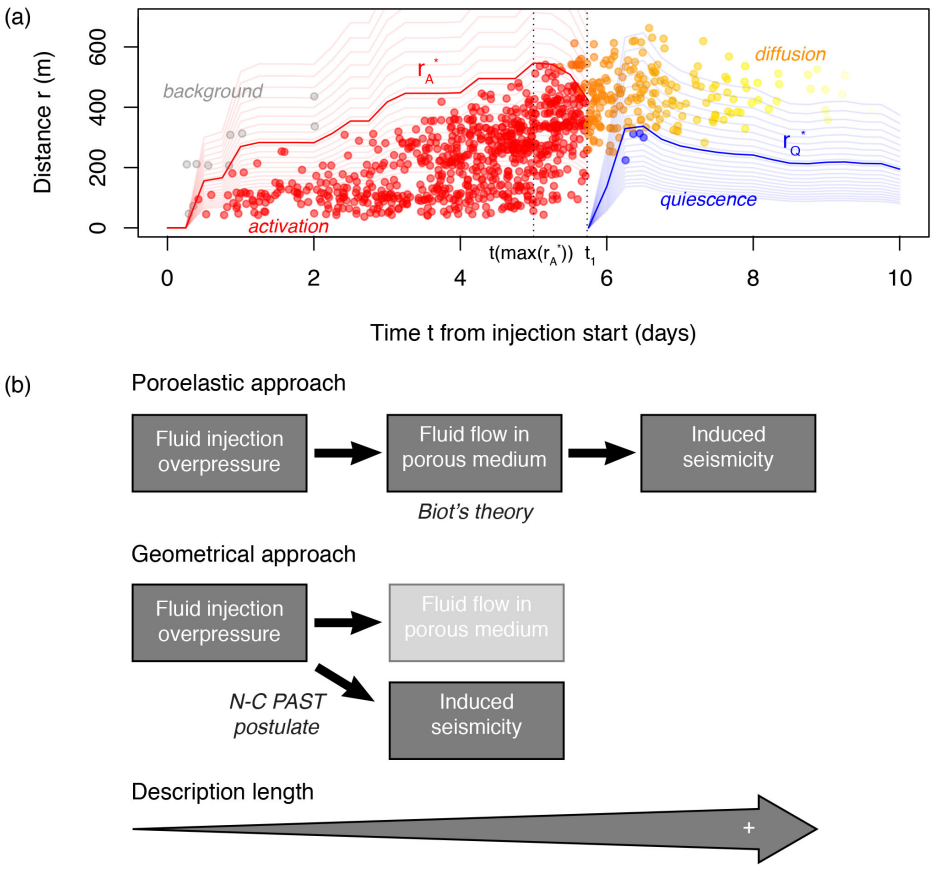

Fig. 1 (a) Spatiotemporal distribution of induced seismicity during the 2006 Basel EGS experiment (catalogue from Kraft & Deichmann, 2014) and envelope fits obtained from analytic geometry. (b) Description length defined as the number of physical steps required to describe induced seismicity, in poroelasticity and in the newly proposed geometrical approach. In the latter, Biot's theory is entirely bypassed. Redrawn from Mignan (2016).

References: Kraft, T. & N. Deichmann (2014), Geothermics, 52, 59-73, doi: 10.1016/j.geothermics.2014.05.014; Mignan, A. (2016), NPG, 23, 107-113, doi: 10.5194/npg-23-107-2016

Scaling of postinjection-induced seismicity – An approach to better understand fluid injection-related processes

Lisa Johann[1], Carsten Dinske[1], Serge A. Shapiro[1]

1FU Berlin, FR Geophysik, Germany, lisajohann@zedat.fu-berlin.de;

Subsurface fluid injections are frequently accompanied by microseismicity. This seismic activity often continues after the injection stop. A valuable tool for the determination of hydraulic transport properties, understanding of seismicity-related processes, as well as for hazard assessment, is the analysis of seismic event distributions in space and time. On the assumption that microseismic events are induced by the diffusion of pore-fluid pressure, Shapiro et al. (1997) use the triggering front of the microseimic cloud in order to get large-scale estimates of the reservoir diffusivity. This concept was transferred to postinjection-induced events by Parotidis et al. (2004), who introduced the back front. Yet, in case of high-pressure fluid injections, the hydraulic diffusivity becomes a function of pressure and pore-fluid pressure diffusion becomes non-linear. Parameters that control postinjection-induced seismicity are still poorly understood.

To describe the temporal behavior of postinjection seismicity in case of non-linear pore-fluid pressure diffusion, we derive scaling laws for the triggering front and for the back front (Johann et al., 2016). We show that both fronts are sensitive to the degree of non-linear pore-fluid pressure diffusion (n) as well as to the Euclidean dimension of the dominant growth of seismic clouds (d), given by $r \propto t^{1/(2+dn)}$. We numerically model non-linear pore-fluid pressure diffusion in 3D, applying two different models regarding postinjection behavior of the hydraulic diffusivity: an elastic diffusivity model and a frozen diffusivity model (see Hummel et al., 2016). We compare synthetic seismicity and also real data examples to the theory.

As shown in Figure 1, the proposed asymptotic scaling law can well describe the evolution of seismicity back fronts in space and time within a 95 % confidence interval (squares and diamond shapes). Therefore, the scaling can be used to get estimates of the dimension of seismic cloud growth and/or the degree of non-linear pore-fluid pressure diffusion, if one of the parameters is unknown in real fluid-injection operations. Thus, we apply the back front scaling to hydraulic fracturing and enhanced geothermal system case studies from literature (circles and triangles).

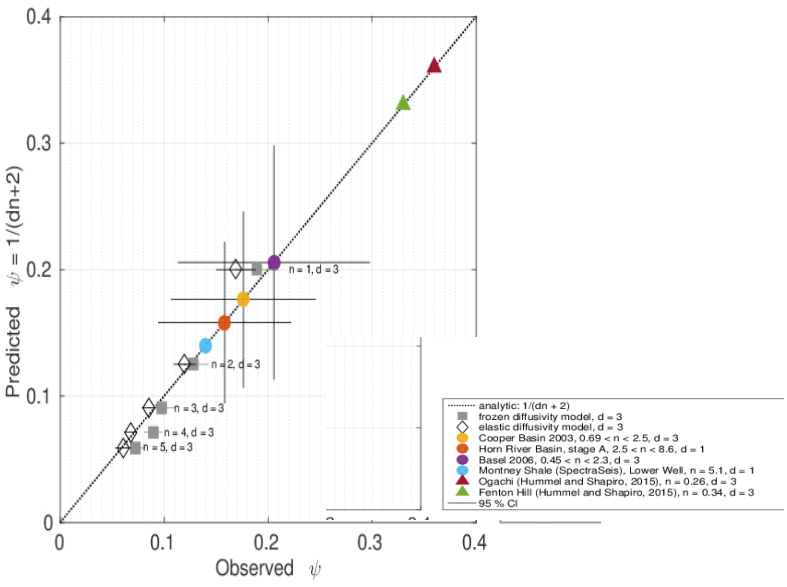

Fig. 1 Numerically determined back front exponents (squares and diamonds) compared to the scaling law. A best fit of fluid injection case studies can be used to determine the influence of non-linearity n (Figure by Johann et al, 2016)

References

Johann, L., C. Dinske, and S.A. Shapiro (2016), Scaling of seismicity induced by nonlinear fluid-rock interaction after an injection stop, Geophys. J. Int., 121, doi:10.1002/2016JB012949.

Parotidis, M., S. A. Shapiro, and E. Rothert (2004), Back front of seismicity induced after termination of borehole fluid injection, Geophys. Res. Lett., 31, L02612, doi:10.1029/2003GL018987.

Shapiro, S. A., E. Huenges, and G. Borm (1997), Estimating the permeability from fluid-injection induced seismic emission at the KTB site, Geophys. J. Int., 131, F15–F18.

Statistical distributions of seismicity in the Cooper Basin geothermal field – a way towards predictive models of induced seismicity

Andreas Barth[1], Pia Carstens[2], Stefan Baisch[2]

1 Karlsruhe Institute for Technology (KIT), Germany, a.barth@kit,edu; **2** Q-con GmbH, Bad Bergzabern, Germany

The Cooper-Basin geothermal field (Australia) produced one of the largest datasets of induced seismicity world-wide. We use these extraordinary observations of localised seismic events to analyse statistical properties that are often presumed in seismic hazard assessment without proving. Comparison with synthetic datasets allows us to evaluate those assumptions in terms of their value as predictors for future seismicity.

Seismic hazard analysis of tectonic seismicity is typically based on the assumption of Poissonian and Gutenberg-Richter (GR) distributed data. For this purpose, datasets are typically declustered to a Poisson distributed dataset by rejecting after- and foreshocks. In a second step a GR distribution above a magnitude of completeness is assumed to represent the magnitude frequencies. The Cooper Basin geothermal field was stimulated in August 2005 with 15,300 events detected. Magnitudes and hypocentral locations were determined for 8,000 events $M_L \geq -0.9$. We perform parameter studies for the declustering process and goodness-of-fit tests to analyse whether the assumptions of Poissonian and GR distributions are valid for the induced seismicity in the Cooper Basin.

We show that the dataset follows an inherent Poisson distribution for moderate rejection rates of timely dependent seismic events (Fig. 1). Single subsets also show GR distributions, when rejection rates are high. Tests with synthetic datasets show that the statistic algorithms are reliably detecting Poissonian and GR distributions. However, uniform distributed datasets may be wrongly identified as Poissonian when high rejection rates are apparent. Even though high rejection rates may be necessary to reveal the statistical properties of declustered subsets, they could be a valuable measure towards an operative control of geothermal production.

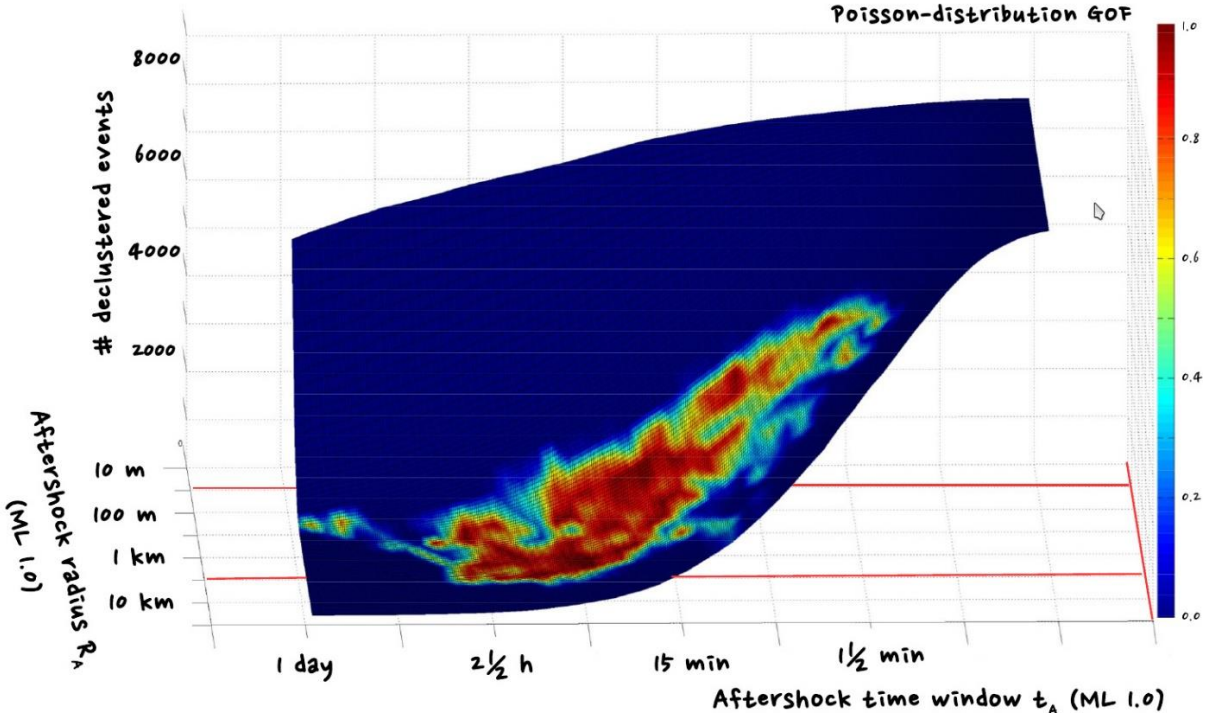

Fig. 1 Goodness-of-fit (GOF) determination regarding a Poisson distribution. Single points on the surface show results of the parameter study for different spatial and temporal aftershock windows.

Seismic valve as a driving mechanism of the 2014 aftershock sequences in West Bohemia

Tomas Fischer[1], Ctirad Matyska[2], Sebastian Hainzl[3], Jens Heinicke[4]

1 Charles University, Faculty of Science, Prague, Czechia, fischer@natur.cuni.cz; **2** Charles University, Faculty of Math. and Physics; Prague, Czechia; **3** GFZ Potsdam, Germany; **4** TU Bergakademie Freiberg, Germany

The West Bohemia/Vogtland region is specific for its collocation of earthquake swarm activity and degassing of CO_2 of mantle origin in a relatively small area. It thus provides a natural analog of injection-induced seismicity. We present an analysis of three mainshock-aftershock sequences that occurred in May-August 2014 and were initiated by M_L 3.5 mainshock on 24 May. Four days later a fast increase of CO_2 flow rate began in the Hartoušov mofette, 9 km apart from the epicentres. During the subsequent 150 days the flow reached the six-fold of the original level. The following decay, which lasts until present, suggests that the seismic activity could have been driven by the fault-valve mechanism.

Our analysis of the spatiotemporal characteristics and focal mechanisms of the relocated aftershock sequences shows that the three mainshocks occurred with unfavorably oriented mechanism in a step-over region of the fault plane with increased coulomb stress due to previous activity. The aftershock decay is of Omori-Utsu type with untypically large c and p parameters. The ETAS modeling shows that an additional aseismic source with an exponentially decaying strength was needed to trigger a large fraction of the aftershocks. Corresponding pore pressure simulations with an exponentially decreasing flow rate show a good agreement with the observed spatial migration front of the aftershocks extending approximately with log(t). Accordingly we propose a scenario that the mainshock opened fluid pathways into the fault plane explaining the unusual high rate of aftershocks, the migration patterns, and the decrease of the aseismic signal due to a finite fluid source. The migrating fluid pulse is then supposed to reach the surface and be observed as a long-term increase of CO2 flow rate in the mofette few days later (Fig. 1).

To verify the likelihood of this scenario we simulated gas flow in a two dimensional model of Earth crust composed of a sealing layer located in the hypocentre depth, which is penetrated with earthquake fault and releases fluid flow from a relatively low-permeable lower crust to vertical high-permeable channel pointing to the surface. We get excellent and robust fit of the simulated flow to the data using a realistic vertical channel diffusivity showing that even this simple model is capable of explaining the observations including the short travel time of the flow pulse from 8 km depth to the surface, the following flow increase and later long-term decrease.

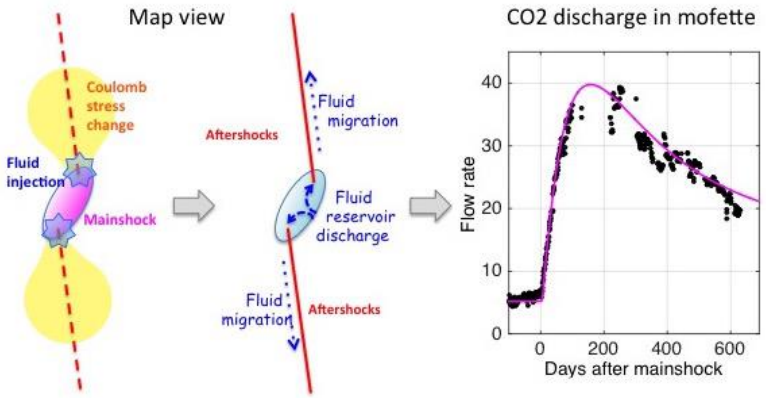

Fig. 1. Mainshock opened fluid pathway to the preexisting fault, where aftershocks were triggered by Coulomb stress and fluid pressure pulse, later CO_2 flow rate increased dramatically in a nearby mofette, compliant with a numerical model.

Abstracts Talks

Session 5

Scaled Experiments

Drilling to probe quasi-static and dynamic seismic ruptures in deep South African gold mines

Hiroshi Ogasawara[1], Y Yabe[2], T Ito[2], G van Aswegen[3], A Cichowicz[4], R Durrheim[5], TC Onstott[6], T Kieft[7], A Ishida[1], HY Ogasawara[1], T Yasutomi[1], A Funato[8], K Imanishi[9], M Okubo[10], M Boettcher[11], P Moyer[11], W Ellsworth[12], M Ziegler[13], S Wiemer[13], C Janssen[14], S Shapiro[15], H Gupta[16], P Dight[17], N Wechsler[18], AK Ward[19], B Liebenberg[20], Y Mukuhira[21], SN Somala[22], JP Hunt[4], S Bucibo[4], N Berset[13], R Harris[6], ED Cason[23]

1 Ritsumeikan University, Japan, ogasawar@se.ritsumei.ac.jp; **2** Tohoku Univ., Japan; **3** Inst. Mine Seismol., South Africa (SA); **4** Council for Geoscience, SA; **5** Univ. Witwatersrand, SA; **6** Princeton Univ., USA; **7** New Mexico Inst.Tech., USA; **8** Fukada Inst., Japan; **9** AIST, Japan; **10** Kochi Univ, Japan; **11** New Hampshire Univ., USA; **12** Stanford Univ., USA; **13** ETH, Switzerland; **14** GFZ, Germany; **15** Freie Universität Berlin, Germany; **16** Nat. Geophys Res. Inst., India; **17** Univ. Western Australia; **18** Tel Aviv Univ., Israel; **19** Seismogen CC, SA; **20** SA; **21** MIT, USA; **22** IITH, India, **23** Free State Univ., SA

The International Continental Scientific Drilling Program (ICDP) approved our project "Drilling into seismogenic zones of M2.0-5.5 earthquakes in South African gold mines (DSeis)". This project aims to probe quasi-static ruptures (with extents < 100 m) and dynamic seismic ruptures (M5.5, M3.5, and M2.8) at depths of 1−4 km from surface. As partly reported in Ogasawara et al. (2013 Schatzalp Workshop), these ruptures have been elucidated by the analysis of seismograms of surface strong ground motion meters (several stations within 10 km from the M5.5 epicenter), in-mine underground dense seismic networks (46 stations within several km from the M5.5 hypocenter), or AE monitoring network (a few tens of sensors within several tens of meters from the quasi-static ruptures) that are significantly more sensitive than the in-mine seismic network. In-situ stress was measured before the M2.8 event and some of the quasi-static ruptures have been exhumed by mining and mapped.

Deep gold mines in South Africa allow us cost-effective drilling by collaring holes at depth and the flexible choice of drilling direction allows for maximum core recovery. We will drill 10−20 holes (50−900 m long) to intersect the ruptures at depths of 1−4 km below surface. We will probe the ruptures by borehole and core logging and by laboratory tests on core samples, which will be cataloged using the ICDP Digital Information System. With in-hole monitoring of seismicity, water, and gas, we further elucidate rupture structures, temporal changes in fault behavior with fault healing or the occasional significant aftershocks. Geomicrobiological investigations focus on the connection of H2 gas generated by cataclastic alteration of quartz during these aftershocks and the activity of the subsurface chemolithoautotroph microorganisms that consume H2. The activity of these microorganisms could provide an extremely sensitive biosensor for H2 (analogous to the canary in the coal mine).

By optimizing the Compact Conic-ended Borehole Overcoring method that the International Society of Rock Mechanics suggests (Sugawara and Obara, 1999 IJRMM), we established an overcoring stress measurement procedure with minimum interference against mining operation, even in earthquake-prone stress conditions. Funato and Ito (2016, IJRMM) developed a method to measure anisotropic elastic expansion of drilled core to estimate differential stress. By combining these methods, we probe stress variation in and around the seismogenic zones.

Seismogenic zones are difficult to access directly and therefore have rarely been probed. In the framework of the DSeis project we will be able to address many fundamental scientific questions on seismogenic zones identified by the ICDP Science Plan 2013−2019.

The first drilling will start in March 2017.

This project is built on the outcomes of the projects in JST-JICA SATREPS program, JSPS Grant-in-Aid, MEXT Japan, Ritsumeikan University, Tohoku University, and DST South Africa. We thank Anglogold Ashanti Ltd., Sibanye Gold Ltd., OHMS Ltd., Seismogen CC, Homeseismo Ltd., and 3D Geoscience Ltd.

Induced micro-seismicity observed during meter-scale hydraulic-fracturing

Valentin Gischig[1], Joseph Doetsch[1], Hannes Krietsch[1], Hansruedi Maurer[2], Florian Amann[1], Keith F. Evans[2], Mohammadreza Jalali[1], Anne Obermann[3], Morteza Nejati[1], Benoît Valley[4], Stefan Wiemer[3]

1 Swiss Competence Center for Energy Research (SCCER-SoE), ETH Zurich, **2** Institute for Geophysics, ETH Zürich, **3** Swiss Seismological Service, ETH Zürich, **4** Centre d'hydrogéologie et de géothermie, Université de Neuchâtel

To characterize the stress field at the Grimsel Test Site (GTS) underground laboratory a series of hydro-fracturing experiments were performed. The experiments were accompanied by seismic monitoring using a network of highly sensitive piezo sensors and accelerometers that was able to record seismic events with magnitudes less than M-3.0. The recorded seismicity was analysed in great detail using a homogeneous anisotropic P-wave velocity model, joint hypocenter determination inferring station corrections as well as cluster analysis and relative localization. Further, we roughly estimated the event magnitudes and analysed focal plane solutions of selected high-quality events. Retrieving reliable event locations proved important as the seismicity cloud orientation is considered an important method to infer the stress field orientation. In addition to hydro-fractures, so-called overcoring tests were carried out to get independent stress measurements that allow inferring the six independent components of the stress tensor. The stress field orientation found from the seismicity cloud and from overcoring tests differs significantly; unlike expected, the seismicity cloud is not perpendicular to the σ3 (minimum principle stress) direction found from the overcoring tests. Thus, characteristics of seismicity is used to discuss possible fracture growth mechanisms that are likely affected by strength anisotropy and near-wellbore effects in combination with a low degree of stress anisotropy at the GTS.

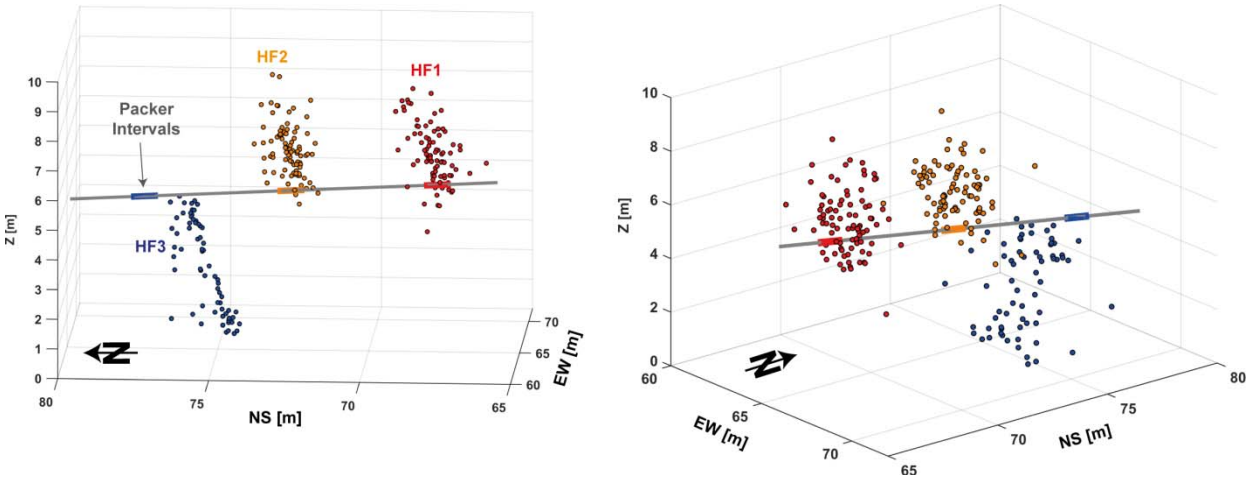

Fig. 1 3D seismicity clouds of three hydro-fractures (HF, HF2, and HF3) performed in a sub-horizontal borehole. The seismicity clouds are roughly oriented East-West.

Insight into subdecimeter fracturing processes during hydraulic fracture experiment in Äspö hard rock laboratory, Sweden

Grzegorz Kwiatek[1], Patricia Martínez-Garzón[1], Katrin Plenkers[2], Maria Leonhardt[1], Arno Zang[1], Georg Dresen[1,3], and Marco Bohnhoff[1,4]

1 Helmholtz Centre Potsdam, GFZ German Research Centre for Geosciences, Potsdam, Germany; kwiatek@gfz-potsdam.de; **2** GMuG Gesellschaft für Materialprüfung und Geophysik mbH, 61231 Bad Nauheim, Germany; **3** University of Potsdam, Potsdam, Germany; **4** Free University Berlin, Berlin, Germany

In this study we analyze the nano- and picoseismicity recorded during a hydraulic fracturing in-situ experiment performed in Äspö Hard Rock Laboratory, Sweden. The fracturing experiment included six fracture stages driven by three different water injection schemes (continuous, progressive and pulse pressurization) and was performed inside a 28 m long, horizontal borehole located at 410 m depth. The fracturing process was monitored with two different seismic networks covering a wide frequency band between 0.01 Hz and 100000 Hz and included broadband seismometers, geophones, high-frequency accelerometers and acoustic emission sensors.

The combined seismic network allowed for detection and detailed analysis of seismicity with moment magnitudes M_W<-4 (source sizes approx. on cm scale) that occurred solely during the hydraulic fracturing and refracturing stages. We relocated the seismicity catalog using the double-difference technique and calculated the source parameters (seismic moment, source size, stress drop, focal mechanism and seismic moment tensors). The physical characteristics of induced seismicity are compared to the stimulation parameters and to the formation parameters of the site. The seismic activity varies significantly depending on stimulation strategy with conventional, continuous stimulation being the most seismogenic. We find a systematic spatio-temporal migration of microseismic events (propagation away and towards wellbore injection interval) and temporal transitions in source mechanisms (opening – shearing - collapse) both being controlled by changes in fluid injection pressure. The derived focal mechanism parameters are in accordance with the local stress field orientation, and signify the reactivation of pre-existing rock flaws. The seismicity follows statistical and source scaling relations observed at different scales elsewhere, however, at an extremely low level of seismic efficiency.

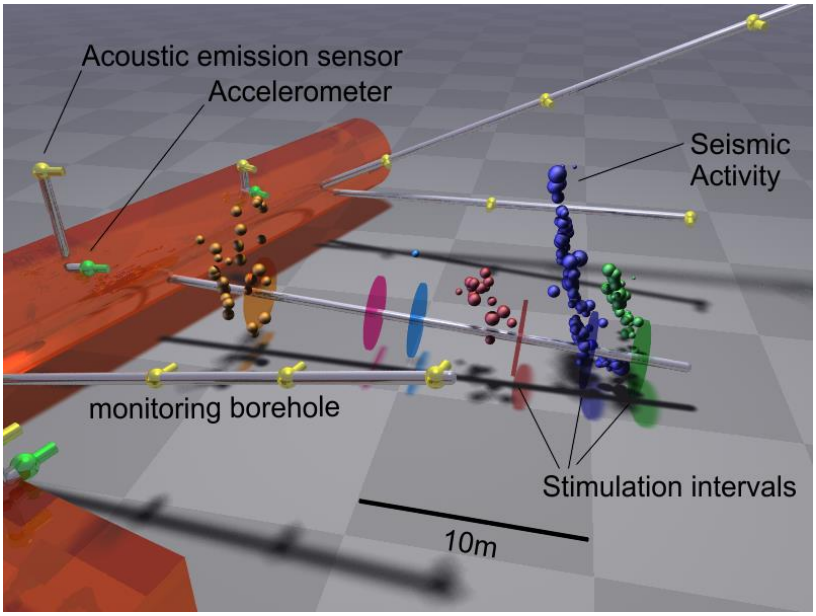

Fig. 1 Perspective view of relocated seismic activity (spheres of different colors) with moment magnitudes between -5.7 and -4.7, corresponding to fractures of ~cm scale, recorded during different stimulation phases (colorful discs). Different stimulations schemes resulted in drastically different seismic response.

Aseismic fault slip and leakage preceding an earthquake induced during an in-situ fault reactivation experiment in the Opalinus Clay, Mont Terri rock laboratory, Switzerland

Christophe Nussbaum[1], Yves Guglielmi[2], Louis De Barros[3], Jens Birkholzer[2], Frederic Cappa[3]

1 swisstopo, Swiss Geological Survey, Wabern, Switzerland, christophe.nussbaum@swisstopo.ch; **2** Lawrence Berkeley National Laboratory, Earth and Environmental Sciences Area, Berkeley, USA; **3** Géoazur, University Côte d'Azur, Sophia Antipolis, France

Understanding fault reactivation is critical in hydraulic fracturing, and CO_2 sequestration because it may result in enhanced fault permeability, potentially inducing fluid leakage from the injection zone through overlying caprock and eventually triggering shallow seismic events. We present preliminary results from a controlled field stimulation experiment (FS experiment dedicated to the hydro-mechanical characterization of in-situ clay fault slip) conducted in a N140°-dipping 50-to-60°SE fault in a claystone formation in the Mont Terri underground rock laboratory. We measure fault slip and seismicity induced by fluid-injection in a natural fault zone, called Main Fault, at a depth of 300 m (**Fig.1**). We observe multiple dilatant slip events (~ 30 μm/s) associated with factor-of-1000 increase of permeability, and a magnitude ~ -2.5 main seismic event associated with a swarm of very small magnitude ones. Seismicity occurs after aseismic slip has been initiated within the fluid-pressurized zone of the fault. Two monitoring points set across the fault allow estimating that, at the onset of the seismicity, the radius of the fault patch invaded by pressurized fluid is ~ 5-to-7m which is larger than the approximate location of the seismic events. The seismic source radius which was estimated to ~ 1.2m indicates that only a fraction of the activated fault patch experienced unstable slip. Significantly different slip/dilation signals at the two monitoring points tend to show that patches of different fault hydro-mechanical properties could be controlling the slip stability. Furthermore, using the slip tendency analysis and 3DEC modelling, we estimate the variability of the stress tensor across the fault zone by fitting the measured 3D displacement vectors with the fault planes geometry.

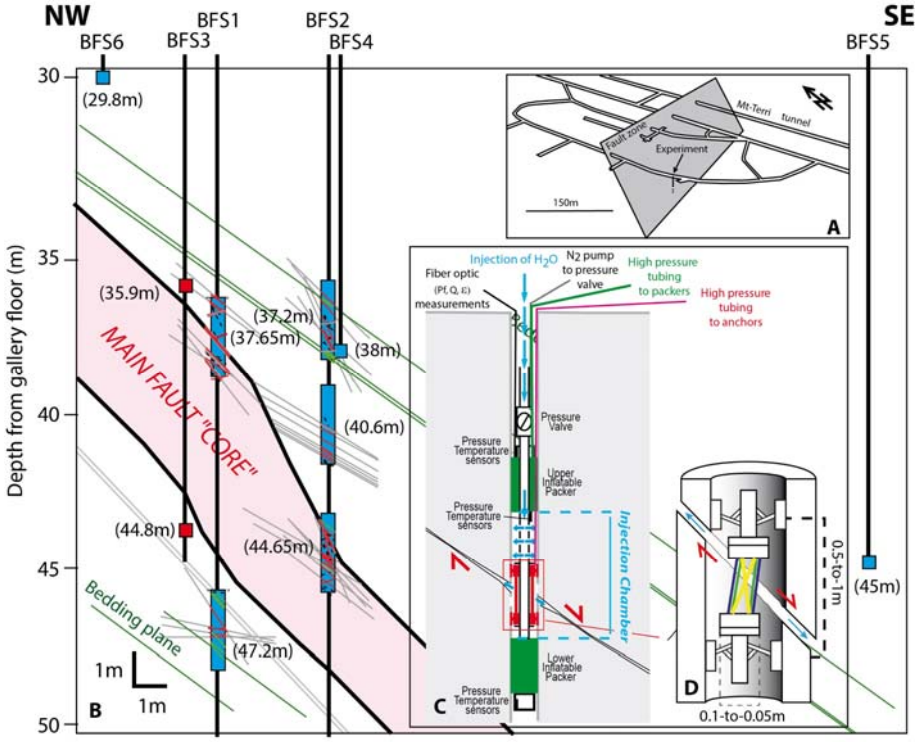

Fig. 1 A) Three-dimensional view of the Main Fault plane with the location of the FS experiment; (B) Simplified cross section of the Main Fault with the blue rectangles indicating the location of the packed-off sections; (C) SIMFIP test equipment setup; (D) Schematic view of the three-dimensional deformation unit. Tubes are differently colored to show that they display different deformations when there is a relative movement of the rings anchored to the borehole wall across the activated fracture.

Unstable slip events on large-scale experimental faults with variable along-fault lithologies

Loes Buijze[1,2], Yanshuang Guo[3], Andre Niemeijer[1], Shengli Ma[3], Christopher Spiers[1]

1 HPT Laboratory, Faculty of Geoscience, Utrecht University, The Netherlands, loes.buijze@tno.nl; **2** Netherlands Organisation for Applied Scientific Research – TNO, Utrecht, The Netherlands; **3** State Key Laboratory of Earthquake Dynamics, Institute of Geology, China Earthquake Administration, Beijing, China

Heterogeneous fault mechanical properties along a fault's dip or strike (e.g. strong – weak fault segments, stable – unstable fault segments) are expected to impose an important control on the nucleation and propagation of (induced) seismic events on these faults. This is highly relevant in the framework of induced seismicity to determine for example where seismic events are likely to nucleate, and whether they will remain restricted within certain lithologies. We designed a scaled experimental setup to investigate the effects of heterogeneous fault properties on the nucleation and propagation of unstable slip events. A vertical fault was created along the diagonal of a 30 x 20 x 5 cm block of PMMA (plexiglass, which was selected for its low stiffness, thus lowering the critical nucleation size), along which a 2 mm thick gouge layer was deposited. The sample was placed in a biaxial deformation apparatus and loaded biaxially to 5 MPa. Shear loading on the fault was induced by continued loading from one side. Different gouge materials were used (kaolinite, quartz, gypsum), which had also been tested previously in a smaller scale sample assembly within a triaxial apparatus. A number of experiments were conducted using only gypsum, which exhibits unstable sliding at the imposed conditions. In other experiments, we created mineralogically different segments along the fault, which exhibit either stable or unstable sliding. Acoustic emissions were continuously recorded at 3 MHz, and were used to determine the location and size of the slip events. Photo-elastic effects (indicative of the differential stress) were recorded in a transparent set of PMMA blocks using a high-speed camera (5000 fps). In a different experiment, particle tracking was conducted on a speckle painted set of PMMA wall-rocks to study the wall-rock's deformation, using the same high-speed camera. The unstable events (stick-slip events) occurred at a specific location along the fault for the gypsum-only faults. This 'asperity' showed up clearly in the photo-elastic patterns in the wall-rock as a highly stressed region, and remained constant during a single experiment. However, when multiple gouge segments were included along the fault, the differential stress differences in the wall-rock were much larger, clearly indicating the position of the strong/unstable segment (see Fig. 1). The unstable events always started from the edge of the unstable segment. We conclude that our experiments can help to understand scaling from small scale to large scale experiments, understand deformation on heterogeneous faults, and provide insight on the relative influence of mineral and stress heterogeneities on the location of nucleation of slip as well as on the magnitude of slip events.

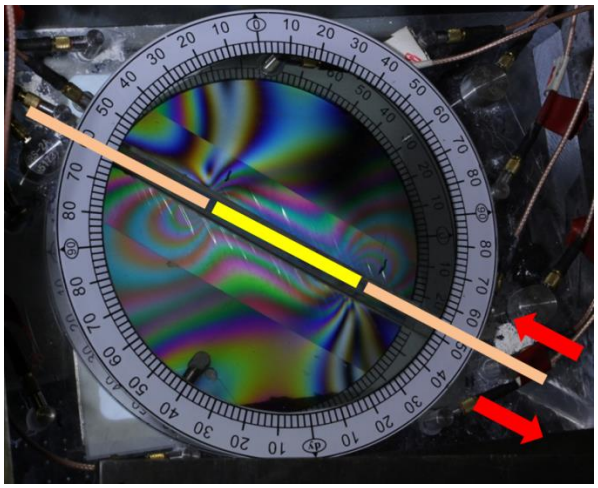

Fig. 1 Fringe patterns indicative of differential stress in PMMA wall-rock sandwiching a multimaterial, vertically oriented strike-slip fault in a biaxial setup. Yellow: gypsum (strong, unstable), pink: kaolinite (weak, stable). Stress concentrations form at the edge of the gypsum segment.

Direct measurements of asperity evolution in the laboratory relating to fault reactivation in stimulated reservoirs

Paul Selvadurai[1], Steve Glaser[2], Thessa Tormann[1], Stefan Wiemer[1]

1 SED, ETH Zurich, Switzerland (paul.selvadurai@sed.ethz.ch); **2** University of California, Berkeley, USA

Fault reactivation and induced seismicity caused by hydraulic stimulation of subsurface reservoirs is an unfavorable byproduct of geothermal energy production. Mechanisms leading to fault reactivation in the stimulated rock mass are difficult to isolate due to, e.g. the unknown stress states, the complex fracture networks and the heterogeneity of material properties, among others factors. During fault reactivation, one source of seismicity can be the result of localized failure of highly-stressed asperities on a relatively weak fault plane.

We performed experiments on a laboratory fault subjected to a variety normal stress conditions, in order to develop a better understanding of how asperities form and the subsequent relationship to the experimentally measured seismicity. We studied a frictional fault formed between two roughened blocks of polymethyl methacrylate (PMMA) in a direct shear configuration. When pressed together, the self-affine surfaces touched at contact points called asperities. Asperities were characterized using two methodologies. (*i*) Static measurements of asperity distribution was initially made by compressing of a pressure sensitive film between the two specimens. The pressure film was used to located, size and measure normal stress on individual asperities. (*ii*) Dynamic measurements were taken once the pressure film and after the fault was reloaded normally, then sheared until failure. An optical video camera measured changes in the light transmitted across individual asperities within the field of view (FOV) – taking advantage of the translucent nature of PMMA.

From the pressure sensitive film, we found the initial distributions of asperities displayed an exponential relationship between asperity area A_{asp} and the number of asperities above a certain size N_{asp}. Figure 1 shows these two distributions for high (blue) and low (red) levels of normal stress. As the interface was sheared, premonitory slip accumulated causing a slip front to move along the fault. As the slip front moved into the FOV, we observed a decrease in the average level of light transmitted across a population of asperities. Locally, this decrease was explained by slight dimming of larger asperities and the complete disappearance of smaller asperities. This resulted in a changing distribution of asperities sizes prior to failure and was measured using the video camera and image detection techniques. Using piezoelectric sensors we detected foreshocks that displayed impulsive signals with source radii ranging between 0.21 and 1.09 mm. The average source radius of the foreshocks increased with applied normal stress suggesting that higher normal stress conditions may promote localized dynamic failure of large asperities to tend to break together.

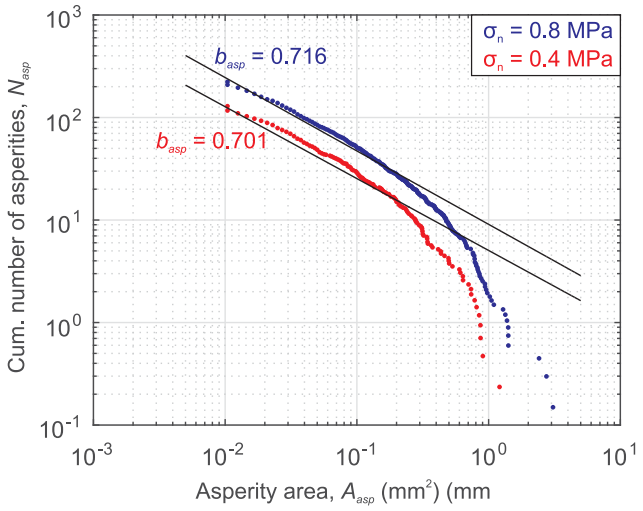

Figure 1. The exponential relationship between asperity area (A_{asp}) and the number of asperities above a certain size (N_{asp}) for a low and high levels of applied normal stress. The relationship is given as $log_{10}(N_{asp}) = a - b_{asp} A_{asp}$ and the slope b_{asp} is shown directly.

Abstracts Talks

Sessions 6 and 7

Monitoring and Analysis of Induced Seismicity

Assessing Potential Magnitudes of Injection-Induced Seismicity on Faults in Crystalline Basement and Overlaying Sedimentary rocks

Mark D Zoback[1], F. Rall Walsh[1], H. Sone[2], A. Kohli[1], F. Rassouli[1], M. Weingarten and S. Xu[1]

1 Department of Geophysics, Stanford University, USA zoback@stanford.edu; **2** Department of Geological Engineering, University of Wisconsin, USA

In this talk, we will address the likelihood of assessing the potential for injection-induced fault slip and possible earthquake magnitudes from two perspective. First, we present a methodology that applies Quantitative Risk Assessment to calculate the probability of a fault exceeding Mohr-Coulomb slip criteria. The program utilizes information about the local state of stress, fault strike and dip and the estimated pore pressure perturbation to predict the probability of the fault slip as a function of time. Uncertainties in the input parameters are utilized to assess the probability of slip on known faults due to the predictable pore pressure perturbations. Application to known faults in Oklahoma has been presented by Walsh and Zoback (*Geology*, 2016). This has been updated with application to the previously unknown faults associated with M $\geq$5 earthquakes in the state (Fig. 1). Second, we will discuss two geologic factors that limit the magnitudes of earthquakes (either natural or induced) in sedimentary sequences. Fundamentally, the layered nature of sedimentary rocks means that seismogenic fault slip will be limited by *i*) the velocity strengthening frictional properties of clay- and carbonate-rich rock sequences (Kohli and Zoback, *JGR*, 2013; in prep) and *ii)* viscoplastic stress relaxation in rocks with similar composition (Sone and Zoback, *Geophysics,* 2013a, b, , *IJRM*, 2014; Rassouli and Zoback, in prep). In the former case, if fault slip occurred in these types of rocks, it would likely be aseismic due the velocity strengthening behavior of faults in the formations. In the latter case, the stress relaxation could result in rupture termination.

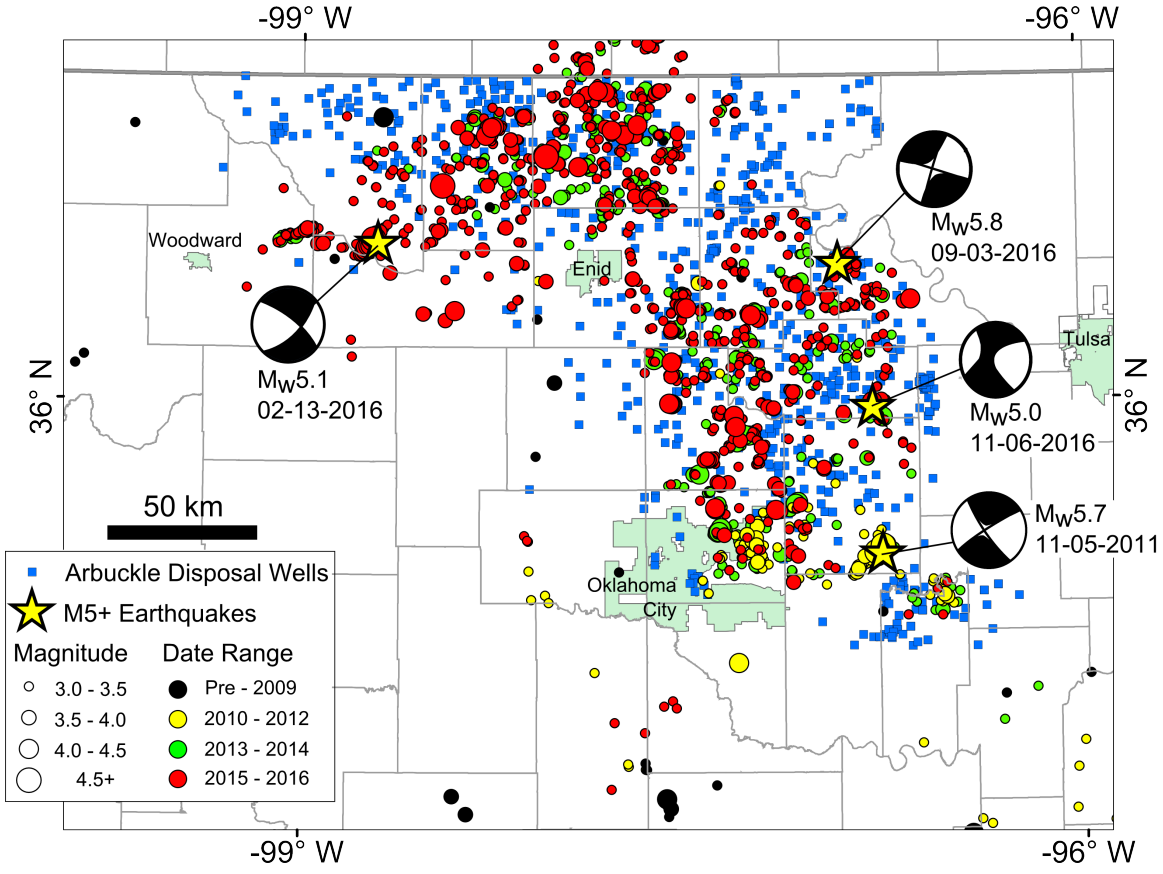

Fig. 1 Historic and recent seismicity, injection wells and the locations of M$\geq$5 earthquakes in Oklahoma.

The induced earthquake sequence of St. Gallen, Switzerland: Fault reactivation and fluid interactions imaged by microseismicity

Tobias Diehl[1], Toni Kraft[1], Edi Kissling[2], Stefan Wiemer[1]

1 Swiss Seismological Service, ETH Zurich, 8092, Switzerland, tobias.diehl@sed.ethz.ch; **2** Institute of Geophysics, ETH Zurich, 8092, Switzerland

Between July and November 2013, a sequence of more than 300 earthquakes was triggered by stimulation and well-control procedures in a planned hydrothermal reservoir close to the city of St. Gallen, Switzerland. The sequence culminated in an M_L3.5 strike-slip earthquake, which was widely felt by the population. In this study, we demonstrate how the coupled hypocenter-velocity structure problem, combined with 3D reflection seismic data, can constrain the absolute position of the reactivated fault strand. The proposed joint interpretation of passive and active seismic data suggest that the majority of the triggered seismicity occurred in the pre-Mesozoic basement, on a previously undetected fault below the targeted hydrothermal reservoir (Fig. 1). Double-difference relocations of fore- and aftershocks precisely image the strike and dip of the M_L3.5 rupture plane and resolve the spatio-temporal evolution of the sequence. The correlation between seismicity and borehole operations, as well as a possible small-scale V_P/V_S anomaly imaged at the border of the M_L3.5 rupture, suggest a hydraulic connectivity between the reactivated fault and the borehole. The proposed connectivity extends over a distance of hundred meters and across different lithologies (Fig. 1). A gap in microseismicity northeast of the M_L3.5 rupture might be related to an asperity and first-order differences in propagation velocities of seismicity indicate along-strike variations in the hydraulic diffusivity on the fault. In summary, our results document the complexity to be expected for upper-crustal fault systems in terms of structure, stress distribution, and hydraulic conditions, which also challenge the degree of predictability of underground fluid injections.

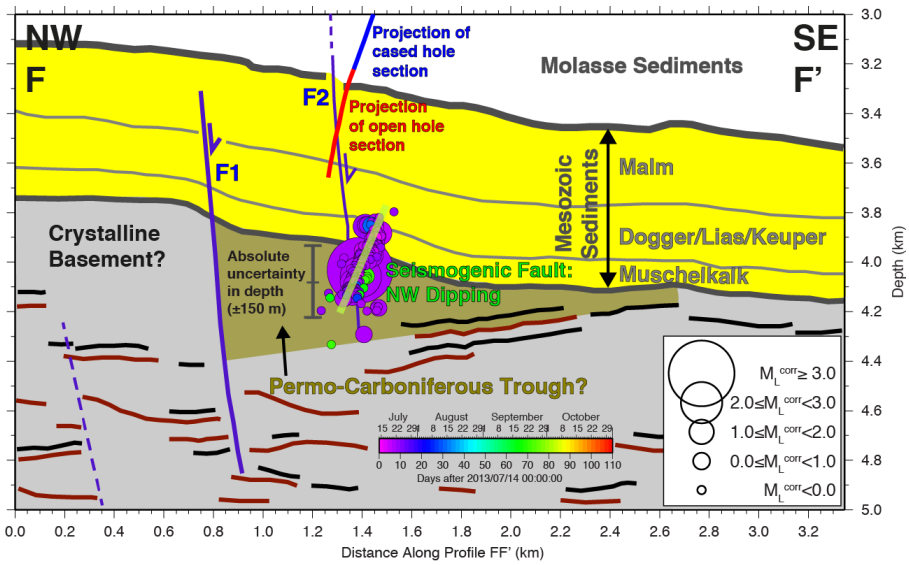

Fig. 1 Location summary figure with double-difference relocated seismicity and interpretation of reflection seismic model after Heuberger et al. [2016] (Heuberger, S., P. Roth, O. Zingg, H. Naef, and B. P. Meier (2016), The St. Gallen Fault Zone: a long-lived, multiphase structure in the North Alpine Foreland Basin revealed by 3D seismic data, Swiss J. Geosci, 109(1), 83-102, doi:10.1007/s00015-016-0208-5.). Bold black and red lines sketch prominent reflectors identified in the 3D reflection images. Faults F1 and F2 are SE dipping normal faults proposed by Heuberger et al. [2016] based on the tracking of vertical offsets in the reflection horizons. The seismogenic fault hosting the induced M_L3.5 event is dipping towards NW.

Interaction between reservoir and basement revealed by CO_2-induced seismicity at Decatur

Bettina Goertz-Allmann[1], Volker Oye[1], Steven Gibbons[1], Robert Bauer[2], Robert Will[3]

1 NORSAR, Norway, Bettina@norsar.no; **2** Illinois State Geological Survey, U.S.; **3** Schlumberger Carbon Services, U.S.

We perform a detailed characterization of microseismicity induced at the Illinois Basin Decatur Project (IBDP). More than 10,000 microseismic events were detected at deep borehole sensors during the injection of 1 Mio metric tons of CO_2 over the course of 3 years. The seismicity occurs in distinct clusters and shows little to no correlation to the progressing CO_2 front. For geomechanical reservoir characterization and seal integrity assessment, we need very high depth resolution for the event locations, such that events can be unambiguously attributed to specific formations. We apply a waveform cross-correlation method to achieve a high level of event depth resolution. Within one cluster, we can distinguish between events in the reservoir and in the uppermost basement, which are some 10ths of meters deeper (Fig 1). Further analysis of source parameters from seismic waveforms such as Brune stress drop and Gutenberg b-value, as well as the general spatio-temporal evolution of the event cloud within a cluster reveal a fluid-driven behaviour of seismicity at the cluster level, and a punctual hydraulic connection between the reservoir and the basement. We observe an increase of stress drop and a decrease of b-value with distance from the cluster nucleation point. We speculate that the clustered microseismicity at Decatur occurs around weak zones associated with basement faults cutting into the reservoir or adjacent sedimentary formations.

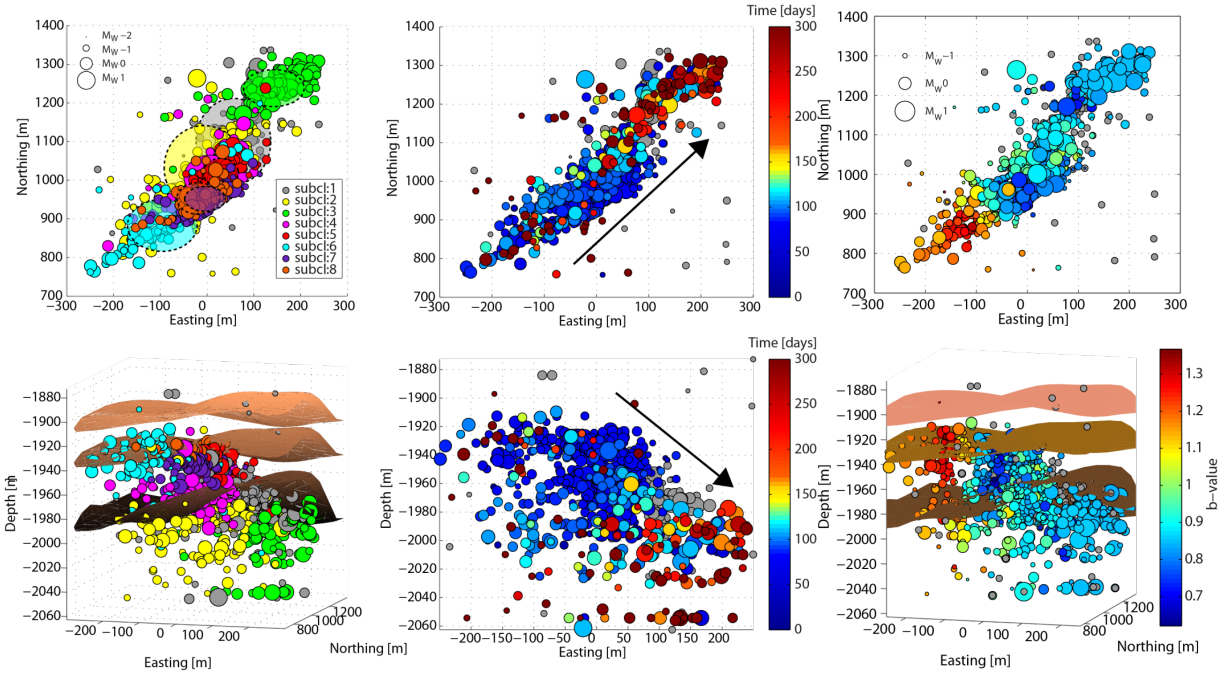

Fig. 1: Left column: sub-clusters in the reservoir (blue, purple, red) and in the basement (yellow, green), revealed by waveform cross-correlation. The colored ellipsoids indicate the mean sub-cluster location and extension. Center column: Color-coding by time of occurrence. Seismicity cluster nucleates in the reservoir and then later migrates into the basement. Right column: Color-coding by b-value. Note a decrease of b-value with distance from SW corner. Top row: map view. Bottom: 3D view including interfaces for Lower Mt. Simon, Argenta, and Precambrian. The black arrow indicates the direction of chronological occurrence of events.

A macroscopic study of the spatio-temporal evolution of induced seismicity on single faults in Oklahoma and Southern Kansas

Martin Schoenball, William L. Ellsworth

Stanford University, Department of Geophysics, United States, schoenball@stanford.edu

For much of Oklahoma, augmentation of the seismic network with new stations in the activated areas has followed rather than preceded the spread of seismicity across the state, and consequently the network geometry is often unfavorable for resolving the underlying fault structures. With this study we augment the existing ANSS catalog with data from two industry operated networks for the period May 2013 to March 2016. These networks include 40 seismic stations and cover seismically active north-central Oklahoma with a station spacing on the order of 25 km. Absolute locations with horizontal errors of about 300 m and relative locations obtained from waveform cross-correlation better than 100 m reveal a striking pattern of seismicity illuminating many previously unmapped faults. Depths are usually well constrained to within 1 km. Relocated epicenters tend to cluster in linear trends of less than 1 km to more than 10 km in length. In areas with stations closer than 10 km, we are able to resolve fault planes by strike and dip. These are generally in agreement with surface wave-derived moment tensors.

Using this data set, we test our understanding of the mechanical conditions for reactivation of dormant faults in the region by elevated pore pressure. Several faults are found to be oriented non-optimally with respect to a homogeneous stress field model for the region. Since pore pressure perturbations by wastewater disposal are generally below 2 MPa, we conclude that local heterogeneities of the stress field in magnitude and orientation play an important role on whether a fault will be reactivated by elevated pore pressure or not.

We further study the spatio-temporal evolution of earthquakes along these faults and find a variety of migration behaviors. For most awakened faults, seismicity tends to initiate at shallower depth and migrates deeper along the faults as the sequence proceeds. However, there are faults where seismicity gets shallower as the sequences progress. Other faults show a radial migration of seismicity or a mixture as shown in Figure 1.

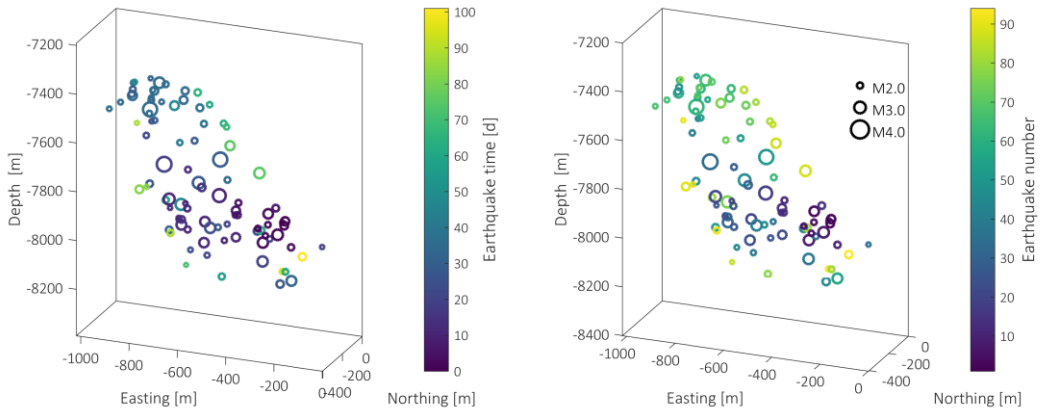

Fig. 1 Relocated seismicity on a fault color-coded by (left) occurrence time and (right) number in the earthquake sequence.

Assessment and Mitigation of Ground Motion Hazards from Induced Seismicity

Gail M. Atkinson

Dept. Earth Sciences, Western University, London, Canada. gmatkinson@aol.com

Induced seismicity poses a consequential increase in hazard to vulnerable high-consequence infrastructure. The likelihood of damaging motions depends on numerous factors including: the activation probability (i.e. the likelihood that a seismicity sequence will be triggered); the magnitude-recurrence characteristics of sequences; ground-motion scaling attributes; and the response characteristics of the structure. Each of these factors has significant associated uncertainty, with the compound uncertainty in the likelihood of damage being orders of magnitude. Moreover, the damage probability is non-stationary in time and space. The high levels of uncertainty in assessing the hazard is problematic when devising mitigation strategies. This is particularly so for high-consequence structures for which the acceptable probability of damage may be extremely low.

Despite the lack of precision in estimating damage probability, a probabilistic seismic hazard assessment for induced seismicity is useful because it provides insight into which factors control the hazard. A case study illustrates the process for the Fox Creek area of Alberta, Canada, where hydraulic fracturing has triggered numerous sequences of earthquakes of M>3. The analysis is conducted using Monte Carlo techniques, assuming activation rates and sequence characteristics typical for the region. The exercise shows that there are two types of events that should be addressed in hazard mitigation plans for specific facilities of consequence: (i) moderate events (M4 to 5) at very close distance (<10 km), having ground motions one or more standard deviations above the median; and (ii) larger events (M5 to 6) that might occur at greater distances (5 to 25 km). A two-pronged mitigation strategy is therefore suggested. It may be necessary to preclude events at very close distances from important or sensitive structures by implementing an exclusion zone for development (typically of the order of 5 km for high-consequence facilities). To reduce the hazard from potential events at distances beyond the exclusion zone, a real-time monitoring and response protocol can be implemented, in which the goal is to monitor and control the event occurrence rate – and hence the likelihood of strong-ground motion.

Long lasting seismicity swarm related to conventional gas production : Lacq gas field, France, 1969-2017

Jean-Robert Grasso[1], Abror Karimov[1], Mathieu Sylvander[2]

1 ISterre,Osug, université de Grenoble-Alpes, France, jean-robert.grasso@univ-grenoble-alpes.fr;
2 IRAP, OMP Toulouse, France

The Lacq gas field is known since the 70's as a significant case study where gas extraction and local seismic deformation interrelate. The still on-going seismicity,(M_{max}=4, 2013, 2016), contemporary to vanishing gas production questions the complex interrelationship between seismicity and reservoir depletion. In this context we discuss possible control parameters of this unexpected long lasting (up to 50 yrs) seismic sequence, including production and pore-pressure drop history and regional tectonic earthquakes.
The interaction between Lacq gas extraction and local seismic deformation was demonstrated on the basis of the overlap between volume where poro-elastic stress changes and seismicity location (Segall, Grasso, Mossop, 1994). The rate and the size of the recorded earthquakes (25 M>3, 1969-2016), which early climax occurred in the mid 90's are still on going now with a new peak of energy released in the 2013-2016 period (M=4 2013, 2016). In this study, we revisit the 1962-2016 seismic activity both in the immediate vicinity of the Lacq gas field and on the Pyrenean fault located 20 km apart. How the long term Lacq seismicity patterns evolve in response to production and pore-pressure drop history, (these later decreasing to vanishingly small amounts since 2010) are compared to others endogenous or exogenous forcing (e.g. the seismic response of the Lacq field to nearby large M>5 Pyrenean earthquake, the endogenous aftershock triggering by the largest Lacq earthquakes). During the 1980-2000 period the reservoir depletion rate smoothly decreases from 1.5 to 0.2 MPa/yrs. It still decreases from 0.2 MPa/yrs to vanishingly small value up to 2010, with a formal production end in November 2013. When the decrease in the seismicity rate after the 1990 peak value correlates with the decrease in depletion rate and the production rate, the long lasting seismicity since 2000, including the 2013-2016 peak of energy release are evidence for the difficulty to predict both (i) how long the still ongoing seismicity will last, and (ii) the local M_{max} value. When compared to seismic tectonic rate (by using the nearby Pyrenees seismicity) we define sub-tectonic rate regime for the Lacq seismicity 1969-1985, followed by over-tectonic rate 1985-1995 and a recession to a sub-tectonic rate since 2000. During the sub-tectonic rate regime, we do not resolve any direct co-seismic effects for 2 nearby Pyrenean M5 events on the Lacq seismicity. The Lacq M3 events have a smaller efficiency to trigger shocks nearby than their Pyrenees counterparts. Alternatively, endogenous triggering patterns are resolved for M3 within the Lacq gas field, when the reservoir length is used as control parameter instead of the mainshock size length. It supports a larger correlation length in the Lacq field than in a regular tectonic area. It suggests the reservoir scale to be a characteristic length for the cascading seismicity swarms. We review possible mechanisms that may reproduce the seismicity patterns. In a more general context of conventional oil and gas extraction, we analyze reported M_{max} values for several oil and gas fields worldwide to discuss on how to possibly constrain the M_{max} event each field operation may trigger.

Insights from 75,000 earthquakes induced in the Cooper Basin Enhanced Geothermal System

Stefan Baisch

Q-con GmbH, Germany, baisch@q-con.de

Geothermal exploration in the Cooper Basin (Australia) was performed between 2002 and 2013. Six deep wells have been drilled into the granite and several large volume hydraulic stimulations were conducted, inducing ~75,000 earthquakes in the magnitude range M_L-2.3 to M_L3.7. Seismicity was time-continuously monitored providing one of the largest and best controlled data sets of induced seismicity in a geothermal reservoir. In this presentation I summarize key findings associated with induced seismicity observations.

Induced seismicity played a key role for characterizing the stimulated reservoir. From hypocenter distributions it was recognized that the reservoir is dominated by a single, large scale fault. Spatial reservoir mapping and model forecasts of the hydraulic conductivity were largely based on recorded seismicity. For example, Figure 1 shows the cumulative shear slip induced on the main, subhorizontal reservoir fault as deduced from earthquake source parameters. Within the concept of self-propping, cumulative shear slip serves as a proxy for the local hydraulic conductivity and turned out to be a key parameter for calibrating numerical reservoir models.

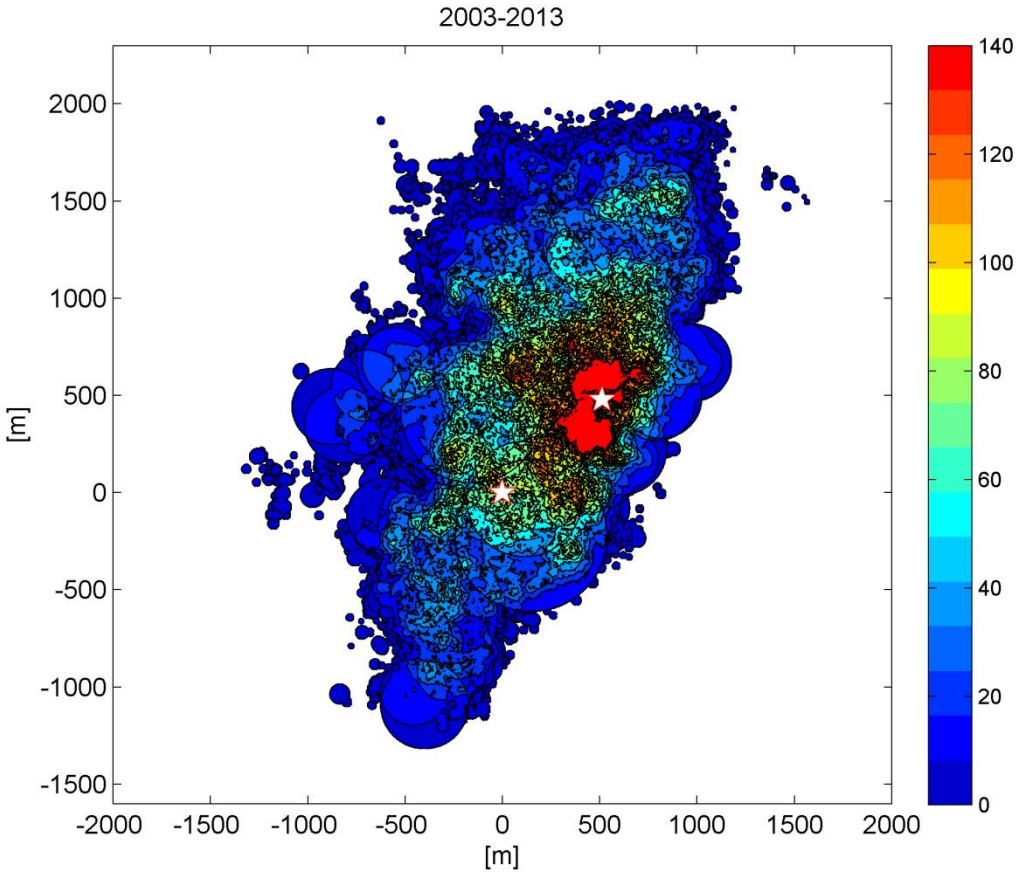

Fig. 1 Cumulative shear slip induced between November 2003 and January 2013 in map view. Shear slip is displayed in millimeters according to the colormap. Stars denote the location of two injection wells.

Induced seismicity at the UK 'Hot Dry Rock' test site for geothermal energy production: a new synthesis

Ian Main[1], Xun Li[1,2], Andrew Jupe[3]

1 University of Edinburgh, School of GeoSciences, Edinburgh, UK, ian.main@ed.ac.uk; **2** Colorado School of Mines, Golden, Colorado, US; **3** Altcom Ltd, London, UK.

Seismicity is routinely monitored at geothermal sites to infer the response of the host reservoir to fluid injection and extraction, including its effective permeability, the architecture of its flow channels, and to assess the risk of inducing felt or damaging events. However, the precise triggering mechanism involved, and the relationship of induced micro-earthquakes to new and pre-existing fracture networks is still the subject of some debate. Here we investigate the triggering mechanism for induced micro-earthquakes at the UK 'hot dry rock' experimental geothermal site at Rosemanowes in Cornwall. We re-analyse a pre-existing data set to quantify the processes involved. The results show a low strain partition coefficient of 0.01%, implying aseismic processes dominate. The strain partition factor decreases with ongoing injection, indicating a decelerating rather than an accelerating (more critical) response to the stress perturbation. The spatio-temporal distribution of hypocentres are used to test competing hypotheses for (a) isotropic pore-pressure relaxation (b) anisotropic pore pressure relaxation and (c) hydraulic tensile fracturing, noting the likely architecture of the fracture network in the present-day stress field. The results are not consistent with (a) but are consistent both with (b) and (c) as a special case of (b). The principal axes of the diffusivity or permeability tensor inferred from the spatial distribution of earthquake foci are aligned parallel to the present-day stress field, although the maximum permeability is vertical, whereas the maximum principal stress is horizontal. This implies a pre-existing permeable vertical structure. We propose a new hypothesis for the mechanism of induced seismicity during fluid injection at the site, constrained by the present-day stress field, the pre-existing joint orientation in the host granite rock, and the focal mechanisms of the micro-earthquakes. The resulting phenomenological model is consistent with all of the know constraints, and involves aseismic slip on a set of optimally-oriented pre-existing joints that are 'unclamped' by an increase in pore pressure and concomitant decrease in normal stress, ultimately fed by fluid flow channeling along stress-aligned tensile cracks. This in turn induces seismic slip on new Riedel P-shear planes connecting the major shear slip surfaces. This hypothesis provides a new scenario to consider for risk assessment of projects involving geothermal energy extraction from jointed crystalline hot rocks, in Cornwall and elsewhere.

Discriminating Features of Induced Seismicity in Application to Sakhalin Offshore Hydrocarbon Fields

Sergey Turuntaev[1,2], Alexey Konovalov[3], Andrey Stepnov[3], Elena Slinkova[1], Anna Gubanova[1,2]

1 Institute of Geosphere Dynamics, Russian Academy of Sciences, Russia (s.turuntaev@gmail.com); **2** Moscow Institute of Physics and Technology, Russia; **3** Institute of Marine Geology & Geophysics of FEB RAS, Russia

Comparison of induced and natural seismicity data allowed to suggest the following discriminating features of them: 1) *b*-value of magnitude-frequency relationship (the value is higher in case of the induced seismicity than in case of the natural earthquakes); 2) the distribution of the time intervals between the seismic events (in case of induced seismicity that distribution is the Weibull distribution with form factor less than 1); 3) migration of the earthquake hypocenters to/from man activity zone; 4) the presence of deterministic component in the induced seismic activity variations, diminishing of correlation dimension; 5) correlation between the seismic activity variations and the variations of man action characteristics (injection pressure, injection and/or production volumes and so on). Change of the above parameters in the regions of industrial activities can be considered as an indication of seismicity induced by that activity.

Sakhalin Island offshore hydrocarbon fields (Russia) are located in the region of high natural seismic activity. That causes a concern on the possibility to trigger catastrophic earthquake by hydrocarbon field developments in this region. The concern is backed by probably triggering nature of the catastrophic Neftegorsk earthquake in 1995 (Mw=7.2). That is why a local seismic network was installed along the eastern shore of Northern Sakhalin in 2006 prior to active phase of the offshore hydrocarbon field developments. The results of analysis of the seismic activity registered by this seismic network are considered in comparison with the natural seismicity registered by the regional seismic network in 1950-1990. It was found that while there are no proved sings of the seismic activity increase due to oil and gas production in the controlled region, some changes in the seismic regime take place: *b*-value became a bit higher than it was before; the distribution of the time intervals between successive events became of the Weibull type with the form parameter less than 1; local maximums of the seismic activity spatial distribution became closer to the boundaries of the developed hydrocarbon fields (Fig.1); the correlation dimension became smaller. All these changes are typical for induced seismicity. It can be concluded, that there are indications of offshore hydrocarbon field development influence on the seismicity in the region of Northen Sakhalin, while this influence did not responsible yet for the seismicity increase.

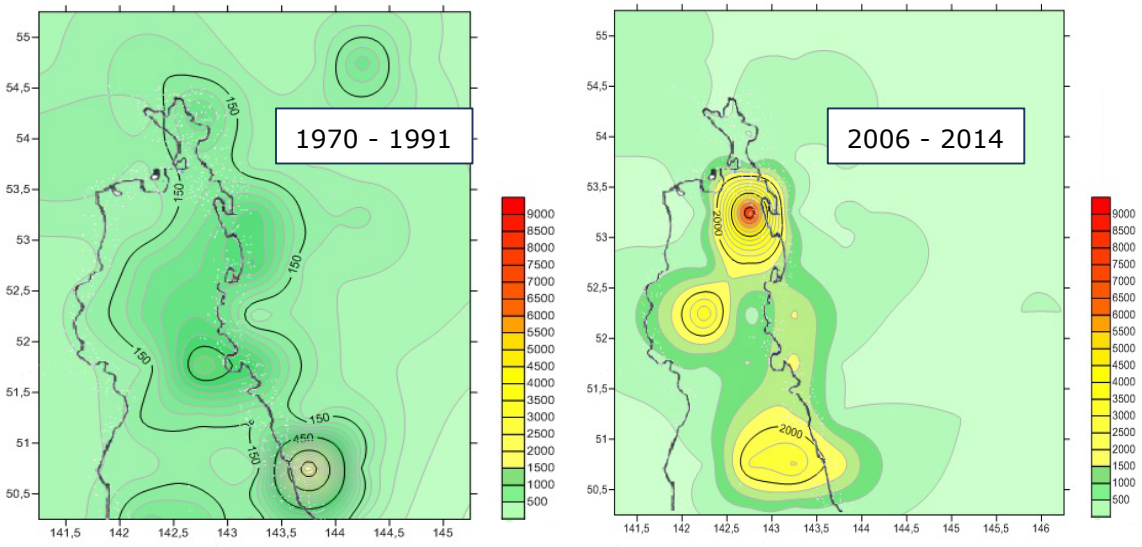

Fig. 1. Change of seismic activity spatial distribution in the area of hydrocarbon fields of Sakhalin after the offshore field development beginning.

Dynamics of fault activation by hydraulic fracturing

David Eaton[1] and Xuewei Bao[2]

1 Department of Geoscience, University of Calgary, Canada eatond@ucalgary.ca

2 School of Earth Sciences, Zhejiang University, Hangzhou, China

Earthquakes up to M_W 4.6 have been triggered by hydraulic fracturing, an industrial process wherein fluids are injected under high pressure to induce localized fracturing of a rock formation; yet, physical links to fault activation remain incompletely understood. This study focuses on a 400-km^2 region in Alberta, Canada where uniquely comprehensive data during a 4-month period from December 2014 to March 2015 characterize dynamic interactions between induced seismicity and well completions at 6 drilling pads. Seismicity is strongly clustered in space and time, exhibiting spatially varying persistence and activation threshold. The largest event during this period (M_L 4.4) can be reconciled with a previously postulated upper bound on magnitude if the cumulative effect of multiple treatment stages is considered. Events in this cluster exhibit contrasting seismicity patterns on parallel fault strands, which are interpreted to reflect different signatures of fault activation by Coulomb stress effects and fluid diffusion, respectively. Related research is currently focused on: 1) the role of shale dynamic overpressure due to hydrocarbon generation, and 2) finite-element modeling of triggering processes for the case of inactive faults where cohesion is non-negligible.

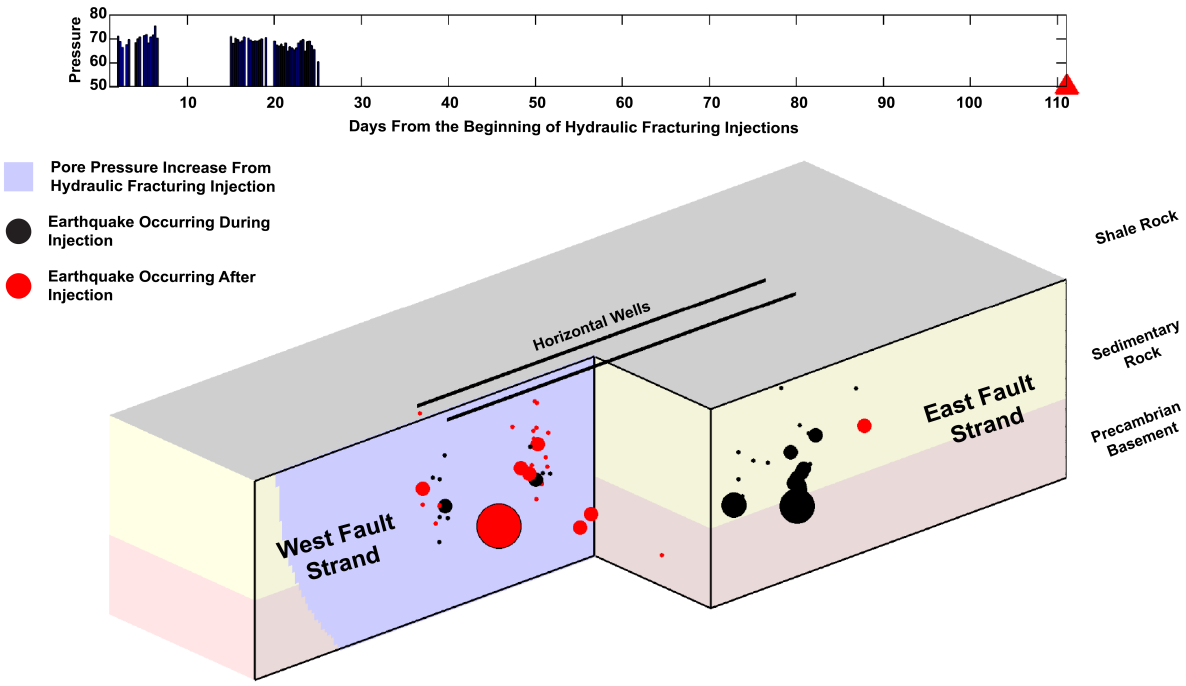

Fig. 1 Upper graphs shows surface injection pressure from hydraulic fracturing in two horizontal wells. Block diagram depicts several clusters of induced seismicity. Black symbols show events that occurred during hydraulic fracturing while red symbols show seismicity that persisted for several months after completion. East and west fault strands inferred from double-difference event locations reveal contrasting fault activation behavior. The largest event occurred in the west fault strand and nucleated in the Precambrian basement two weeks after completion of hydraulic stimulation, likely from fault pressurization. Data from Bao and Eaton (2016).

Reference: Bao, X. and Eaton, D., 2016. Fault activation by hydraulic fracturing in western Canada. Science, DOI: 10.1126/science.aag2583.

Why M_L and M_W for small earthquakes scale as 1:1.5 instead of 1:1

Nicholas Deichmann

Swiss Seismological Service, ETH Zurich, Switzerland

At least part of any strategy to estimate the hazard associated with induced seismicity relies on the extrapolation of the probability of occurence of a larger and thus potentially damaging earthquake from the rate of occurrence of very small seismic events. Reliable magnitudes and a linear relation between the cumulative frequency of occurrence versus magnitude (the Gutenberg-Richter relation) are essential prerequisites. Recent observations of a break in the M_L/M_W scaling relation between small and large earthquakes have raised some fundamental questions concerning the choice of magnitude scale and the physical basis and applicability of the G-R relation over the required magnitude range. For a set of earthquakes in a perfectly elastic medium and assuming that stress-drop and rupture velocity do not vary systematically as a function of magnitude and provided that the instrument response has been corrected for, M_L is proportional to M_W over the entire range for which M_L can be determined. In practice, however, we observe that M_L and M_W deviate from this 1:1 scaling relation. Analysis of an earthquake cluster induced by the geothermal project of Basel in 2006 shows that, for small events (M_W below about 2), M_L is proportional to $1.5M_W$, in agreement with the results of other studies. This behaviour can be reproduced with synthetic earthquake source-time functions convolved with a causal Q-operator using independently determined Q-values (Fig. 1). A key result of both the data analysis and the modelling exercise is that, for small events below a certain magnitude, pulse-widths and equivalently corner frequencies remain practically constant. Thus, in an attenuating medium, the signals of small earthquakes constitute essentially the impulse-response of the medium, scaled by the seismic moment. A simple theoretical demonstration shows that under these circumstances the observed proportionality of 1.5 between M_L and M_W is a necessary consequence of the intrinsic scaling properties of amplitude and duration of the moment-rate function versus seismic moment, as well as of the frequency response of an attenuating medium. As a consequence of this and of the bias introduced by the response of the Wood-Anderson seismometer for the larger events, the G-R relation based on M_L loses its physical justification and, with respect to M_W, leads to different b-values for small and large events.

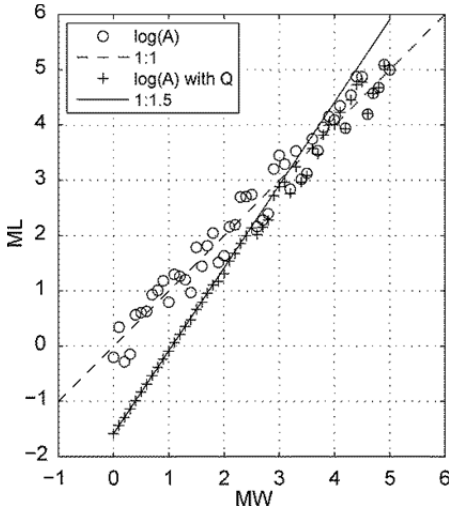

Fig. 1 Plot of M_L against M_W with random variations of stress drop, for synthetic moment-rate functions without attenuation (circles) and with attenuation (crosses). The instrument response of the Wood-Anderson seismometer is not included in these simulations. The attenuation was modelled as for the Basel seismicity with t* = 0.029. The apparent moment-rate functions were computed for a take-off angle of 30 degrees and with a constant rupture velocity of 2.9 km/s. For reference, ML was arbitrarily set equal to M_W for M_W = 5.0 with stress drop = 3 MPa. For all other events, stress drop was allowed to vary randomly between 0.1 and 100 MPa, which is the cause of the scatter of M_L relative to the 1:1 relation. Below about M_W = 2, pulse widths and corner frequencies in an attenuating medium remain constant: in this range M_L scales as $1.5M_W$ and variations in stress drop are no longer visible. (Figure 7 of Deichmann, N.: Theoretical basis for the observed break in M_L/M_W scaling between small and large earthquakes. BSSA, 107, 2, 2017, doi: 10.1785/0120160318)

Abstracts Talks

Session 8

Risk Governance, Societal Acceptance, and License to Operate

Categorizing seismic risk for the onshore gas fields in the Netherlands

Karin van Thienen-Visser[1], Joost Roholl[1], Bart van Kempen[1]

1 TNO – Geological survey of the Netherlands, The Netherlands, Karin van Thienen-Visser, karin.vanthienen@tno.nl

In recent years public awareness on induced events due to gas production has increased in the Netherlands. This has been caused by the larger magnitudes (M_L=3.6) in 2012 occurring in the Groningen gas field, which is the largest gas field in Western Europe with a GIIP of originally close to 3000 billion cubic meters (bcm), and the overall increase in the number of induced events caused by the Groningen gas production. Besides in the Groningen gas field, induced seismicity has been observed in 31 smaller gas fields located on land or in the area close to the Dutch coast. Event magnitudes as high as M_L=3.0-3.5 have been observed in these other fields, which has led to damage of buildings. Since more attention is given to the induced seismicity occurring in the Groningen field, public awareness is growing as well for the induced seismicity of other gas fields.

In 2016 State Supervision of Mines, with input from TNO-Geological Survey of the Netherlands, and the onshore operators proposed a guideline for a qualitative seismic risk analysis for gas fields in the Netherlands. The guideline follows international practices for risk assessment using expert judgement, causes and consequences, influence factors and results in a risk matrix. We have performed this qualitative seismic risk analysis for all the onshore gas fields in the Netherlands. The result is shown in figure 1. The Groningen gas field has the highest risk followed by gas fields in the north and east of the Netherlands. The resulting score is a qualitative measure and should be considered as an ordering of gas fields in terms of seismic risk for monitoring purposes, mitigation measures and legislation.

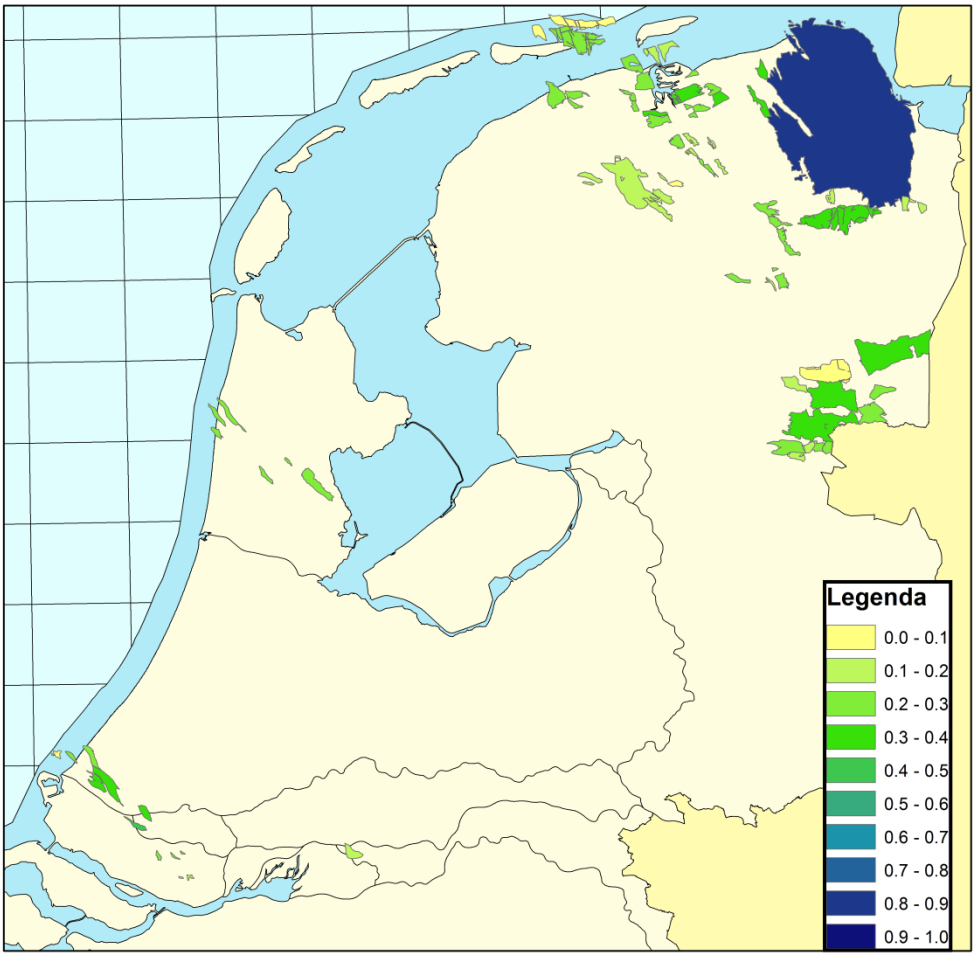

Fig. 1 Normalized risk for the producing fields in the Netherlands. The south of the Netherlands is not shown as gas fields do not exist in this area. Non producing and negligible risk gas fields are not indicated.

How will induced seismicity in Oklahoma respond to decreased saltwater injection rates?

Cornelius Langenbruch[1] and Mark D. Zoback[1]

1 Stanford University, Department of Geophysics, USA, langenbr@stanford.edu

In response to the marked number of injection-induced earthquakes in north-central Oklahoma, regulators recently called for a 40% reduction in the volume of saltwater being injected in the seismically active areas. We present a calibrated statistical model that predicts that widely felt M ≥ 3 earthquakes in the affected areas, as well as the probability of potentially damaging larger events, should significantly decrease by the end of 2016 and approach historic levels within the next ten years.

We modify the Seismogenic Index (SI) model of Shapiro et al. to quantify future earthquake probabilities in Oklahoma based on future injection volumes. Current seismic hazard models in Oklahoma are solely based on earthquake history and do not consider injection rates. Fig. 1 shows observed earthquake rates (M ≥ 3) in Oklahoma and SI models calibrated over different time scales. We find that earthquake rates increase proportional to saltwater injection rates above a critical threshold. In addition, we find a time delay of several months between injection of fluid and occurrence of earthquakes. As predicted by our model the earthquake rate is declining several months after the injection rates start to decrease. To describe the decay of seismicity after injection rates significantly decreased, we use a modification of Omori's law (Langenbruch and Shapiro, 2010). Although the earthquake rate significantly decreased by the end of 2016 the seismic hazard in Oklahoma is still high. Before 2009 only about one M ≥ 3 earthquake has been observed each year. For 2017 our model predicts about 250 M ≥ 3 earthquakes and a 40% probability to exceed M=5. The probability to exceed M=5 during the next five years is 70% (5% to exceed M=6). Without reduction of saltwater injection rates the probability to exceed M=5 would likely have been as high as 80% each year. At the workshop we will also discuss the performance of our model in the next months.

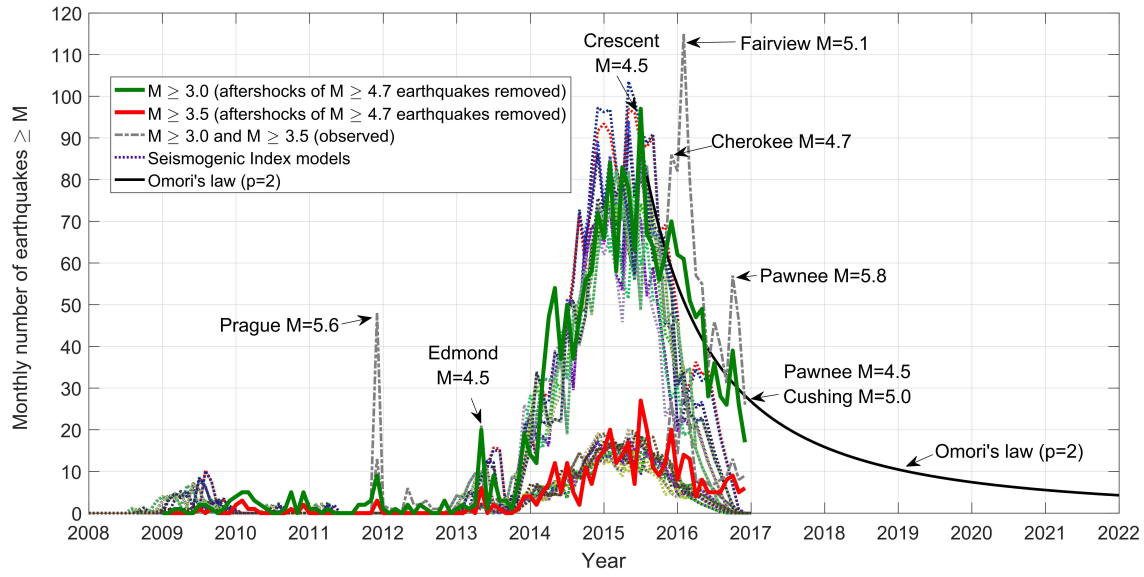

Fig. 1. Observation and prediction of induced seismicity in Oklahoma. Solid colored lines show the combined monthly number of observed earthquakes (green, M ≥ 3; red, M ≥ 3.5) in Oklahoma (aftershocks of M ≥ 4.7 events have been removed). The gray dashed lines present the complete earthquake catalog. The colored dotted lines present SI models calibrated through different times between June 2014 and December 2015. The black solid line shows a decay of M ≥ 3 earthquakes according to a modification of Omori's law. Changes of the earthquake rates are caused by changes of saltwater injection rates.
(Modified from: *Langenbruch and Zoback, 2016, Science Advances, doi: 10.1126/sciadv.1601542*).

Expert agreements and disagreements on induced seismicity by Enhanced Geothermal Systems

Evelina Trutnevyte[1], Ines L. Azevedo[2]

1 ETH Zurich, Department of Environmental Systems Science, Switzerland, tevelina@ethz.ch; **2** Carnegie Mellon University, Department of Engineering and Public Policy, United States of America

Induced seismicity is a concern for multiple geoenergy applications, including low-carbon Enhanced Geothermal Systems (EGS). With only a handful of EGS worldwide, empirical evidence is sparse and epistemic uncertainties are ubiquitous. We present results of an international expert elicitation (N=14) on EGS induced seismicity hazard and risk. A state-of-the-art expert elicitation method is used: it combines technical analysis with behavioral science-informed techniques to minimize subjectivity.

Using a hypothetical scenario of an EGS plant and its geological context, we show that expert best-guess estimates of annualized exceedance probabilities of a M≥3 event range from 0.2% to 95% during reservoir stimulation and 0.2% to 100% during operation. Most experts believe that M≥3 event has less-than-even annualized chance during both stimulation and operation. Best-guess annualized exceedance probabilities of M≥5 event span from 0.002% to 2% during stimulation and 0.003% to 3% during operation. Assuming that tectonic M7 events could occur, some experts do not exclude induced (triggered) events of up to M6 or M7 too.

If induced M=3 event happens at 5 km depth beneath a town with 10 thousand inhabitants, most experts estimate 50% probability that the loss is contained within 0.5 million USD without any injuries or fatalities. In case of induced M=5 event, there is 50% chance that the loss is below 50 million USD with the most-likely outcome of 50 injuries and 1 or no fatality.

As we observe vast diversity in quantitative expert judgements and underlying mental models, we conclude with the needs for future research and improvements of induced seismicity assessment and management processes.

Switzerland's support for geothermal energy

Gunter Siddiqi

Swiss Federal Office of Energy, 3003 Berne Switzerland

The implementation of Switzerland's energy strategy 2050 has recently achieved an important milestone with Swiss Parliament having enacted a completely revised Energy Act and associated with a partially revised CO_2-Act. Both acts contain major new policy initiatives in support of geothermal energy development, both for direct use and for power generation.

The implementation rules have been specified in subordinate ordinances to both acts. Among other rules, geothermal power project developers wishing to benefit from grants for prospecting and exploration or from geothermal guarantees have to provide evidence for appropriate and risk-based hazards and effects management processes, hazard operability studies as well as the provision of fit-for-purpose risk management measures.

Similar rules apply for project developers wishing to benefit from financial support measures for projects that aim for direct use of geothermal energy to offset CO_2-emissions from alternate fuels used for heating.

Special attention will be given to hazards and risks in connection to induced seismicity.

Abstracts Posters, Part I

Session 1 and 2

Case Studies

Characterization of near surface effects by V_s estimation using a combined approach and waveform modelling in the area of the natural gas fields in Northern Germany.

Moritz Fehr[1,2], Simon Kremers[2], Ralf Fritschen[2]

1 Ruhr-University Bochum, Institute of Geology, Mineralogy and Geophysics, Germany, moritz.fehr@ruhr-uni.de; **2** DMT GmbH & Co. KG, Germany;

In recent years, several seismic events occurred in the apparently aseismic region of Northern Germany. A large amount of these events revealed a spatial clustering in the proximity of natural gas fields. Since some of these events could be felt at the surface an evaluation of the influences of seismic waves especially the effects of ground motion on the surface is required. The events were recorded with a sparse network of surface stations that does not clearly cover the whole affected area. It cannot be ruled out that site effects can cause high amplifications of the surface vibrations. For one seismic event damages have been reported although the recorded vibrations were below any damage threshold. Therefore the characterization of site effects due to local underground variations (V_s and layer thickness) is of paramount importance for hazard assessment. The local soil conditions have to be examined to detect areas where vibrations could be amplified. This study focuses on the estimation of 1D shear wave velocity profiles at three test sites by using a combined approach of small aperture 2D array ambient noise and small scaled active 1D measurements. The commonly used high-resolution frequency-wavenumber method (HRFK) was applied to the data, various array sizes and the active measurement have jointly allowed obtaining phase velocity dispersion curves covering a wide frequency range. The inversion has provided average S-Wave velocity profiles down to depths of 100 – 250 m. A comparison with available borehole data has shown an overall good correlation.

In addition, a parameter study was conducted to investigate the influences of simple shallow sediment underground structure models by using waveform modelling. The modelling of various layer thicknesses with typical soil parameters of Northern Germany has gained a catalogue of amplifying factors depending on signal frequency.

It was demonstrated that the combined approach represents a promising tool of the determination of near surface 1D shear wave velocity profiles. The catalogue allows to quickly identify regions with high amplification from the geological surface map. The measurements can be used to verify the local soil conditions or map regions, where the near surface geology is unknown. Finally these findings can lead to a better understanding of near surface effects and hence give the opportunity to improve hazard assessment in the area of natural gas fields of Northern Germany.

2016 Hydraulic Fracture Induced Earthquakes in Ohio

Paul A. Friberg[1]

1 Instrumental Software Technologies Inc., Saratoga Springs, New York 12866, P.Friberg@isti.com

In the past three years the oil and gas industry's production activity in the Utica shale play in Ohio has induced over 6 sequences of positive magnitude earthquakes. Some have been as large as magnitude 3.0 and a couple of earthquakes were felt (Friberg et al, 2014; Skoumal et al, 2014). Case studies in hydraulic fracture induced seismicity are important for understanding both the causation and for operators and regulators to under take proactive measures to prevent larger earthquakes. In August of 2016, a series of small earthquakes, magnitude 1.0 to 2.0, were triggered in Guernsey County Ohio that were tied to hydraulic fracture stimulations on several wells that were being zipper fracked at the time. A second sequence was observed during November of 2016 in Harrison County, to the east of three prior induced sequences. The November sequence resulted in two ML 2.5 earthquakes and was preceded by many smaller earthquakes. The zipper style hydraulic fracture completion operations on wells above the location of the November earthquakes were all coincident in time with both the smaller and larger earthquakes. The location of the events and differences in b-value measurements indicate that the Harrison County sequence was on an extension of an East-West oriented strike-slip fault system, documented by the prior sequences (Friberg et al, 2014; Friberg et al, 2016).

A template-matching algorithm was applied to the largest earthquakes in the August and November sequences and a number of smaller earthquakes were observed that preceded the largest event in the sequence. Each of these template detections was coincident with hydraulic fracture stages being stimulated at the time. There were no earthquakes in this area prior to well completion operations, and following a temporary shut-in of the wells implicated in the August sequence, the earthquake activity ceased. Changes in the completion operations in the November sequence also effected later events. We will present the results from the analysis of these two sequences of hydraulic fracture induced earthquakes and how changes in the stimulation process affected the earthquakes during further stages.

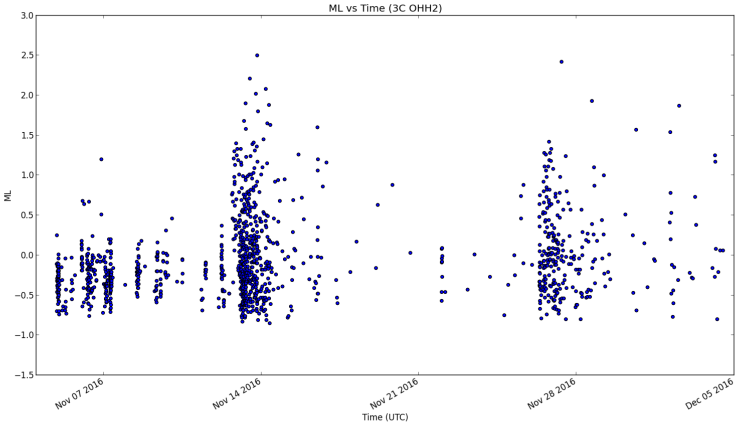

1200 template-matching earthquake detections determined with a single three-component station using three candidate templates against a 12X Median Absolute Deviation threshold.

Induced Seismicity Protocol for the First Enhanced Geothermal Systems Project in Pohang, Korea

Kwang-Il Kim[1], Ki-Bok Min[1], Kwang-Yeom Kim[2], Jae-Won Choi[3], Kern-Shin Yoon[3], Woon Sang Yoon[3], Byungjoon Yoon[4], Tae Jong Lee[4] and Yoonho Song[4]

1 Seoul National University, Korea, kbmin@snu.ac.kr; **2** Korea Institute of Civil Engineering and Building Technology, Korea; **3** NexGeo Corporation, Korea; **4** Korea Institute of Geoscience and Mineral Resources, Korea

Induced microseismicity has been regarded as a key component for the first EGS project initiated in Pohang, Korea which started in 2010. A regional case study of geothermal energy development in South Korea focusing on the comprehensive protocol addressing induced microseismicity is presented in this study. The protocol largely follows the seven steps suggested by the Department of Energy in United States with site specific adjustment and improvement as necessary. Site selection procedure, outreach program, establishment of local seismic network, and methodology in establishing traffic light system are introduced together with analysis of induced microseismicity from the first hydraulic stimulation campaign. An estimated equation for blasting vibration was converted to an equation relating PGV (Peak Ground Velocity) to magnitude by using conversion equations between the amount of charge, radiated energy and magnitude. The site specific traffic light system was suggested based on the PGV-magnitude relating equation whose site specific parameters was determined by natural earthquake having occurred within 50km from Pohang EGS site. The basic frame of the traffic light system referred to the that used for the Basel EGS project. The traffic light system was applied to the first hydraulic stimulation operated in January and February of 2016, and calibrated with surface detected induced microseismicity (Fig. 1).

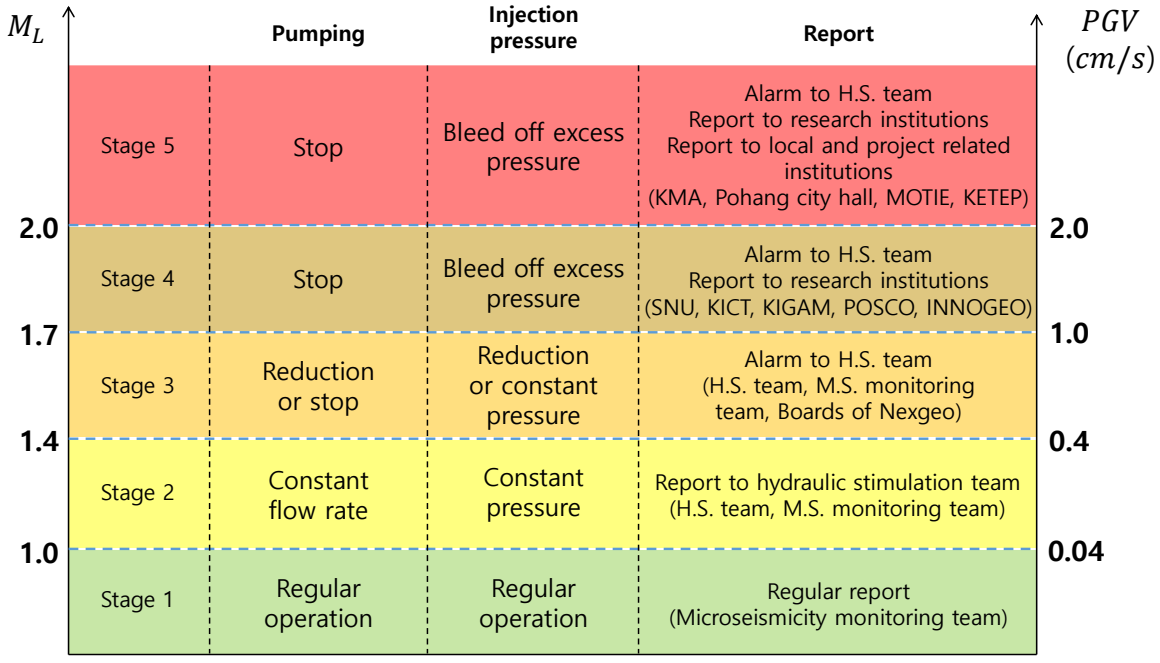

Fig. 1 The traffic light system for Pohang EGS project

The effect of induced earthquakes on buried water pipelines. A case study in Groningen, Netherlands.

Boris Kreike[1], Giuliana Scuderi[1],

1 HZ University of Applied Sciences, Netherlands, B.kreike@hotmail.com

Since 1963, in the province of Groningen, Netherlands, natural gas has been extracted at a depth of 3km from a porous sandstone layer. Due to the extraction, this sandstone layer has experienced a pressure drop from 350 to 150 bars, while the pressure due to the above soil layers leads to a rise in tension in the ground, finally resulting in induced earthquakes.

In the Netherlands, infrastructural systems have not been designed to bear seismic loads, due to the fact that earthquakes did not occur as frequent and strong as nowadays. Nevertheless, induced earthquakes in Groningen might have caused already several damages to visible infrastructure. In addition, the Netherlands is located for a substantial part below sea level: buried pipelines are crossing dikes that protect the hinterland from the sea and rivers. It is still uncertain to what extend these induced earthquakes have and will damage existing pipes, with all consequences that entails such as ensuring continuity of water transportation. In addition to this, water loss during transportation through pipes, could go unnoticed when being damaged. As result seepage could weaken the dike body that protects the hinterland. It is of high importance to ensure water availability to people as protecting them from water.

The presented research aims at understanding the effects of induced earthquakes through a case study, where the focus is on the impact of temporary soil movement on a steel continuous buried water pipe. The case study applies Newmark's theory to simplify the relation for the analysis of ground motion according to wave propagation effects. Desk research studies and existing numerical simulations have indicated that the inertia forces arising from the interaction between the pipe and the soil are much smaller than the forces induced by permanent soil deformation. This preliminary result allows to reduce the soil-pipeline interaction problem to a static problem, where the pipeline is deformed by the passage of a displacement wave, without considering dynamic effects.

Within this case study, the soil motion is represented by a single sinusoidal wave, whereby the amplitude of the sinusoidal wave is the maximum ground deformation. In order to take into account, the worst scenario, the particle motion is implemented along the pipeline axis. These forces have been studied using the finite element program Pipeline Engineering for Windows (Ple4Win). Firstly, the pipeline, including its material properties and its initial stresses were modelled in the program, in order to identify the location of the high stress parts along its axis. Secondly, a wave in direction of the pipeline axis was implemented as a vertical soil subsidence. The initial stress of the pipeline has been compared with the additional stress during an earthquake event. The results show that the additional stress caused by seismic loading effects on the pipe in operation was smaller than when the pipeline is empty. However, the total stresses on the pipeline in operation were higher, thus decisive in this case. The stress increases significantly when a pipeline is in operation, with as result that the total stress is higher. Calculations of soil parameters have been performed in this case study for the drained situation

The preliminary results of this research indicate that temporary soil movement in Groningen has no significant impact on the investigated pipeline case study. However, future research into the effect of earthquakes on appurtenances as on dikes next to pipelines and other constructions connected to pipelines are necessary. Due to the fact these objects could damage the pipeline during an earthquake indirectly.

On-going seismic monitoring of the Rittershoffen and the Soultz EGS projects (Alsace, France)

Vincent Maurer[1], Nicolas Cuenot[2], Alexandre Richard[1], Marc Grunberg[3]

1 ÉS-Géothermie, France, vincent.maurer@es.fr; **2** GEIE "Exploitation Minière de la Chaleur", France; **3** Université de Strasbourg, EOST, France

The scientific pilot power plant at Soultz-sous-Forêts, established in a deep fractured granitic massif, has resulted in the development of the EGS (Enhanced Geothermal System) concept and has provided the international scientific community with a unique high quality data set with no equivalence anywhere in the world. After a complete renovation of the facilities, the plant has been exploiting a geothermal brine at 150-160°C with a flowrate of about 30 l/s to produce a net power of about 1.4 MWe since the beginning of July 2016. Currently the brine is pumped out of GPK-2 and reinjected into GPK-3.

The recent geothermal project located at Rittershoffen, 6 km east of Soultz-sous-Forêts, in Northern Alsace, exploits a geothermal brine trapped in the fractured hard rocks. This geothermal project is designed to produce 24 MWth (170°C, 70 l/s) which is delivered to a bio-refinery located 15 km away. The exploitation of the geothermal plant started end of May 2016. Two deep wells have been drilled between 2012 and 2014 to 2500 m TVD (True Vertical Depth) for targeting local normal-faults located close to the interface between the clastic Triassic sediments and the top crystalline basement. Due to a poor initial injectivity index, the first well was developed by using various thermo-mechanical and chemical treatments. The results were positive, since the initial well injectivity index was multiplied by a factor of five. The second well was good enough hydraulically after drilling operation and thus, it was not necessary to enhance its natural permeability.

A seismic network has been deployed in order to monitor the induced seismic activity during drilling, reservoir development, and exploitation phases. Thus, before, during and after drilling operations, induced seismicity was continuously monitored by a surface seismological network. In order to detect any rise of micro-seismicity induced by the geothermal operation, the mining authorities required the deployment of a permanent seismic network, composed of 5 surface stations. Since 2012, the micro-seismicity activity of both Rittershoffen and Soultz geothermal projects has been monitored by a permanent seismic network composed of 12 surface short-period stations and by temporary surface networks (see Fig.1).

On the Rittershoffen site, in December 2015, the down-hole pump was installed at depth in the production well, GRT-2, and end of in May 2016 an almost continuous production and re-injection loop was performed. As low magnitude seismic events are occasionally associated with deep circulations of such projects, the micro-seismic activity has been carefully monitored in real–time since the beginning of the production. Since then and until November 2016, 73 induced low magnitude earthquakes were detected (Ml_{max} = 1.1), all located in the vicinity of the downhole section of the injection well GRT-1.

On the Soultz site, after the dismantling of the previous facilities in 2015, a new geothermal loop and a new ORC unit have been built since the beginning of 2016. The new power plant was commissioned in July 2016 and has been running successfully since then. After 5 months of almost continuous operation, no induced seismicity was detected, probably because of the low reinjection pressure in the GPK-3 well.

The induced seismicity occurred recently in Rittershoffen and the observations made in the past in Soultz-sous-Forêts highlight the need to continue the seismic monitoring, even during the exploitation phase of power plants, which is now explicitly required by the French mining authorities for getting the exploitation license.

Microseismic monitoring of fault re-activation during hydraulic fracturing

James P. Verdon[1], J-Michael Kendall[1], Max Werner[1]

1 University of Bristol, School of Earth Sciences, U.K., James.Verdon@bristol.ac.uk

Hydraulic fracturing in North America has produced a number of cases of induced seismicity, with the largest events having magnitudes M_L > 4. Unfortunately, in many such cases, the nearest seismic monitoring stations have been some distance from the site, limiting the extent to which we can learn about the processes that cause fault re-activation.

In this paper we present 2 case studies from Devonian shales in North America where pre-existing faults were re-activated during multi-well hydraulic stimulation at approximately 2km depth. At these sites, downhole geophone arrays had been deployed to monitor microseismic activity during stimulation. Due to the high sensitivity of these arrays, events with magnitudes as low as -3 were detected and located, providing robust, world-class microseismic datasets with over 100,000 microseismic events detected and located during each of these two operations. The faults in these case studies do not pose any risk to the public with respect to aquifer proximity or the possibility of generating large magnitude events. However, they allow us to examine mechanisms of fault re-activation in greater detail than many past case studies.

The re-activation of pre-existing faults is apparent upon examination of the microseismic data, including (i) the locations of events, which show planar features extending significant distances from the injection points (as shown in Fig. 1); (ii) from the sizes of events, which become far larger than is typically the case for events during normal hydraulic fracture propagation (in this case M_{MAX} = 1.3); and (iii) from the Gutenberg-Richter *b* value of the frequency-magnitude distributions, which was higher during most stages, but dropped to $b \approx 1$ for stages where faults were reactivated.

We use these datasets to investigate the processes that generate hydraulic fracturing-induced seismicity. We find that stages that reactivate faults correlate with areas of increased faulting as imaged by 3D reflection seismic data. In addition, where faults are reactivated, events can propagate hundreds of meters away from the stimulated zone (Fig 1), and the largest events are often found some distance from the stimulation zone. However, event loci in such cases reveal fault planes that in every case run through or very close to the perforations and stimulated region of that stage. Where faults and stimulated zones do not intersect, the faults are not re-activated. This indicates that poroelastic effects such as stress and/or pore pressure transfer through the rock frame at greater distances are not sufficient to re-activate faults.

We examine Mohr-Coulomb stress changes associated with fault re-activation. We find that stress sources (dilation and seismic slip) near the injection point generate insignificant Coulomb stress changes on faults. However, stress sources further from the injection point and at later times generate significant and positive stress changes. This indicates that it is injection of pressurized stimulation fluid into a fault that initiates rupture, rather than stress transfer from initial seismic events. However, once a fault is re-activated the associated Mohr-Coulomb stress changes can promote further seismic activity.

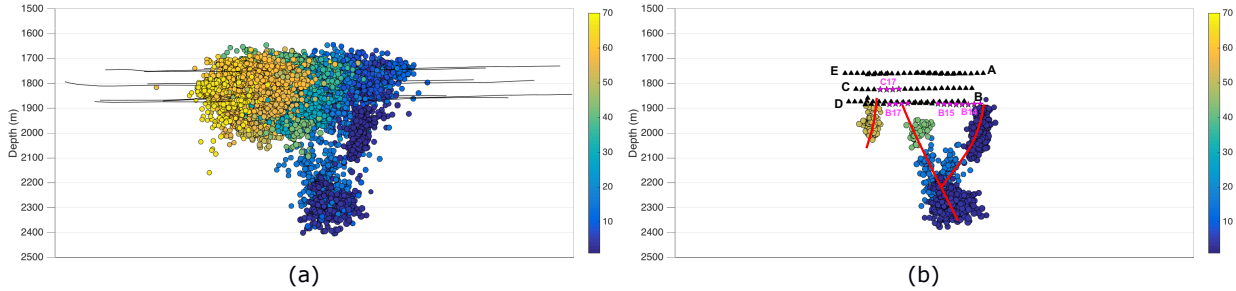

Fig. 1 Cross-section showing a subset of microseismic events detected during hydraulic fracturing. Events are coloured by stage number. In (a) we show all events recorded, while in (b) we show only events that occur in clusters with low *b* values, indicating fault re-activation.

Abstracts Posters, Part I

Session 3 and 4

Understanding and Modeling of Induced Seismicity

PROBABILISTIC QUANTIFICATION OF INDUCED SEISMIC NON-STRUCTURAL DAMAGE TO UNREINFORCED MASONRY

G. Abbiati[1], M. Didier[1], M. Broccardo[1], B. Stojadinović[1]

1 ETH Zurich, Department of Civil, Environmental and Geomatic Engineering (D-BAUG), Institute of Structural Engineering (IBK), Switzerland, abbiati@ibk.baug.ethz.ch, didier@ibk.baug.ethz.ch, broccardo@ibk.baug.ethz.ch, stojadinovic@ibk.baug.ethz.ch

Two deep geothermal energy projects have been recently conducted in Basel and St. Galen using hydraulic fracking and hydro-shearing. These operations induced numerous earthquakes, the strongest reaching magnitudes of 3.4 and 3.5, respectively. Hairline cracks were observed on plaster of near-by masonry buildings after one of the two projects, while no structural damage was observed in either project. The need for quantifying plaster cracking and other forms of non-structural damage on unreinforced masonry walls caused by induced ground motions, motivated the authors to develop fatigue tests, which were recently conducted at ETH Zürich.

In greater detail, ten plastered 1.20m x 1.20m x 0.15m unreinforced masonry wall specimens were tested in a cantilever configuration under constant gravity load by applying cyclic horizontal displacement sequences at constant amplitude. A previous testing campaign based on incremental displacement load sequences and small number of cycles revealed that cosmetics cracks occur above 2mm of horizontal displacement. Therefore, three 100-cycle displacement sequences of 3mm, 5mm and 7mm amplitude were selected to assess low-cycle fatigue behavior of walls.

In order to quantify plaster damage, crack length per unit area and average crack width were measured via Digital Image Correlation (DIC). Finally, a low-cycle fatigue damage model based on Gaussian Process (GP) was calibrated and implemented into a structural finite element code to support nonstructural fragility analyses.

Main results of this study are presented and discussed.

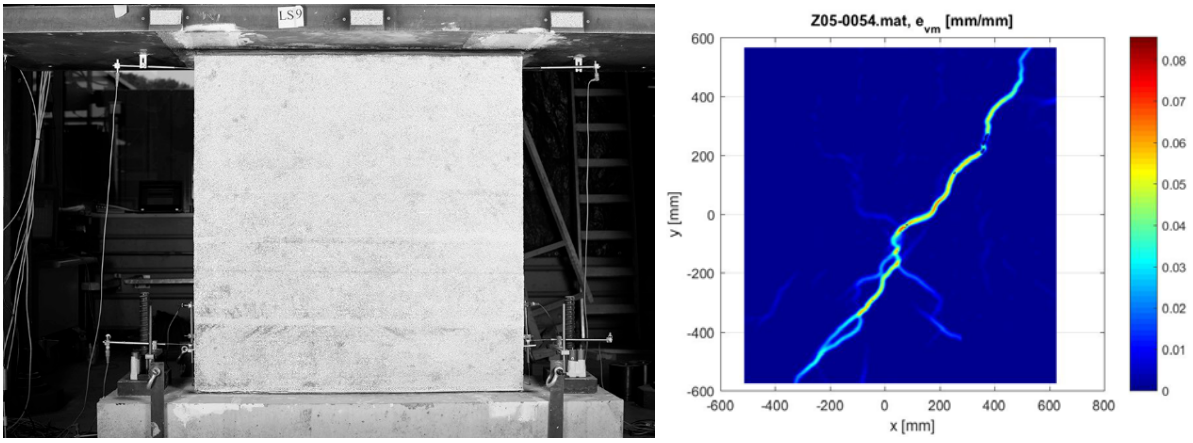

a **b**

Fig. 1 a) Experimental setup; b) example of Von Mises strain field measured via DIC

Optimization of operational strategies in producing gas fields mitigating induced seismic risk.

Alin Chitu[1], Olwijn Leeuwenburgh[1], Thibault Candela[1], Dirk Kraaijpoel[1], Brecht Wassing[1]

[1] TNO, The Netherlands, dirk.kraaijpoel@tno.nl

The extraction of hydrocarbons from the subsurface is associated with the risk of induced seismicity. Pore pressure changes caused by the production of gas from reservoir rocks result in reservoir compaction, stress changes on faults, potential fault reactivation and related seismic activity. This seismic activity is expected to be affected by the amount of pressure change, the spatial distribution of the pressure changes relative to the distribution of the faults and the rate at which the pressure changes occur. One of the options to mitigate seismicity in the field during ongoing depletion is to reduce production in areas of high seismicity rates and/or to maintain pressures by local injection. Therefore, seismic activity can potentially be reduced by optimizing the production strategy of a field.

We have developed a workflow to find optimized production strategies that takes into account the risk of induced seismicity. The seismic risk can have two distinct roles. First, from the perspective of safety, regulations usually determine a maximum acceptable (seismic) risk level, leading to a constrained optimization. Second, seismic risk may be regarded as an operational or economical factor, by quantifying the (expected) cost of damage repairs and/or mitigation measures. These costs may then be incorporated in the net present value of the project, or they can be treated separately as a second objective to be minimized in a multi-objective optimization. In both cases the calculation of the seismic risk needs to be quantified in terms of operational production parameters. In the approach that will be presented, we use a seismological model that relates reservoir strain, differential strain and strain rate (i.e. cumulative compaction and compaction rates) to the rate of seismicity. Other, more advanced types of seismological models, for example based on stress developments in the reservoir, can also be incorporated.

We have implemented an optimization scheme based on approximate gradients, that is flexible, allows for many opererational parameters, and can account for all kinds of uncertainty. The optimization workflow is applied to a gas field model that is inspired by an existing gas field in the Netherlands. First we discuss the calibration of the parameters of the seismic risk model. The performance of the optimization is subsequently demonstrated in a series of experiments in which we constrain total production or let the total production be determined during the optimization by balancing with the objective to minimize seismic risk. The results of these experiments demonstrate the potential for model-based reservoir management workflows to contribute to safe production of hydrocarbon resources.

Numerical modeling of injection induced shear failure in fractured reservoir using extended finite volume method

Rajdeep Deb[1], Patrick Jenny[1]

1 Institute of Fluid Dynamics, ETH Zurich, Switzerland, debr@ethz.ch;

A numerical modeling framework to simulate shear failure in fractured reservoir is developed using a finite volume method. A hierarchical fracture representation is employed to solve for fluid flow and shear failure in the fractured reservoir without refining the grids around fractures. Shear failure along the fracture manifolds is resolved by discontinuous basis function. The Coulumb friction law is applied to describe the failure criterion. Further, in order to obtain the fluid injection induced shear failure in a grid and timestep size independent manner, the choice of suitable timestep size depending on the grid resolution has been formulated. This timestep size scales with the square of the fracture segment size, which strongly affects the computational complexity as the grids gets refined. An alternate approach based on Prakash and Clifton friction law with a flow dependent timescale is proposed. This timescale models the shear strength relaxation due to decreasing compressive stress on the fracture manifold following the fluid injection. This modeling approach replaces the grid dependent timestep size in the Coulumb friction law by a timescale parameter.

The numerical modeling framework is used to study injection induced seismicity in single and multi fracture domains. The moment magnitude is obtained, which follows the Guttenberg-Richter law. With these testcases it has been demonstrated that the b-value of the moment magnitude becomes grid and timestep size independent.

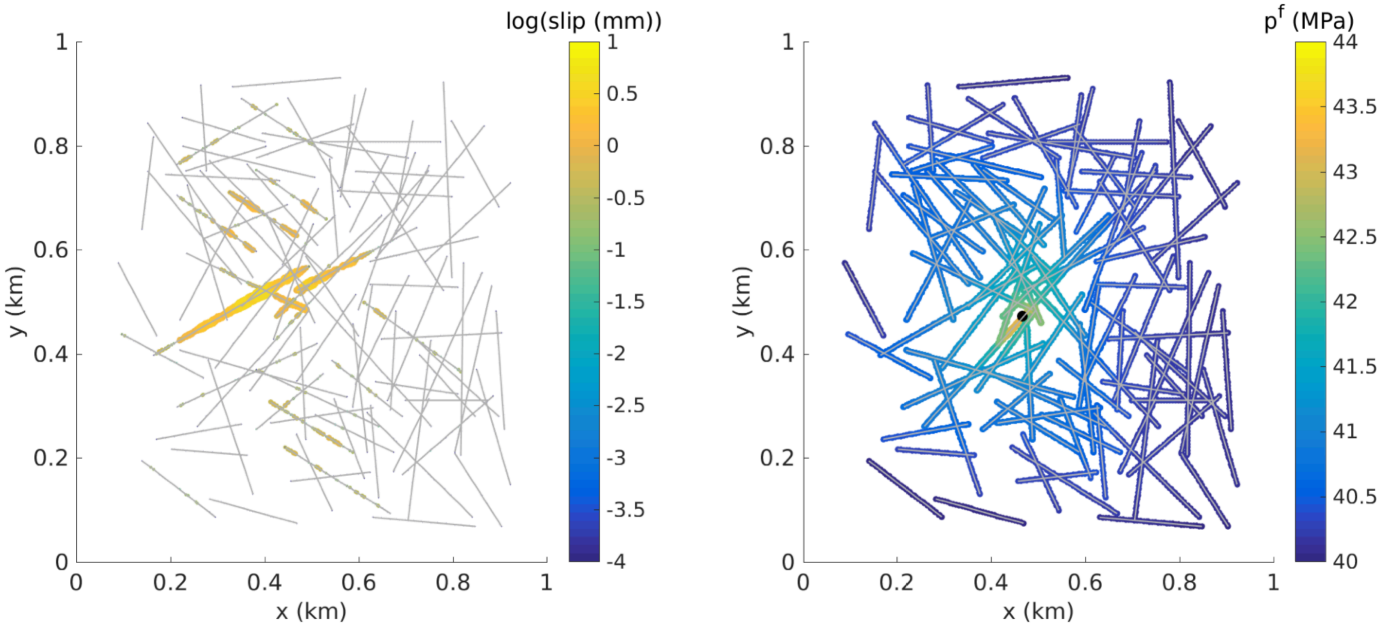

Fig. 1 The slip (left figure) and the pressure (right figure) solutions induced by fluid injection in a stochastically generated fractured domain.

Thermo-Hydro-Mechanic-Seismicity Simulation of Enhanced Geothermal Systems via an Adaptive Hybrid Numerical Method

Mohammadreza Jalali[1], Dimitrios Karvounis[2]

1 ETH Zurich, Sonneggstrasse 5, 8092, Zurich, Switzerland, mohammadreza.jalali@erdw.ethz.ch; **2** Swiss Seismological Service – ETH Zurich, Sonneggstrasse 5, 8092, Zurich, Switzerland

Presence of natural and induced fractures play a crucial role in different disciplines, including hydrogeology, oil and gas industry, waste disposal and geothermal industry, as these discontinuites introduce lithological heterogeneity as well as fabric complexity to the host rock. An adaptive hybrid numerical model - iterative coupling of finite volume method (pressure, temperature) with displacement discontinuity method (stress and displacement) - is implemented in this study to simulate thermo-hydro-mechanic-seismicity (THMS) coupled behavior of a host crystalline rock with pre-existing fractures. Seismic characteristics of the model consists of two approaches, i.e. deterministic calculation of the seismic moment via calculation of slip area and magnitude for the discrete fractures and semi-stochastic estimation of the seismic moment for the host rock, especially damaged zone around the fractures using seed model. Adaptivity of the time marching between flow and mechanical simulators significantly enhance the computational time of the simulation in comparison with fully coupled models. Such an approach aims to shed light on the effects which microseismicity has on the hydraulic and mechanical properties of important fractures and could perhaps be employed for multi-scale EGS simulations.

Modeling induced seismicity in abandoned enhanced geothermal systems

Dimitrios Karvounis[1], Antonio P. Rinaldi[1], Luca Urpi[1]

1 Swiss Seismological Service - ETH Zurich, Switzerland, karvounis@sed.ethz.ch;

Technologies like Enhanced Geothermal Systems (EGS) that require reservoir stimulation, rely their commerciality on safely generating several induced seismicity events between the wells. Although the technology is expected to mature with time and financially self sustainable EGS power plants will play an important role in the energy mix of Switzerland, the scenario of premature abandonment of a well or of an entire reservoir must be considered. This is the case with the abandoned stimulated reservoir in Basel. Both the local authorities and the EGS investors are facing the question when will eventually the rate of seismicity due to the performed stimulation be nullified.

Here, we employ our repository of modeling approaches for induced seismicity, ranging from finite element method to discrete fracture network and coupling finite-difference/finite-element method, to give a first answer on the importance of different hydraulic and mechanical mechanisms that could lead to further seismicity in the long run. Processes relevant to the reactivation of faults and fracture during the short-term fluid injection and in the closure phase are considered, assessing the long term importance regarding their potential for induced seismicity.

Adaptively Smoothed Seismicity Models of Injection-Induced Seismicity in Oklahoma and southern Kansas

Gareth Maver[1], Max Werner[1]

1 University of Bristol, School of Earth Sciences, Bristol, UK, max.werner@bristol.ac.uk

The seismic hazard associated with injection-induced earthquakes in northern Oklahoma and southern Kansas is a growing concern. Wastewater injections are the likely drivers of the sharp increase of seismicity. Here, we calibrate a smoothed seismicity model to earthquake catalogs and conduct tests to optimise retrospective forecasts. We use a method developed for California that estimates seismicity rates by smoothing past earthquakes using adaptive kernels in space and time (Helmstetter and Werner, 2012). Retrospective likelihood testing indicates that the probability gain per earthquake for the forecast model is highest when using the most recent year of seismic data and including small $M \geq 2.5$ events to forecast larger events. The forecast model achieves a probability gain of 7.7 compared to 2.75 for the forecast component of the 2016 USGS model by Moschetti et al. (2016) at identical model magnitude and catalogue choices. This encouraging performance suggests that the adaptive kernel smoothing method is a potential alternative to the fixed-bandwidth smoothing method currently used by the USGS. We also identify optimal look-back periods for 6-month and 1-year forecast (see Figure 1). A one year calibration period generates the greatest probability gains. The results suggest that smoothed seismicity models provide significant predictive skill despite the non-stationary nature of induced seismicity.

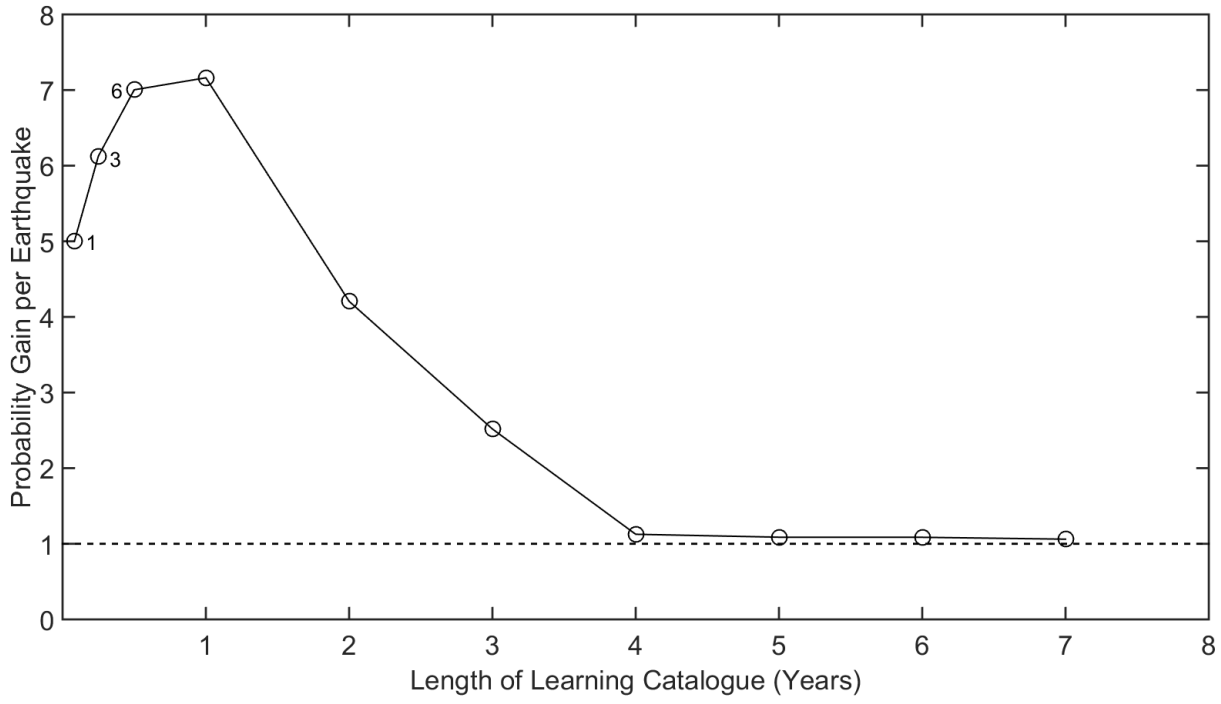

Figure 1: Probability gain per earthquake as a function of the length of the learning catalogue relative to a testing period of July 2015 – December 2015. The end of the learning period is June 2015. The number labels indicated the learning catalogue length in months (e.g. *6* = 6-month learning period beginning January 2015). The other model choices are M_d = 2.5, M_t = 3.5 and T = 20 days. The dashed line represents the probability gain of a uniform rate model.

Massively Parallel and Scalable Solvers for Simulating frictional Contact on Rough Surfaces

Cyrill von Planta[1], Alena Kopanicakova[1], Maria Nestola[1], Rolf Krause[1], Daniel Vogler[2], Patrick Zulian[1]

1 Università della Svizzera Italiana, Institute for Computational Science, Switzerland, cyrill.von.planta@usi.ch; **2** ETH Zurich, Geothermal Energy and Geofluids, Switzerland

Enhanced geothermal systems (EGS) are a promising option for renewable energy production, and are part of the energy strategy 2050 in Switzerland. Operating EGS projects are scarce, which can be partially attributed to the unsatisfactory understanding of hydraulic stimulation mechanisms. Hydraulic stimulations increase EGS fluid production rates by high-pressure fluid injection into a fracture, and subsequent fracture opening and permeability increase. The stimulation process is driven by the contact stress distribution in the fracture, where rough fracture surfaces cause a nonlinear relationship between fracture normal stress, contact area and fracture opening/closure. Unfortunately, current industry and academic reservoir simulation tools do not have the computational efficiency needed to simulate large complex systems.

In order to overcome this difficulty, we employ a parallel and scalable monotone multigrid method [1]. The monotone multigrid method is a substantial improvement compared to active set strategies and penalty methods. It is based on the direct minimization of the nonlinear energy functional and does not depend on a penalty parameter. It is of optimal complexity and and globally convergent. Our monotone multigrid method is implemented as a modification of a standard linear multigrid cycle and uses L^2-projections [2] with biorthogonal basis functions and Galerkin assembly for the setup of the coarse grid spaces. This allows application to arbitrarily complex geometries. For the pre- and postsmoothing steps we use a parallel nonlinear block Gauss-Seidel smoother. The main advantage of our method is that it extends multigrid efficiency from elliptic linear problems to a wider range of nonlinear problems. In the domain of geophysics suitable problems include apart from linear elasticity itself, multibody frictional contact of nonmatching rock surfaces and fracture growth using the phasefield approach.

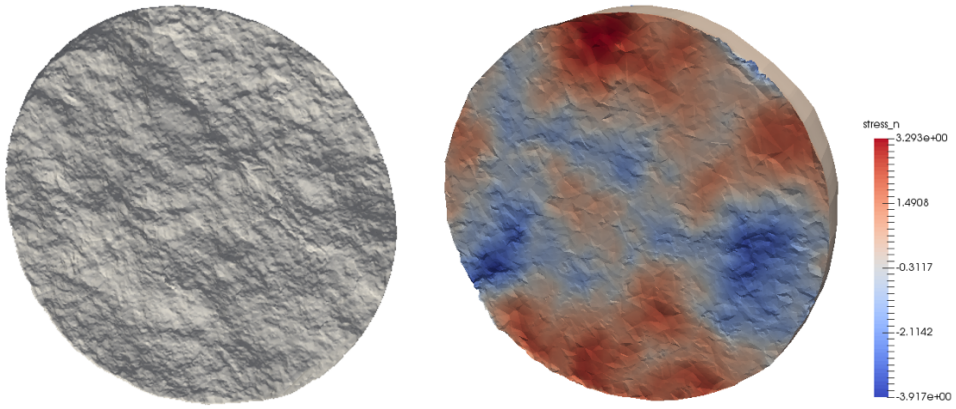

Fig. 1 Left: Surface scan from granitic sample of the Grimsel site (from [3]). Right: Contact stresses of rocksurface in contact simulated using the monotone multigrid method.

In this work we show how the monotone multigrid method can be applied to a three dimensional frictionless contact problem using an unstructured grid and weakly discretized contact conditions. We simulate a rock surface, taken from the SCCER experiments on the Grimsel [3], in contact. We show the weak and strong scaling of the monotone multigrid and give an outlook how the method can be adapted to solve multibody contact problems and fracture growth in phasefield models.

References:

[1] Dickopf, Krause 2009, Efficient simulation of multi-body contact problems on complex geometries: A flexible decomposition approach using constrained minimization, J. Numer. Meth.
[2] R. Krause, P. Zulian 2016, A Parallel Approach to the Variational Transfer of Discrete Fields between Arbitrarily Distributed Unstructured Finite Element Meshes, SIAM
[3] D. Vogler, R.R. Settgast, C. Annavarapu, C. Madonna, P. Bayer and F.Amann 2016, Experiments and Simulations of Fully Hydro-Mechanically coupled Response of Rough Fractures exposed to High Pressure Fluid Injection, JGR-Solid Earth (submitted)

Seismicity induced by seasonal variation of reservoir level: the case of Pertusillo lake, Val D'Agri (Italy)

Antonio P. Rinaldi[1], Flaminia Catalli[2], Luca Urpi[1], Luigi Improta[3], Mauro Buttinelli[3]

1 Swiss Seismological Service, ETH Zurich , Switzerland, antoniopio.rinaldi@sed.ethz.ch; **2** Deutsches GeoForschung-Zentrum, GFZ – Potsdam, Germany; **3** Istituto Nazionale di Geofisica e Vulcanologia, Rome, Italy

Water level reservoir affects the underlying crust stress state through the poroelastic response to the weight of the water volume stored and by the consequent fluid movement.
The perturbation of crustal stress state has been associated in some cases with small to large seismic events, with maximum magnitudes up to 6.3, as recorded in the largest confirmed case of Reservoir-Induced Seismicity (RIS), that took place at the Konya reservoir in India.
The artificial lake of Pertusillo in Val d'Agri (Italy) is one of the known water reservoirs showing protracted seismic activity for several years after the initial filling in 1963. More than 800 small-magnitude events (ML <3; Mc=1.1) were located between 2001 and 2013 by a monitoring network of a local industry operator supplemented by permanent and temporary stations of the Istituto Nazionale di Geofisica e Vulcanologia. Hypocenters concentrate at a shallow depth (< 5 km) to the south of the lake. During the same period the reservoir water level fluctuated in average of tens of meters between summer and winter periods. The observed seismicity rate positively correlates with these seasonal oscillations.
In this work we present two modeling approaches aimed at understanding the seismicity that occurred at Pertusillo lake. The first approach accounts for green function solutions given for a homogeneous, porous-elastic half-space and considering the decoupled approximation when solving the governing partial differential equations (i.e. elastic stresses influence the pore pressure but not vice versa). Then the calculated effective stresses are used to compute seismicity rate changes through the rate-and-state nucleation model. The second approach employs forward numerical modeling (finite element) in order to properly understand the triggering processes and to discriminate between the undrained and the drained response. The 3-dimensional model presented here allows inclusion of heterogeneous elastic and hydraulic parameters. Stress and strain are calculated for a transient evolution of the water level, and the calculation allows to compute dCFS (change in Coulomb failure stress) and to identify promotion of failure on different planes at different time of reservoir activities.
On one side, the semi-analytical approach shows that the proposed model reproduces consistently the time behavior of seismicity and its positive correlation to the water level fluctuations; it allows also for understanding the relative importance of the driving forces. However, our approach is a generalization of the problem of reservoir-induced earthquakes because we are not considering information of the crustal structure in the study area, such as for example the presence of different layers with different physical characteristics. Discrepancies between forecasted and observed seismicity may suggest that some parameters of the modelling need a better fit and/or that the simplicity of some assumptions needs to be revised, allowing for a better understanding of the phenomena at play.
On the other side, the numerical modeling approach allows a more complete study of the properties and layering of the medium. The short-term undrained response strongly depends on the elastic properties and can be amplified in a heterogeneous layered elastic media, especially for a media being stiffer with increasing depth. The long-term response depends on the hydraulic properties and it can play a role even if the reservoir is hydraulically isolated from the underlying units. The calculated perturbation of stresses and pressure in space and time can be provided as an input to a statistical model to investigate the evolution of seismicity and the earthquake triggering potential for nearby fault system.

Potential for induced seismicity from the operation of a deep geological repository.

Luca Urpi[1], Antonio P. Rinaldi[1], Stefan Wiemer[1]

1 Swiss Seismological Service, ETH Zurich, Switzerland, luca.urpi@sed.ethz.ch

The geological storage of high-level radioactive waste has been evaluated to be the safest option in the long term by a number of nations, among them Switzerland. The challenge of understanding and predicting the behavior of the stored waste and the rock mass for the next hundresds of thousands of years obviously involves also seismological aspects. With this work, we present preliminary results on the assessment of thermoelastic stress and pressure changes on a failure plane, to evaluate if rupture takes place.

Recent numerical investigations supported by field scale experiment (performed with an electric heater) shows that the heat produced by the nuclear waste is affecting the rock mass not only by means of increase in temperature, but also by a strong pressurization that takes place in the first couple of thousands of years. We represented an idealized storage scenario with the coupled TOUGH2-FLAC solvers, where an elastoplastic fault modelled with the ubiquitous joints is embedded in an elastic material and the forcing imposed by the high-level waste is explicitly represented by imposing pressure and temperature curves derived from previous studies.

Numerical Simulations of Hydraulic Fracturing during Reservoir Stimulation at the Grimsel Test Site, Switzerland

D. Vogler[1], R.R. Settgast[2], C.S. Sherman[2], V.S. Gischig[1], R. Jalali[1], J. Doetsch[1], B. Valley[3], K.F. Evans[1], M.O. Saar[1], F. Amann[1]

1 ETH Swiss Federal Institute of Technology Zurich, Zurich, Switzerland, davogler@ethz.ch;

2 Lawrence Livermore National Laboratory, Livermore, USA; **3** University of Neuchatel, Neuchatel, Switzerland

In-situ hydraulic stimulation has been performed on the decameter scale in the Deep Underground rock Laboratory (DUG Lab) at the Grimsel Test Site (GTS), Switzerland. The test site consists of granodiorite with a low fracture density and has been well characterized. The GTS is chosen as it represents physical properties representative for crystalline basement where the development of deep enhanced geothermal systems are planned for the future. Conducted stimulation was performed in a number of boreholes, with 3-4 packer intervals in each borehole subjected to repeated stimulation. During each stimulation event, fluid injection pressure, injection flow rate and microseismic events were recorded amongst others.

Fully coupled 3D simulations have been performed with the LLNL's GEOS simulation framework. The methods applied in the simulation of the experiments address physical processes such as rock deformation/stress, LEFM fracture mechanics, fluid flow in the fracture and matrix, and the generation of micro-seismic events. This allows investigation in which we may estimate the distance of fracture penetration during the injection phase and correlate the simulated injection pressure with experimental data during injection, as well as post shut-in. Additionally, the extent of the fracture resulting from the numerical model are compared with the spatial distribution of the microseismic events recorded in the experiment.

Hydro-mechanical modelling of induced seismicity during the deep geothermal project in St. Gallen, Switzerland

Dominik Zbinden[1], Antonio Pio Rinaldi[1], Toni Kraft[1], Tobias Diehl[1], Stefan Wiemer[1]

1 ETH Zurich, Swiss Seismological Service, Switzerland, dominik.zbinden@sed.ethz.ch

The St. Gallen deep geothermal project in 2013 was the second geothermal project in Switzerland with the objective of power production after the Enhanced Geothermal System in Basel in 2006. In St. Gallen, the seismic risk was expected to be smaller than in Basel, since the hydrothermal resource was an aquifer at a depth of about 4 km, not expected to require permeability enhancement and associated hydroshearing of the rock. However, after an injectivity test and two acid stimulations, unexpected gas release from an unidentified source forced the operators to inject drilling mud into the well to fight the gas kick. Subsequently, several seismic events were induced, the largest one having an M_L 3.5, which was distinctly felt by the nearby living population. Even though the induced seismicity could not be handled properly, the community still strongly supported the geothermal project. The project was however halted because the target formation was not as permeable as required to deliver sufficient power. Still, controlling induced seismicity during deep geothermal projects is a key factor to successfully operate future geothermal projects. Hence, it is crucial to understand the physical relations of fluid injection, pressure and stress response at reservoir depth as well as associated induced seismicity. To date, these processes are yet not fully understood.

In this study, we aim at developing a hydro-mechanical model reproducing the main features of the induced seismic sequence at the St. Gallen geothermal site. Here, we present the conceptual model and preliminary results accounting for hydraulic and mechanical parameters from the geothermal well, geological information from a seismic survey conducted in the St. Gallen region, and actual fluid injection rates from the injectivity tests. In a future step, we are going to use this model to simulate the physical interaction of injected fluid, gas release, hydraulic response of the rock, and induced seismicity during the St. Gallen project. The results will then allow us to more accurately estimate the seismic hazard for future geothermal projects.

Abstracts Posters, Part I

Session 5

Scaled Experiments

Effect of pore pressure on earthquake dynamic rupture: insights from stick slip experiments on granite.

Mateo Acosta[1], François Passelègue[2], Alexandre Schubnel[3], Marie Violay[1]

1 LEMR, ENAC, École polytechnique fédérale de Lausanne (EPFL), Lausanne, CH ; mateo.acosta@epfl.ch; **2** School of Earth, Atmospheric and Environmental Sciences, University of Manchester, Manchester, UK; **3** Laboratoire de Géologie, Ecole Normale Supérieure de Paris, CNRS UMR8538, 24 rue Lhomond, 75005 Paris, FR.

Fluids play a crucial role in fault zone stability and in earthquake generation. Fluid injection induced earthquakes in geothermal reservoirs are direct evidence of the effect of fluid pressure on faults' mechanical behaviour. Here, we try to understand how fluid pressure affects: (1) fault strength, during earthquake nucleation, propagation and arrest; (2) the dynamic rupture. To this end, we conducted stick slip experiments in the laboratory, on thermally-treated, westerly granite samples. The saw-cut cylinders were solicited under triaxial loading ($\sigma1>\sigma2=\sigma3$) at identical effective confining pressures (Pceff=$\sigma3$'= Pc-Pp) for 3 different configurations: (1) Nominally DRY experiments at 70 MPa confining pressure and room humidity conditions, (2) water saturated (or WET) experiments at low pore pressures (Pc= 71 MPa and Pp= 1 MPa), and (3) WET experiments at high pore pressures near hydrostatic configuration (Pc=95 MPa, Pp=25MPa). The samples were instrumented with four strain gages recorded at high frequencies and one thermocouple located at 2 mm from the fault plane allowing the measurement of dynamic shear stress drops and temperature elevation near the artificial fault. Rupture initiation locations and rupture speeds were assessed during the experiments through an acoustic monitoring array. In total, around 100 stick slip events were recorded for these 3 configurations. Results showed: (1) Under DRY conditions peak static friction ranged from 0.80 to 0.87 resulting in large final slip (from 210 to 280 µm) and high static and dynamic stress drops (respectively from 20 to 40 MPa and from 80 to 95 MPa). Sliding is accompanied by frictional melting of the asperities. (2)Under low pore pressure conditions, peak static friction ranged from 0.60 to 0.72 resulting in shorter slip from 160 to 250 µm but larger dynamic shear stress drop (80 to 120 MPa) even though smaller static stress drops were recorded (from 12 to 40 MPa). Similarly to dry conditions, deformation is accompanied by frictional melting. Finally, under high pore pressure conditions, peak static friction ranged from 0.7 to 0.87. Both static and dynamic shear stress drops (respectively ranging from 3 to 20 MPa and from 17 to 40 MPa) were strongly reduced and were accompanied by short slip (from 30 to 100 µm). No evidence of melting was observed in this case. These results highlight the importance of pore pressure presence and level in the dynamic frictional behaviour of granitic rocks. High water pressure in fault zones strongly reduce dynamic weakening mechanisms, inhibiting flash melting of the asperities, and so, rupture propagation.

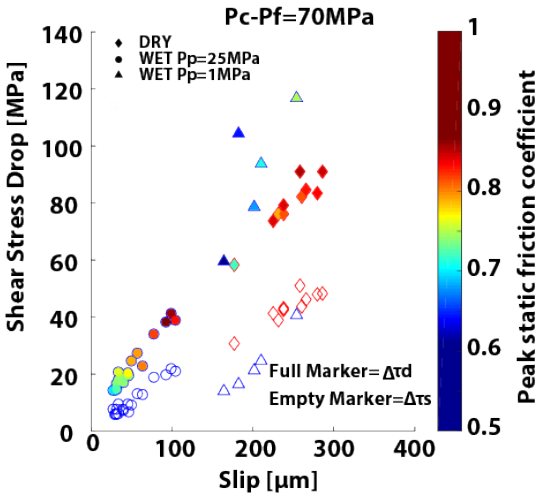

Fig. 1: Experimental data of Stick-slip events in Westerly Granite at 70 MPa effective confining pressure Pceff = Pc - Pp: [a.] Shear stress drop [MPa] VS Slip [mm]. Static shear stress drop presented in empty markers and dynamic shear stress drop presented in full markers.

Modelling of fluid injection into a frictional weakening dilatant fault

Federico Ciardo[1], Brice Lecampion[1]

1 EPFL Lausanne, Geo-Energy Laboratory – Gaznat Chair on Geo-Energy (GEL), Switzerland,
federico.ciardo@epfl.ch & brice.lecampion@epfl.ch

Shearing pre-exiting fractures/faults via fluid injection (hydraulic stimulation) is a mechanism that enhance the permeability in deep geothermal reservoirs (Enhanced Geothermal Systems), whose efficacy rely on the shear-induced dilation.

Locally elevated pore pressure associated with fluid injection leads to a reduction of the fault frictional strength (product of the local normal effective stress and the slip-weakening friction coefficient) which may fall below the background shear stress. As a result, a shear crack will start to propagate. Its propagation can be *ultimately stable* or *unstable*, depending on the ratio between the background (initial) shear stress τ^b and the ambient frictional strength as well as on the values of the overpressure. For small values of the initial shear stress (w.r.t the peak frictional strength of the fault) and moderate overpressure the fault exhibits an ultimately stable regime. The overpressure is just enough to activate the slip at the fault center. The subsequent shear crack propagates quasi-statically (stable) toward the initial point of instability; then a dynamic rupture occurs (see Figure 1 – red arrows). As soon as the residual friction is reached, it arrests and subsequently keeps growing quasi-statically. On the other hand, for large background shear stress (ultimately unstable regime), a fault can host either a dynamic instability (without arrest) or a nucleation of dynamic instability followed by an arrest and a re-nucleation of instability (τ^b/τ_p = 0.65 – see Figure 1). Larger nucleation time are therefore expected for stable faults, whereas larger dynamic ruptures are expected for ultimately unstable faults.

In this contribution, we investigate the effect of shear dilatancy on both stable and unstable faults. Dilatancy locally leads to a pore-pressure drop during high slip rates. As a consequence, the fault shear strength increase during dynamic events, leading to a stabilizing effect.

We formulate a 2D model of fluid injection in a shear dilatant fault exhibiting linear slip weakening friction. The model couples elastic deformation, shear weakening Coulomb friction with dilatancy and fluid flow along the fault. We develop a numerical scheme based on boundary element (displacement discontinuity method) for elastic deformation and a finite volume scheme for fluid flow. We verify our solver first on the non-dilatant case by comparing our results with the semi-analytical solution of Garagash & Germanovich, 2012 (see Figure 1). We then investigate the effect of shear-dilatancy and its feedback on the nucleation of dynamic rupture (especially for ultimately unstable faults).

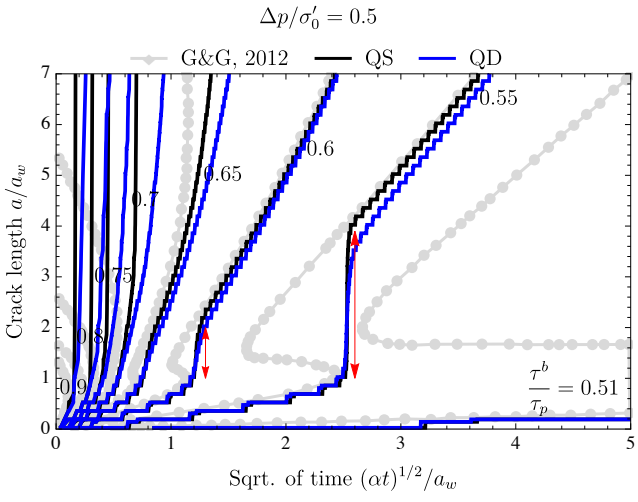

Fig. 1 Quasi-static (QS) and quasi-dynamic (QD) development of the normalized crack half-length under moderate constant overpressure for various values of the normalized fault background stress and a linear frictional weakening law (f_r/f_p=0.6) The marked lines correspond to the G&G's results (2012) for quasi-static crack propagation (benchmark).

Fluid driven fracture mechanics in highly anisotropic shale: a laboratory study with application to hydraulic fracturing

Stephan Gehne[1], Philip Benson[1], Mark Enfield[2], Nick Koor[1]

1 University of Portsmouth, Portsmouth, UK, stephan.gehne@port.ac.uk; **2** P.D.F. Limited, Ewelme, Wallingford, UK

The finding of considerable volumes of hydrocarbon resources within tight sedimentary rock formations in the UK led to focused attention on the fundamental fracture properties of low permeability rock types and hydraulic fracturing. Despite much research in these fields, there remains a scarcity of available experimental data concerning the fracture mechanics of fluid driven fracturing and the fracture properties of anisotropic, low permeability rock types.

In this study, hydraulic fracturing is simulated in a controlled laboratory environment to track fracture nucleation (location) and propagation (velocity) in space and time and assess how environmental factors and rock properties influence the fracture process and the developing fracture network.

Here we report data on employing fluid overpressure to generate a permeable network of micro tensile fractures in a highly anisotropic shale (~50% P-wave velocity anisotropy). Experiments are carried out in a triaxial deformation apparatus using cylindrical samples. The bedding planes are orientated either parallel or normal to the major principal stress direction (σ1). A newly developed technique, using a steel guide arrangement to direct pressurised fluid into a sealed section of an axially drilled conduit, allows the pore fluid to contact the rock directly and to initiate tensile fractures from the pre-defined zone inside the sample. Acoustic Emission location is used to record and map the nucleation and development of the micro-fracture network.

Indirect tensile strength measurements at atmospheric pressure show a high tensile strength anisotropy (~60%) of the shale. Depending on the relative bedding orientation within the stress field, we find that fluid induced fractures in the sample propagate in two of the three principal fracture orientations: Divider and Short-Transverse. The fracture progresses parallel to the bedding plane (Short-Transverse orientation) if the bedding plane is aligned (parallel) with the direction of σ1. Conversely, the crack plane develops perpendicular to the bedding plane, if the bedding plane is orientated normal to σ1. Fracture initiation pressures are higher in the Divider orientation (~24MPa) than in the Short-Transverse orientation (~14MPa) showing a tensile strength anisotropy (~42%) comparable to ambient tensile strength results. We then use X-Ray Computed Tomography (CT) 3D-images to evaluate the evolved fracture network in terms of fracture pattern, aperture and post-test water permeability. For both fracture orientations, very fine, axial fractures evolve over the entire length of the sample.

Test data from fluid driven fracturing experiments suggest that fracture pattern, fracture propagation trajectories and fracturing fluid pressure (initiation and propagation pressure) are predominantly controlled by the interaction between the anisotropic mechanical properties of the shale and the anisotropic stress environment. The orientation of inherent rock anisotropy relative to the principal stress directions seems to be the main control on fracture orientation and required fracturing pressure.

Insights into the seismic signature of gas-bursts, volcanic explosions and permeable gasflow under controlled laboratory conditions

Bettina Scheu[1], Alejandra Arciniega-Ceballos[2], Miguel Alatorre-Ibargüengoitia[3], Donald B. Dingwell[1]

1 Department für Geo- und Umweltwissenschaften, LMU München, Deutschland, b.scheu@lmu.de; **2** Instituto de Geofísica, UNAM Ciudad Universitaria, Coyoacán, Mexico; **3** Centro de Investigación en Gestión de Riesgos,Universidad de Ciencias y Artes de Chiapas, Tuxtla Gutiérrez, Mexico

We present laboratory experiments designed to investigate the seismic signature associated with volcanic and hydrothermal activity. Volcanic eruptions for instance generate different types of seismic signals in a wide frequency bandwidth; their source may involve brittle failure (of host rock and/or magma), fluid transport (volatiles and/or magma), bubble collapse, fluid depressurization, degassing or a combination of these processes. Several of these processes are also typical for seismicity induced by mining activity or geothermal exploration, especially of high enthalpy resources.

The experiments are conducted using shock-tube apparatus, where several high-pressure (HP) sections can be attached allowing for instance high-temperature or visible conditions of the sample inside (e.g. gas, ash, dry or liquid-saturated rocks). The physical mechanism consists of a slow pressurization of the HP section (by Argon gas) followed by its rapid decompression. The sample is ejected into a large low-pressure (LP) section from where it can be recovered for further analysis. Here we show results of experiments at room temperature under controlled pressure conditions from 4 to 20 MPa. Seismic signals were detected during the depressurization process using High Dynamic Piezo Film (HDPF) sensors (PDF, 0.001 - 10 G Hz analog bandwidth, low impedance), fixed and distributed along the HP section. In addition, dynamic pressure sensors record the pressure evolution within the HP section, high-speed cameras can be employed to monitor the events in the HP section as for instance sample fragmentation as well as the ejection of gas and particles into the LP section; all sensors and cameras are synchronized. The resonance of the empty apparatus was characterized in order to distinguish between the signals generated by depressurization of the system and the sample. Preliminary results of this experimental approach provide insights in the recognition and interpretation of seismic signals characteristics and physical properties of their associated source process.

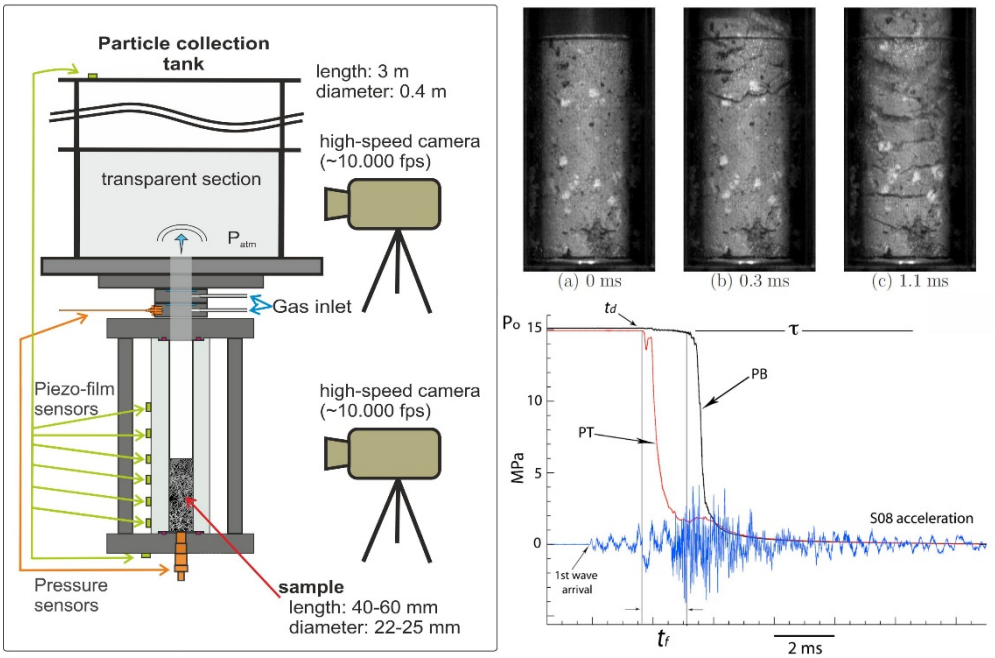

Fig. 1 Schematic experimental setup with sensors attached to transparent HP section (left); still frames showing a rock fragmenting (recorded at 10.000 fps) and signals recorded during such an event (right).

Towards Distributed Acoustic Sensing as a Viable Microseismic Monitoring Tool: Results from the Field

Matt Wilks[1], Andreas Wuestefeld[1], Volker Oye[1], Peter Thomas[2], Erling Kolltveit[2]

1 NORSAR, Gunnar Randers vei 15, 2007 Kjeller, Norway. matt@norsar.no;

2 Christian Michelsen Research AS, Fantoftvegen 38, 5072 Bergen, Norway.

Distributed Acoustic Sensing (DAS) has gained increasing attention in recent years as a highly cost-effective seismic monitoring technique of induced seismicity. DAS exploits Rayleigh backscattering of coherent laser radiation for probing the dynamic location of natural inhomogeneities in the glass structure of the fiber, which modulates with the impingement of seismic waves. In this scenario, the entire cable becomes the monitoring sensor and offers vast reaches, near-real time recording, low attenuation, easy installation and high sampling resolutions in otherwise challenging (i.e. regarding temperatures, pressures and chemistries) recording environments. These factors provide obvious advantages to more-conventional geophone sensing arrays.

Although dramatic improvements in optical fibre technology has led to an increasing number of experimental studies, field tests and research into the capabilities of DAS for geophysical applications, there remains significant challenges, including high noise-floors and directional insensitivity to 'broadside' incident waves. Despite this, the potential of DAS is of high interest to the fossil and renewable energy industries and to many other monitoring applications.

In this study we perform field tests using a DAS set-up provided by CMR to record man-made hammer blows in different recording environments. We vary the recording cable geometry and shot point locations to investigate the directional sensitivity of the set-up. We investigate the noise floor and signal to noise characteristics of the data and test different methods of coupling the cable to the ground. These field experiments are compared to synthetic cases, where we evaluate the capabilities of DAS monitoring for subsequent use.

We also examine routines for the large processing requirements of near-real time monitoring at high spatial and temporal sampling rates. Here we compare detection and location methods that may be utilized in the future.

Acknowledgement: This work was funded by the Norwegian Research Council, through the CLIMIT program, project 254748 "Distributed seismic monitoring for geological carbon sequestration"

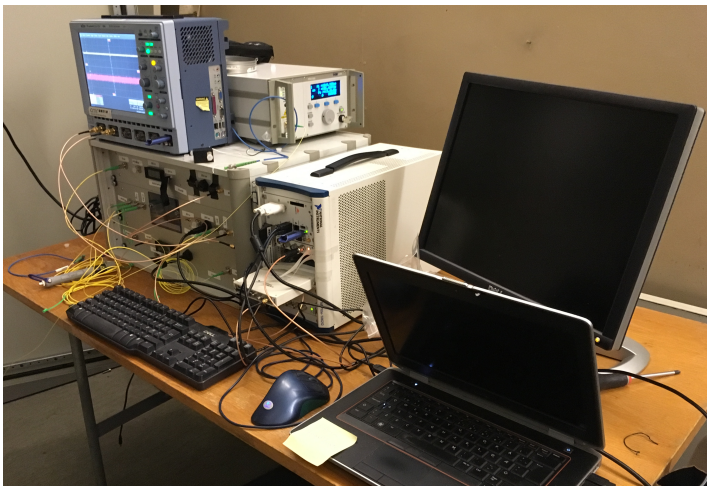

Fig. 1: DAS system used in the investigations (copyright CMR)

Abstracts Posters, Part I

Session 6 and 7

Monitoring and Analysis of Induced Seismicity

Characteristics of seismicity induced by gas production in Northern Germany

Monika Bischoff[1], Nicolai Gestermann[2], Thomas Plenefisch[2], Stefan Viola[1], Joachim Fritz[1]

1 State Authority of Mining, Energy and Geology (LBEG), Germany, monika.bischoff@lbeg.niedersachsen.de;
2 Federal Institute for Geosciences and Natural Resources (BGR), Germany

The Northern German Basin is a tectonic region of low natural seismicity. No damaging earthquake is known from historical archives. With instrumental recordings only few and relatively weak events were observed in the recent decades. The most seismically active part spans the region of gas production of about 400 km in east-west and about 70 km in north-south directions from the Dutch-German border to the Altmark region. The strongest events had local magnitudes (M_L) of 4.5 and 4.0. They occurred near Rotenburg in 2004 and near Soltau in 1977, respectively. These events were widely felt. Weaker events with magnitudes of about 3 are usually felt up to 15 km. Events below magnitude 1.8 are not felt. In total 75 seismic events with local magnitudes (M_L) between 0.5 and 4.5 have been observed since 1977.

The seismic events in the gas production region are classified as induced events due to the following reasons: 1) events cluster in the region of gas production whereas no seismicity is observed at larger distances in the surroundings with the same geologic and tectonic setting; 2) seismicity has only been observed after gas production had started, no seismic event was observed before; 3) for some, especially for the M_L>3 events in recent years, reliable hypocenters were determined at shallow depths correlating well with the gas reservoirs at depths of about 5 km.

Monitoring has significantly improved over time. Early events were recorded at very few stations at large distances. Therefore location uncertainties can easily exceed 10 km. The magnitude of completeness (M_C) is about 3.0. In the mid-nineties the German Regional Seismic Network (GRSN) was installed and the detection threshold was significantly lowered to about 2.0. Location uncertainties were still high due to the lack of local stations and inappropriate azimuthal coverage. First stations designed for gas field monitoring were installed after the Rotenburg event in 2004. The number of stations has been increasing since. Today 45 stations are operated by the industry and 10 stations by the Federal Institute for Geosciences and Natural Resources (BGR). Epicenters can be determined with high accuracies of about 3 km. Relatively bad signal-to-noise conditions as a result of thick sedimentary layers impede the further lowering of the detection capability for the whole region. Overall M_C 2.0 has been achieved. In addition, mini-arrays for detailed analysis of the eastern region have been operated by University Stuttgart since 2013.

Seismicity is mainly related to Rotliegend fields and Zechstein carbonates at depths between 3.5 and 5 km. With a total of only 75 events statistical analysis is very poor. Still, the seismic characteristics of the individual gas fields seem to vary. The vast majority of the fields does not show seismicity at all. The most events, i.e. 14 events in the magnitude (M_L) range between 0.5 and 3.1, occurred at the Völkersen field. Only small (M_L < 2.1) but rather regular events are observed at the Walsrode field. At the fields Söhlingen and Klosterseelte/Kirchseelte/Ortholz four of the nine largest events (M_L>2.9) occurred and besides very few aftershocks no smaller events have been recorded. For Völkersen a delay of 14 years between the start of production and the first seismic event (M_L>2) is observed. A significantly larger delay is observed for the Hengstlage field. Comparisons with production parameters show that no simple relations exist between seismicity and cumulative extracted gas volume, extraction rate and the total size of the field.

We will present an overview on the seismicity, including the spatial and temporal distributions with respect to gas production. We will discuss hydraulic fracturing, waste water disposal, pressure depletion and natural causes such as isostatic rebound effects or pure tectonic origin as possible causes of seismicity. We conclude that the most probable reason for seismicity at the natural gas fields in Northern Germany is pore pressure depletion resulting in the compaction of sediments, the increase of stresses at tectonic faults and their release in seismic events. Pure tectonic origin is being discussed for some events in the region of the gas fields located at larger depths of more than 20 km.

Differentiating Induced and Triggered Seismic Responses to Mining

Laura Brown[1], Marty Hudyma[2]

1 PhD Candidate, Laurentian University, Ontario, Canada, lg_brown@laurentian.ca; **2** Associate Professor, Laurentian University, Ontario, Canada

The seismic response to mining varies significantly throughout the mining environment. In some areas of the rock mass, the seismic response is relatively small and proportionate to mining activities. In other locations, the seismic response to mining is extreme and severe rock mass failure may occur. Responses are commonly identified as either induced or triggered. In general terms, an induced response can be attributed directly to rock mass failure from the creation of mining excavations. Induced seismicity typically occurs in close temporal and spatial proximity to mine blasting. A triggered response is primarily attributed to rock mass failure associated with significant geological features. Triggered seismicity is relatively time-independent and typically occurs distant to mine blasting.

Fig. 1 shows Magnitude-Time History charts for two seismic populations from the same deep Canadian mine. The induced seismic population (a) contains relatively few large seismic events. This indicates the seismic response is proportionate in terms of radiated seismic energy - indicative of an induced response. The influence of local development blasts is clearly reflected in "steps" throughout the cumulative number of events line, shown along the secondary y-axis. This local blasting influence is further evident in the significant decrease of events occurring during the mine shutdown period in the beginning of July (approximated by a red box).

The triggered seismic population (b) contains a significant quantity of large seismic events. This indicates the seismic response is disproportionate in terms of radiated seismic energy, particularly considering there is no blasting occurring in proximity to this population. Unlike the induced population, the influence of mine blasting is not evident in the cumulative number of events line. Changes in the slope of the line are not related to any discrete mining activities - indicative of triggered seismicity. The mine shutdown period has little influence on the seismic population, as the event rate increases in the absence of mine blasting in early July.

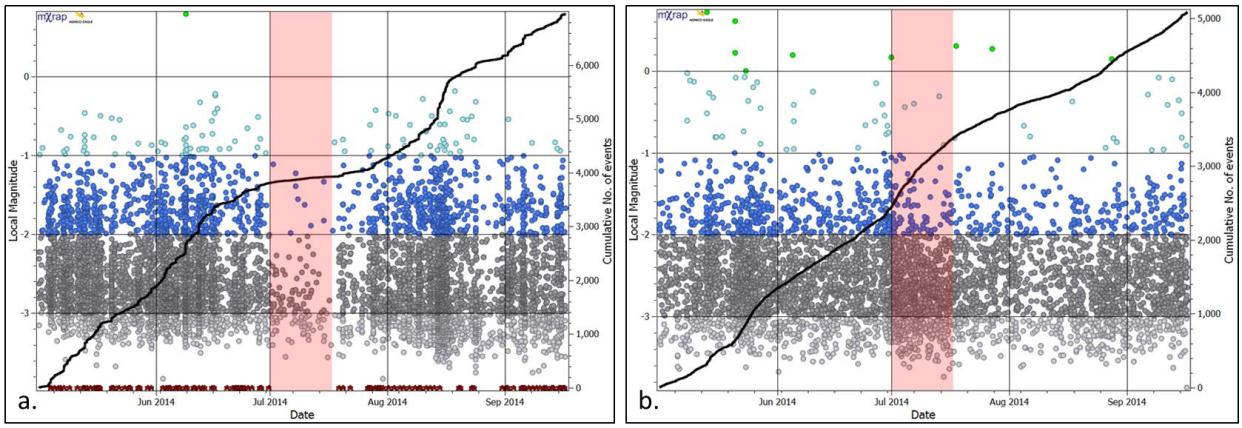

Fig. 1 Magnitude-Time History charts of an induced development seismic population (a) and a triggered deep footwall seismic population (b). Mine blasts contained within the population volume are denoted along the x-axis by red stars. A mine shutdown period is approximated by the red box.

Seismic source parameters such as time, apparent stress and energy, provide insight that can be useful in differentiating between induced and triggered seismicity. Various methodologies for differentiating between and characterizing the induced and triggered seismic response to mining will be presented. All examples will be provided from a single deep Canadian bulk mining operation.

Local Magnitude Scales and Traffic Light Schemes

Antony Butcher[1], Richard Luckett[2], & J-Michael Kendall[1]

1 School of Earth Sciences, University of Bristol, Wills Memorial Building, Queen's Road, Bristol BS8 1RJ, UK, antony.butcher@bristol.ac.uk; **2** British Geological Survey, Earthquake Seismology, The Lyell Centre, Edinburgh, EH14 4AP, UK

Subsurface activities that alter the state of stress of the ground are capable of triggering seismic activity on pre-existing faults. Within the United Kingdom (UK), the production of shale gas using hydraulic fracturing requires the use of a traffic light monitoring scheme to manage this risk. This scheme uses an amber warning set at a magnitude of ML = 0.0, and a red light at ML = 0.5, where injection must cease followed by a 24hr monitoring period. As the UK seismic network operates at a nominal detectability level of ML > 2, the installation of local seismic stations is critical for the operation of this scheme.

We demonstrate that significant discrepancies (up to a unit higher) occur between seismic events recorded on nearby stations (<5km) compared to those at greater distance. Data recorded near New Ollerton (NOL), UK, is used to consider the impact proximity has on magnitude estimates. Events occur as a result of coal mining within sedimentary layers, and we show that at near-event stations the ray path is predominantly within these layers. As sedimentary layers are generally lower in velocity and more attenuating than the underlying crystalline basement rocks, the UK ML scale is inappropriate for near-event stations. As the UK scale is empirical and derived from earthquakes at distance, this is not unexpected, and we use the NOL data to derive an appropriate NOL ML scale for these stations. Using seismic events recorded in basins elsewhere with in the UK, we then consider in more detail the appropriateness of using the NOL scale as part of the traffic light monitoring scheme.

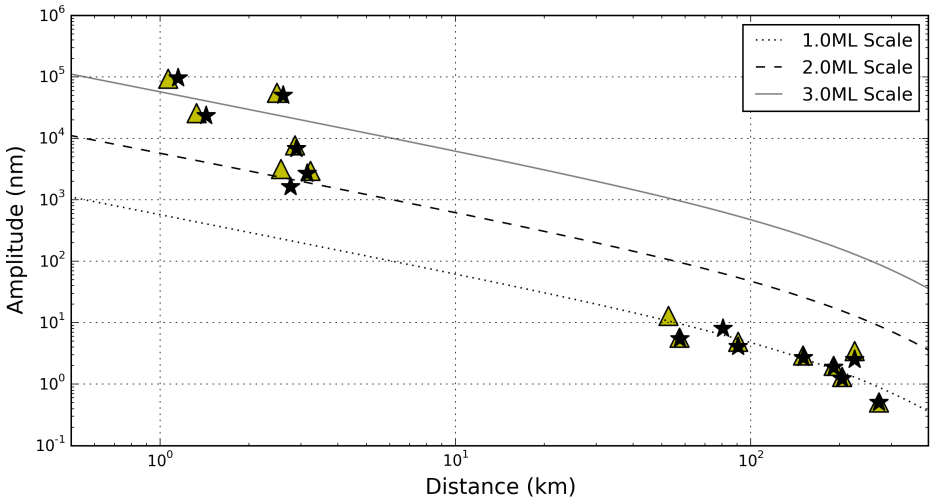

Fig. 1 Displacement amplitude versus distance recorded on both the NOL network (stations < 5km distance) and the UK national network (stations > 50km distance) for two events (2014/02/09 05:33 and 2014/02/12 02:35 coloured yellow and black respectively). Also plotted is the UK scale for ML = 1, 2 and 3 (dotted, dashed and solid lines). On the distant stations, the displacements match well with the UK scale for an ML = 1.0 event. On the nearby stations, displacements are substantially larger, and this discrepancy increases as hypocentral distance decreases.

Revealing full spectrum of triggering processes in induced seismicity

Xiaowei Chen[1], Colin Pennington[1], Nori Nakata[1], Jackson Haffener[1]

1 University of Oklahoma

The earthquake rate in Oklahoma has been dramatically increasing since 2009. Recent management efforts in disposal volume reduction led to reduction in seismicity rate since late 2015. Yet, three M5 earthquakes occurred in 2016 in Oklahoma, including the M5.0 Fairview earthquake in February, the M5.8 Pawnee earthquake in September, and the M5.1 Cushing earthquake in November. Are these earthquakes expected? What we know and we don't know about induced earthquakes in Oklahoma? In this study, we focus on the occurrence patterns of larger events, and demonstrates that full spectrum of earthquake triggering processes need to be considered in understanding the spatial-temporal evolutions of induced seismicity. We begin by an overview of occurrence patterns of earthquakes in Oklahoma, and their relationship with injection zones. Then, we focus on the Fairview/Woodward area in western Oklahoma and the Pawnee county to perform detailed analysis of the relationship between injection and background seismicity; as well as stress interaction between microearthquakes and earthquakes greather than M4. In western Oklahoma along the Fairview fault, microearthquake clustering illuminates locations of M4 earthquakes. In the Pawnee county, active stress interaction between the mainshock fault and a conjugate fault started about 100 days before the mainshock, all the M>3 foreshocks produced positive Coulomb stress at the mainshock hypocenter. In addition, observation of earthquake migration suggests existence of aseismic slip during precursory stage. Compared to the long-time delay between peak injection and peak seismicity rate observed over large spatial scale, we observe nearly instantaneous responses to injection volume variations during the precursory stage before the Pawnee earthquake. These observations lead to the proposal that full spectrum of triggering processes needs to be considered for induced seismicity, and to unravel the occurrence of large earthquakes, detailed analysis of proceeding microearthquakes is of great importance.

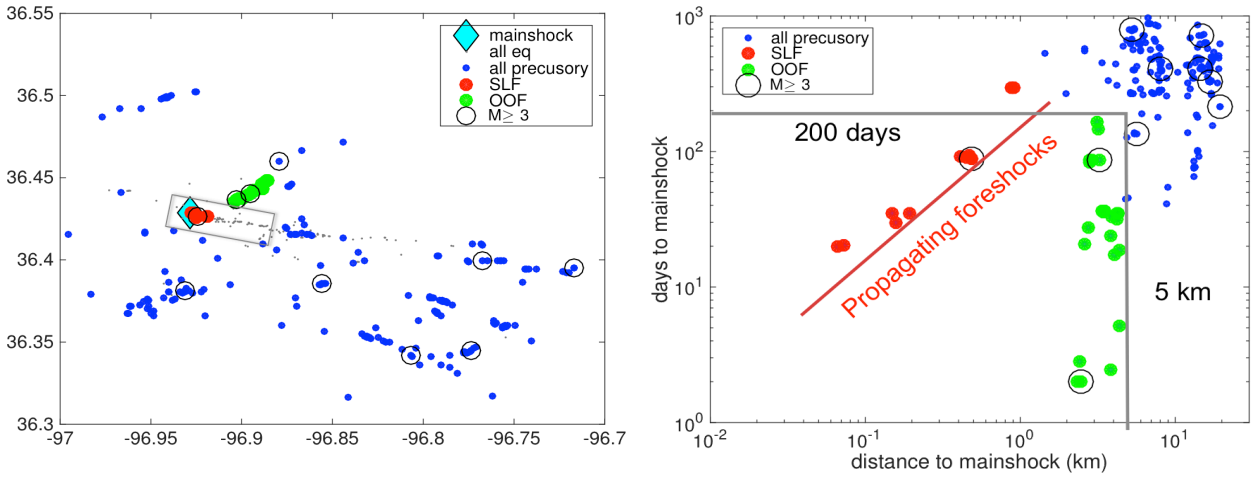

Figure 1. Left: Map view of precursory activities before the Pawnee earthquake (M>2.2). The Green circles denote earthquakes occurred on a previously mapped conjugate fault, which is optimally oriented (OOF). The Red circles denote earthquakes on Sooner Lake Fault (SLF), which is the mainshock rupture fault. The grey box outline the approximate mainshock rupture zone, where the major portion remained locked during the precursory stage. Right: Time (before mainshock) versus Distance (relative to mainshock) during precursory stage. Note that about 100 days before mainshock, all the activities are occurring on the conjugate fault system, while other regions are relatively quiet.

Assessing the monitoring performance and the induced seismicity by hydraulic fracturing at the Wysin site (Poland)

José Ángel López Comino [1], Simone Cesca [1], Marius Kriegerowski [1,2], Sebastian Heimann [1], Torsten Dahm [1], Janusz Mirek [3], Stanislaw Lasocki [3]

1 GFZ German Research Centre for Geosciences, Potsdam, Germany, José Ángel López Comino, jalopez@gfz-potsdam.de; **2** University of Potsdam, Institute of Earth and Environmental Sciences, Potsdam-Golm, Germany; **3** Institute of Geophysics, Polish Academy of Sciences, Krakow, Pola

This work analyses the monitoring performance and the induced seismicity for a hydrofracking experiment monitored in the framework of the SHEER (SHale gas Exploration and Exploitation induced Risks) EU project at the Wysin (Poland) site, located in the central-western part of the Peribaltic synclise, Pomerania. A specific network setup has been installed in autumn 2015, including a distributed network of six broadband stations, three small-scale arrays and three shallow borehole stations. The fracking operations are carried out in June and July 2016 at a depth 4000 m. We propose a hydraulic fracturing analysis in two stages: 1) a microseismic synthetic catalogue and waveform dataset using real noise from the pre-operational phase is generated and used to assess the monitoring performance; 2) Automated full waveform detection and location algorithms are applied to analyze the induced seismicity during and after the fracking operations.

In the synthetic data, background seismicity is modeled by double couple (DC) focal mechanisms and non-DC sources resembling the induced tensile fractures, opening in the direction of the minimal compressive stress and closing in the same direction after the injection. We combine realistic source models with a local crustal model to generate event-based synthetic waveforms. Overlapping station specific noise records we are able to reproduce realistic monitoring conditions. The network detection performance is then assessed in terms of Magnitude of Completeness (Mc) through two different techniques: i) using an amplitude threshold approach, taking into account a station dependent noise level and different values of signal-to-noise ratio (SNR) and ii) through the application of an automatic detection algorithm to the continuous synthetic dataset. In the first case, we compare the maximal amplitude of noise free synthetic waveforms with different noise levels. The Mc is assessed from the known synthetic catalogue, imposing the simultaneous detection at 4 stations. Each station detection can be further adjusted by empirical relationships for different SNR values, what helps to extrapolate Mc estimates to a broader region. We find that different source mechanisms have different detection threshold, with the background seismicity (DC sources) better detectable than induced earthquakes (tensile cracks mechanisms). Assuming a SNR of 2, we estimate a Mc ~ 0.55 around the fracking wells, with an increase of 0.05 during day hours. The value of Mc can be decreased to ~ 0.45, taking advantage by the array installations. The second approach applies a full waveform detection and location algorithm based on the stacking of smooth characteristic function and the identification of high coherence in the signals recorded at different stations. In this case the detection can be improved at the cost of increasing the number of false detections, with an acceptable compromise found for Mc ~ 0.1.

We apply the same detector to real data for the time period May-September 2016, covering pre-operational, fracking and post-operational stages, generating an unsupervised detection catalogue. The strong temporal change (day/night) of the detection performance is confirmed with real data. A manual revision of the detected signals revealed that most detections are associated to local and regional seismic signals, generated far from the injection well. Only two events could be assigned to the volume potentially affected by the fracking operations.

Energy Magnitude as Common Magnitude Scale for Mining Induced Seismicity

Savka Dineva[1], Łukasz Rudziński[2]

1 Luleå Technical University, Luleå, Sweden, sdineva@ltu.se; **2** Institute of Geophysics PAS, Warszawa, Poland

Magnitude is important parameter which describes the strength of the seismic source. Although it is widely used in mining seismology, often it is not exactly the same parameter in different parts of the world. Moreover no attempt for obtaining relationships between different magnitude scales is currently known. In some cases, like in Polish mines, logarithm of the energy (log E) is used instead of the magnitude. In other mines local magnitude or its variations are used. This can affect the transfer of methodologies as well as conclusions about correlation between seismic source parameters, geomechanical properties, and mining operations. Strictly speaking, since the scales are not related to each other, the same magnitude estimated in one mine does not mean exactly the same in another one. The problem is even more serious when different mining areas in the same country are considered. We try to overcome this issue by introducing common magnitude scale.

An attempt was made to obtain a new magnitude scale ME based on the energy of the seismic waves, calibrated with the local magnitude ML, similar to the magnitude used for natural earthquakes. We used the unique opportunity of available records of mining induced seismicity by two types of seismic networks – mining wide and local/regional networks in Lubin - Głogów Copper District, Poland (deep copper mines with exploration level below 1 km) to calculate the original ML magnitude and to calibrate ME with it.

The ME magnitudes are estimated for seismic events in Polish and Swedish mines based on the energy calculated from the records by the mining seismic networks. The ME magnitudes are compared with the estimated moment magnitude Mw from the same data, as well as the available magnitude estimations from national and international data centres. The challenges and advantages of the ME for the mining induced seismicity are discussed.

Seismic Monitoring of Deep Geothermal Energy Drilling

Ladina Glaus[1], Florian Haslinger[2],Toni Kraft[2], John Clinton[2], Philipp Kästli[2], Nils Oesterling[3], Stefan Wiemer[2]

1. SCCER-SoE, ETH Zurich, Switzerland, ladina.glaus@sccer-soe.ethz.ch, **2.** SED, ETHZ, Switzerland, florian.haslinger@sed.ethz.ch, ; **3.** Swisstopo, Switzerland, nils.oesterling@swisstopo.ch

Easy and open access to project data on past and existing geothermal projects is a crucial requirement for project developers and scientists to develop and advance the knowledge and technologies enabling the save and economic exploitation of geothermal energy. To facilitate such developments, the Federal Office for Topography (swisstopo) collects data from boreholes deeper than 500 m from all over Switzerland, in the context of the project GeoTherm. The aim is to publish this data collection as a new layer on the federal geoportal map.geo.admin.ch, spreading the knowledge of the underground. swissopo collaborates with the "Swiss Competence Center for Energy Research - Supply of Electricity" (SCCER-SoE) (www.sccer-soe.ch) for collecting any kind of project data from deep geothermal energy projects (i.e., geological, hydrological, geomechanical, borehole data, seismic survey data, etc.)

Recent deep geothermal projects in Switzerland and Europe were terminated because of induced earthquakes up to magnitude ML3.5. Therefore, seismological data are crucial to develop successful exploration strategies for future projects. The Swiss Seismological Service (SED;www.seismo.ethz.ch) is the federal authority responsible for seismic monitoring and data archiving in Switzerland. In recent year the SED was involved in, or responsible for, the monitoring of most deep geothermal project in Switzerland. In the framework of the GeoTherm project, SED has collected the available seismological meta- (i.e. station inventories and earthquake catalogs) and waveform data recorded for these projects. This data is, or will be made available online via the existing and well-established infrastructure provided by SED for natural seismicity (www.eida.ethz.ch).

In the framework of the GeoTherm project a concepts is in development to make this seismological data available through swisstopo's geoportal map.geo.admin.ch. Seismic data for each monitored deep geothermal project in Switzerland will be linked from map.geo.admin.ch – where other project related data can be found - to the data source at SED map portal. On the SED web portal, a layer for each geothermal project in Switzerland will be created. This layer includes two maps, one with metadata of the active monitoring stations during the geothermal project's operation period and the other map with recorded earthquakes in the monitoring period. A conceptual data model for the layer is under development.

In the end, all data described above shall be open. The User will be able to display and combine the seismological data with any other thematic maps on map.geo.admin.ch.

This poster gives an overview on the GeoTherm database and the geothermal relevant modules, the seismic station network which was established for monitoring deep geothermal projects and first results of the layer generated for the SED website.

Identifying Anthropogenic Seismicity in Colombia by evaluating cumulative distribution functions of earthquakes.

Sebastián Gómez Alba[1], Carlos A. Vargas Jimenez[2]

1 PhD. Candidate in Geosciences. National University of Colombia, Bogota, sagomezalb@unal.edu.co; **2** PhD. Associated Professor. National University of Colombia, Bogota, cavargasj@unal.edu.co

One of the disadvantages that arise when trying to investigate the effect of industrial activities on the seismicity of a specific region is that anthropogenic seismicity may be "hidden" in what could be considered clusters of natural seismicity. It is for this reason that one of the current challenges for the scientific community is to identify which events can be classified as induced / triggered and natural among a random set of events.

Seismic monitoring of human made seismic events have not been well covered, neither understood, in the territory of Colombia. To carry out an analysis of anthropogenic seismicity in the country, the five areas with the highest production of minerals and hydrocarbons were chosen to identify in them which of the events registered by the National Seismological Network of Colombia (NSNC) have the highest probability of being related with industrial activities. Areas are located in different sedimentary basins with diverse geological characteristics. Seismological events in these regions are mainly associated to tectonic features along major fault systems, but also to mineral and hydrocarbon exploitation activities. The areas differ in the type of reservoirs/deposits, the technologies used for the extraction of resources and the operating time. We turn to the theory of probability to identify induced/triggered events from those occurring naturally, and then determine the operational causes responsible for generating these events.

The analysis showed that the origin of anthropogenic seismicity is associated with the detonation of explosive charges for the removal of rock material in the case of mining, and the injection of water into the subsoil in the case of the exploitation of hydrocarbons. The seismic catalogs belong to the National Seismological Network of Colombia (NSNC) and are available on its website.

Automated seismic event location combining waveform stacking based methods with Source Specific Station Corrections Terms

Francesco Grigoli[1], Simone Cesca[2], Lars Krieger[3], Marius Kriegerowski[2], Torsten Dahm[2]

1 ETH Zurich, Swiss Seismological Service (SED), Switzerland, francesco.grigoli@sed.ethz.ch;

2 GFZ-Potsdam, German Research Centre for Geosciences, Germany;

3 Institute for Geothermal Energy Resource Management, Bingen, Germany.

Microseismic monitoring became a common operation in many seismological and industrial (Oil&Gas especially) applications, and in the last decade a significant effort has been spent to develop or improve methodologies able to perform seismological analysis for weak events at a local scale. This effort was accompanied by the improvement of monitoring systems, resulting in an increasing number of large microseismicity catalogues. The interest in microseismic monitoring operations, involving a synergy among different scientific communities, is in part due to their occurrence both in consequence of natural processes in active regions, swarm areas, hydrothermal and volcanic environments, but also in relation to human activities, e.g., in proximity of mining areas, geothermal systems, oil and gas fields, and water reservoirs. The analysis of microseismicity is challenging, because of the large number of recorded events often characterized by a low signal-to-noise ratio. A significant limitation of the traditional location approaches is that automated picking procedures are often done on each seismogram individually, making little or no use of the coherency information between stations. In order to improve the performance of the traditional location methods, in the last year, different full waveform location methods have been proposed. These methods exploits the coherence of the waveforms recorded at different stations and do not require any automated picking procedure. The main advantage of these methods relies on their robustness even when the recorded waveforms are very noisy. On the other hand, like any other location method, the location performance strongly depends on the accuracy of the available velocity model. When dealing with inaccurate velocity models location results can be affected by large errors. In this work we present a location method which combines some features of relative location techniques (such as the source specific station correction term [Richards-Dinger and Shearer 2000]) with a waveform based location method [Grigoli et al 2016]. This location approach inherits all the advantages of the full waveform location methods without the main drawback which characterizes all the absolute location procedures. In fact, this method is less dependent on the knowledge of the velocity model and presents several benefits, which improve the location accuracy: 1) it accounts for phase delays due to local site effects, e.g. surface topography or variable sediment thickness 2) theoretical velocity model are only used to estimate travel time within the source volume, and not along the entire source-sensor path. After successfully testing the method with synthetic data, we applied it to a real dataset related to fluid induced microseismicty associated with magmatic fluid migrations.

References:

Richards-Dinger, K. & Shearer, P., Earthquake locations in southern california obtained using source-speci c station terms. *Journal of Geophysical Research: Solid Earth* (*1978-2012*) **105,** 10939–10960 (2000).

Grigoli, F. *et al.* Automated microseismic event location using Master-Event Waveform Stacking. *Sci. Rep.* **6**, 25744; doi: 10.1038/srep25744 (2016).

A consistent high-resolution catalog of the induced earthquakes in Basel based on template matching

Marcus Herrmann[1], Toni Kraft[1], Thessa Tormann[1], Luca Scarabello[1], Stefan Wiemer[1]

1 Swiss Seismological Service, ETH Zurich, Switzerland, marcus.herrmann@sed.ethz.ch

In December 2006, an extensive fluid injection was carried out below the city of Basel, Switzerland, to stimulate a reservoir for an Enhanced Geothermal System (EGS). A thereby induced and strongly felt M_L3.4 earthquake led to a temporary halt of the project. Three years later, a seismic risk study suggested a substantial threat of further felt and potentially damaging events, which led to the eventual termination of the project. Seismic monitoring, however, continued and has now been running for more than ten years. Until today, the details of the long-term behavior of the induced seismicity at the EGS site remained unexplored since a consistent catalog did not exist. This deficiency is particularly critical since from mid-2012 onwards, seismicity started to occur again reaching magnitudes up to M_L1.9 (June 6, 2013).

Here we present a catalog of the seismic activity in the geothermal reservoir with homogeneous detection sensitivity and consistent magnitude estimates over its whole lifetime. We applied a multi-trace template-matching technique (TM) to extract more information from the existing 10-year-long continuous data of the deepest borehole station (OTER2, 2.7km depth). This station is very close (1.5–2.5km) to the ~4.5km-deep reservoir.

Our TM approach selects templates dynamically from a given catalog based on the similarities between the catalog events. In an initial run, 31 templates were selected from the SED catalog (209 events). We could detect a vast amount of previously unknown microevents. But these templates sample the seismic cloud only sparsely and show considerable waveform dissimilarity. To reach an acceptable coverage of the complex seismicity in the stimulated volume, we performed a cluster analysis using >3'600 event waveforms of the operator's borehole-network catalog and selected >500 reasonably dissimilar events as templates. Due to the high computational demand of scanning with such a large template set, we extended our detector to run on the Euler high-performance computer of the Swiss National Supercomputing Centre.

We detected more than 100'000 events during the six-day-long stimulation in December 2006 alone. All events are clearly linked to well-located earthquakes (templates) by waveform similarity and can thus be confidently classified and approximately located. Previously, only 13'000 amplitude-threshold-triggered detections were known for this period, most of which were neither locatable nor waveform-checked.

Our newly created catalog spans more than ten years featuring a uniform detection threshold and a consistently determined magnitude. The high temporal and spatial resolution of this catalog allowed us to analyze the statistics of the induced Basel earthquakes in great detail. We resolve spatio-temporal variations of the a- and b-value that have not been identified before, which enables us to derive the first high-resolution temporal development of the seismic hazard for the Basel EGS reservoir for the last 10 years.

With our catalog we hope to provide the basis for a better understanding of the processes that drive the induced seismicity in Basel. We have also started to extend our analysis to other induced and natural sequences in Switzerland.

Model testing and a new type of ensemble model to better forecast induced seismicity

Eszter Kiraly-Proag[1], Valentin Gischig[2], J. Douglas Zechar[3], Stefan Wiemer[1]

1 Swiss Seismological Service, ETH Zurich, Switzerland, eszter.kiraly@sed.ethz.ch; **2** Swiss competence Center for Energy Research (SCCER-SoE), ETH Zurich, Switzerland; **3** Little Lebowski Urban Achievers Scholarship Foundation, Beverly Hills, CA, USA

Induced seismicity is unavoidable consequence of fluid injections. It is an important element to monitor reservoir creation, however, it also poses hazard on the population and the infrastructure in the vicinity of the projects. In our view, models to monitor and control induced seismic hazard with traffic light systems should be probabilistic, forward-looking, and updated as new data arrive. Here, we propose an Induced Seismicity Test Bench to test, validate and rank such models. This test bench can be used for model development, model selection, and ensemble model building. We apply the test bench to data from the Basel 2006 and Soultz-sous-Forêts 2004 geothermal stimulation projects. We assess forecasts from two models: Shapiro and Smoothed Seismicity (SaSS) and Hydraulics and Seismics (HySei). These models incorporate a different mix of physics-based elements and stochastic representation of the induced sequences. Our results show that none of the models is fully superior to the other and the shut-in phase is a difficult moment for both models in both reservoirs: the models tend to underpredict the seismicity rate around, and shortly after, shut-in. Forecasts can be improved by combining models. In this work, we also show a new type of ensemble models that outperforms individual models as well as simple ensemble models.

Towards Performance-Driven Monitoring and Early Warning Systems for Induced Seismicity

Konstantinos G. Megalooikonomou[1], Stefano Parolai[1], Massimiliano Pittore[1]

1 GFZ German Research Centre for Geosciences, Germany, kmegal@gfz-potsdam.de

Earthquakes may be induced by a wide range of anthropogenic activities such as mining, fluid injection and extraction, and hydraulic fracturing. In recent years, the increased occurrence of induced seismicity and the impact of some of these earthquakes on the built environment have heightened both public concern and regulatory scrutiny, motivating the need for a framework for the management of induced seismicity. Earthquake early warning systems coupled with non-standard monitoring approaches can prove as valuable tools for mitigating the risk associated with earthquakes. These solutions might include advanced sensors with a number of functions, such as implementing a performance-based on-site early warning and rapid response system for infrastructure but also monitoring the structural response of buildings and infrastructure in real time (Fig.1). Such technical solutions can be used also for validating damage forecasts (performance) determined by probabilistic approaches based on suitable fragility curves. Based on the performance level an alert is designated according to pre-defined thresholds for acceptable levels of motion.

The ultimate objective of any effective program for the management of induced seismicity must be to limit the consequent seismic risk. Towards this goal, the seismic hazard, the exposure and the vulnerability should be defined. Hazard is defined by a measure of the ground shaking, and in order to quantify the likelihood of the risk, the associated frequency or probability of exceedance. Regarding exposure coupling remote sensing with in-situ imaging can be optimized over broad areas for the characterization of the built environment.

Finally, related to vulnerability, for the specific case of induced seismicity different types of consequences might be considered such as non-structural damage to buildings and annoyance of the affected population. It is therefore important to incorporate in an already developed on-site early warning and rapid damage forecasting system (Parolai et. al. 2015) properly derived fragility curves. After reviewing the existing protocols for evaluating the fragility, new proposals are made for analytical fragility curves for typical building types that have been developed for the seismic demands generally imposed upon linear and slightly nonlinear systems of single and multiple degrees of freedom which is the case for induced seismicity demands.

Fig. 1 Multi Parameter Monitoring System

Recent Seismicity in the Northern German Gas Fields – Induced and Tectonic?

Gregor Mokelke [1], Zaneta Heinrich[1], Benjamin Sick[1], Rolf Häfner[1], Patrick Blascheck[1], Marco Walter[1,2], Manfred Joswig[1]

1 Institute for Geophysics, Stuttgart University, Germany, gregor.mokelke@geophys.uni-stuttgart.de;
2 Seismic Solutions, Tübingen, Germany

In the northern German gas fields, several ML 2 to ML 3 earthquakes per year happened during recent years. Seismicity is generally bound to some 5 km depth corresponding to the exploited gas reservoirs in the Rotliegend. Thus this seismicity is assumed to be probably related to the conventional gas extraction. For liability claims, the regional seismic monitoring has improved recently by several new stations operated for the Bundesverband Erdgas, Erdöl und Geoenergie (BVEG) - an industry consortium of gas producers - and the Bundesanstalt für Geowissenschaften und Rohstoffe (BGR) - the German federal governmental agency for geosciences and resources.

In the context of the DGMK research project 761, Stuttgart university has installed an additional, small-scale seismic network that monitored the Rotenburg region for the last two years. The region was chosen on purpose since 2004, the ML 4.5 Rotenburg earthquake was the largest event ever recorded in the vicinity of conventional gas production. For our monitoring, we combined two 10-station array with two tri-partite small arrays and three 3C single stations. Our installation covers an area of 11,5 km by 16 km. Within this area we achieved a detection threshold of ML 0.5 as verified by 35 events in a distance range of up to 100 km. In spite of this sensitivity no small events were observed near Rotenburg as would have been expected from the past seismicity by the two major earthquakes Rotenburg 2004 (ML 4.5) and Visselhövede 2012 (ML 2.9).

Reprocessing BVEG and BGR data from the past by cross correlating seismograms from those 35 recent events we found additional events also clustering at 5 km depth. Additionally we discovered four singular, deeper earthquakes at 25 km to 30 km depth which previously were overlooked in regional monitoring due to many noise bursts by military shooting. Possible source mechanisms for these deeper events will be discussed ranging from the existence of intraplate earthquakes to the stress release from postglacial isostatic relaxation.

PCA-based moment tensor inversion of induced earthquakes in The Geysers geothermal reservoir

Changpeng Yu[1,3], Václav Vavryčuk[2], Petra Admová[2], Grzegorz Kwiatek[1], Marco Bohnhoff[1,3]

1 GFZ Potsdam, Section 4.2, Germany (changpeng.yu@gfz-potsdam.de); **2** Institute of Geophysics, CAS, Czech Republic;
3 Free University of Berlin, Institute of Geological Sciences, Germany

During the long history of production at The Geysers geothermal field, fluid injection significantly increased the rate of local seismicity. Throughout the last decade, the induced seismicity in this area was analyzed using data recorded by short period stations of the LBNL network. In this study, we use broadband data acquired by a local surface network of 33 broadband stations deployed throughout The Geysers geothermal field and operated from February 2012 to July 2013, to determine the source mechanisms of the induced seismicity. Since more than 35,000 events with M_L>1.0 were detected in the reservoir within the period of network operation, manual processing of the dataset is not feasible.

A fast and semi-automatic approach using the principal component analysis (PCA) is implemented in the moment tensor inversion of P-waves. Considering the scales of rupture process and of the observing system, the earthquakes can be assumed as point sources, and the radiated P-waves reaching to different receivers should have similar shapes of waveform. The PCA technique can be advantageously applied to extract the common waveform of the P-waves and return the principal component coefficients for different traces. These coefficients are used as the equivalent amplitudes in the standard amplitude inversion for the moment tensor. In our previous studies, the PCA-based inversion for moment tensor shows a high robustness and accuracy for the synthetic as well as real datasets.

In this paper, we analyze the focal mechanisms of about 1700 events with M_L>2.0 in The Geysers area. The initial analysis of focal mechanisms obtained by using the PCA-based inversion for 50 selected events is presented in Figure 1. Although the events are not selected from a single cluster and scattered over a broad region, the T-axes clearly show clustering along the direction perpendicular to the NNE-SSW trending of the regional maximum horizontal stress (S_{Hmax}). This suggests that the tectonic stress is an important controlling factor of the focal mechanisms. In addition, considerable portions of non-double-couple components are observed for some events. Before the interpretation, the reliability of non-DC components needs to be examined by considering the influence of noise, mislocation and the inaccuracy of velocity model.

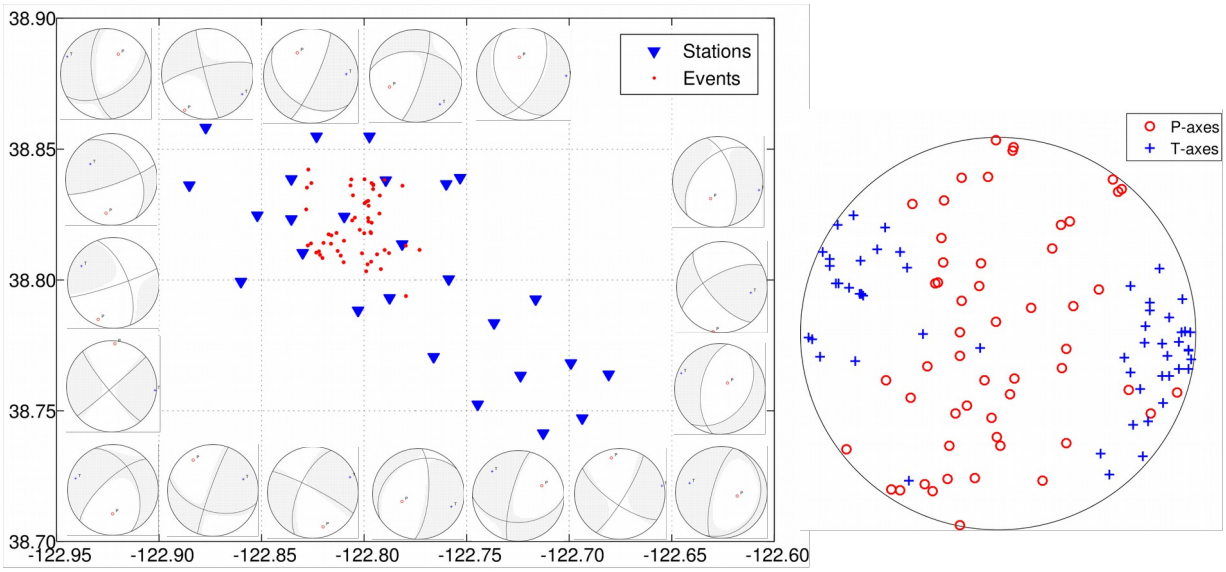

Fig. 1: The initial analysis of the focal mechanisms obtained by using the PCA-based inversion for 50 selected events with ML>2.3. Left: map of the stations and the selected events overlapped by some examples of the focal mechanisms. Right: the P- and T-axes distributions of the selected events.

Abstracts Posters, Part II

Session 1 and 2

Case Studies

Mapping relative principal stresses in the southern United States with application to predicting fault slip potential

Jens-Erik Lund Snee[1], Mark D. Zoback[1], F. Rall Walsh, III[1]

1 Stanford University, Department of Geophysics, California, USA, lundsnee@stanford.edu

We have made more than 250 new measurements of the maximum horizontal stress (S_{Hmax}) orientation in Texas, Oklahoma, and New Mexico, USA. We also map relative principal stress magnitudes (faulting regime) across the south-central United States using the A_ϕ parameter (Fig. 1).

The most robust constraints on A_ϕ are derived from geologic observations of slip sense on active faults, measurements of stress magnitudes made in boreholes, and inversions of dozens of moment tensors. In addition, individual focal mechanisms or observations of microseismic event locations qualitatively indicate the types of active faults (e.g., normal, simultaneous normal and strike-slip, strike-slip, etc.), which can be used to estimate permissible ranges of A_ϕ.

We apply all of these methods to estimate the faulting regime at discrete locations, which we then interpolate across the study area using ordinary kriging (Fig. 1). Because our measurements enable us to obtain relative values for the full stress tensor, we are able to estimate gradients of the tensor components across the south-central United States, which we present at this workshop. We aim to develop maps that show the degree of adherence to the equations of equilibrium.

Our stress mapping also enables us to predict the orientations of faults that are most likely to slip. We calculate the probability of slip on mapped faults at a specified fluid pressure perturbation in several study areas in Oklahoma and Texas. In addition, we present calculations of the fluid pressure perturbation that may have been needed to trigger fault slip in the case of several apparently triggered earthquakes in Texas.

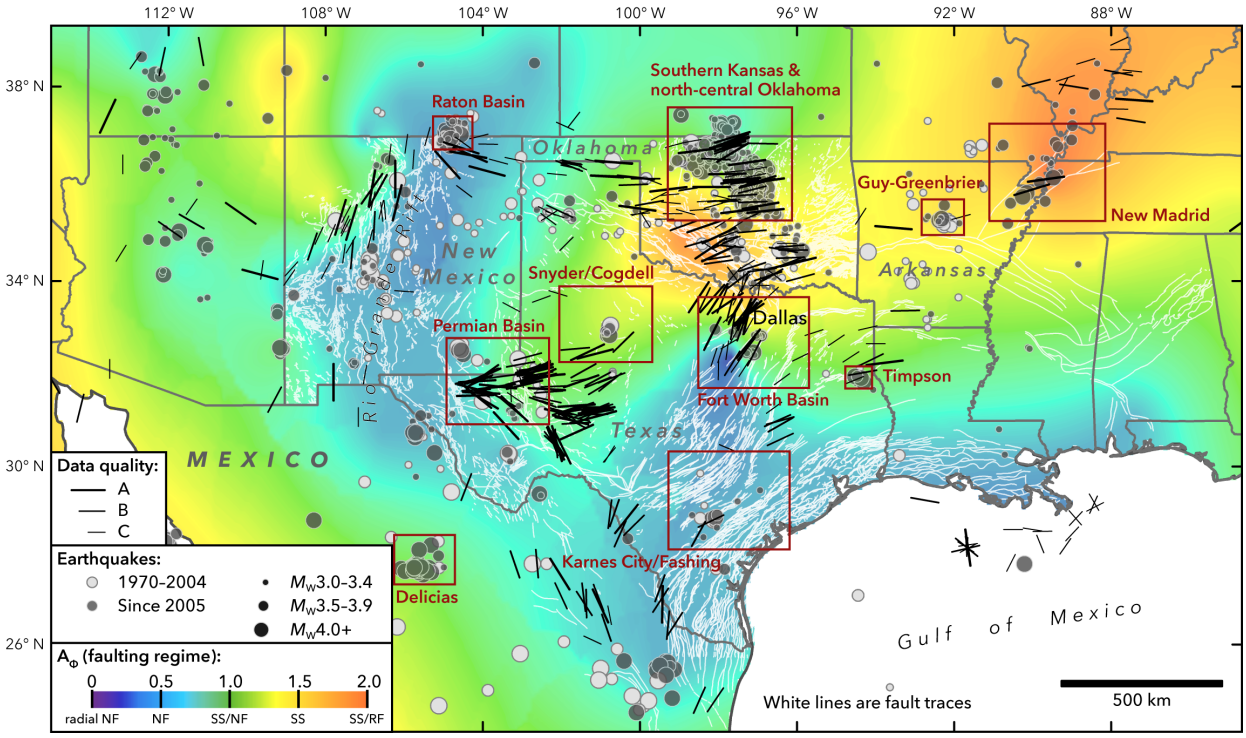

Fig. 1 Preliminary stress map of the south-central United States and northern Mexico. Black lines indicate the maximum horizontal stress (S_{Hmax}) orientation, and the colored background shows the faulting regime displayed using the A_ϕ parameter of Simpson (1997, *Jour. Geop. Res.*). Red boxes show areas that have experienced recent seismicity. References are listed by Lund Snee and Zoback (2016, *Geop. Res. Lett.*).

Induced Seismicity During Hydraulic Stimulation in Pohang (Korea) in Comparison to Basel (Switzerland)

Myungsun Kim[1], Byoungjoon Yoon[1], Falko Bethmann[2], Kwang-Il Kim[3], Ki-Bok Min[3], Choi Jaiwon[4], Peter Meier [2]

1 KIGAM, Korea, mskim@kigam.re.kr, yoonstation@kigam.re.kr; **2** Geo-Energie Suisse, Switzerland, f.bethmann@geo-energie.ch; **3** Seoul National University, Korea; **4** NexGeo, Korea

Since 2011 an important EGS pilot project is under development in Pohang (Korea) by a Korean project consortium (NexGeo, posco, INNOGEO, KIGAM, KICT, SNU). Two deep boreholes (PX1 and PX2, MD 4348 m) and recently one side-track from well PX1 (PX1-ST, MD 4362 m) have been drilled within granitic gneiss.

The project is one of the pilot project sites of the DESTRESS project (Demonstration of soft stimulation treatments of geothermal reservoirs, http://www.destress-h2020.eu/) which is an EU-Horizon 2020 supported program with South Korea and Switzerland as third member participating partners. The project started in March 2016 with a duration of 4 years. The aim is to expand knowledge and to provide solutions for a more economical, sustainable and environmentally responsible exploitation of underground heat using EGS.

Hydraulic stimulation started on December 15th, 2016 by injecting water into the open hole section with a length of 314 m of the recently drilled sidetrack PX-1 ST at a measured depth between 4048 and 4362 m. An extensive seismic monitoring system has been set up by KIGAM with 4 surface monitoring stations, 9 shallow borehole stations and two 1350 and 1550 m deep VSP-chain with 3 sensors in PX2, and a sensor installed within an offset well at a distance of about 2 km from the reservoir at a depth of 2263 m within the crystalline basement. This sensor has been installed previously at the Basel site and was provided by the Swiss seismological service and Geo-Energie Suisse.

The injection rates and injection pressures are comparable to the Basel project during the first days. However, induced seismicity shows a very different behavior compared to Basel. Both, frequency and magnitudes of the measured seismic events are several orders of magnitude lower than in Basel and comparable to the rather low induced seismicity commonly observed in sediments during fracturing operations of the oil and gas industry.

We will present the seismic monitoring system, the data of the first days of stimulation in PX1 ST and a comparison with the Basel data.

The considerable differences between induced seismicity in Pohang and Basel are not understood yet and will be the topic of detailed rock mechanical research by the DESTRESS project partners under the lead of Seoul National University(SNU).

First hypotheses to explain the observed behavior include aseismic shearing, tensile fracture propagation, different rock mechanical parameters, different regional tectonic structural setting, and more. We believe that the data from Pohang and the comparison with Basel will strongly improve the understanding of induced seismicity within crystalline rocks, showing probably two different end members of seismic behavior during hydraulic stimulation. We conjecture that further research based on this data will lead to development of technics and procedures to mitigate seismic risks and improve stimulation efficiency, both being crucial for industrial breakthrough of EGS technology.

Influence of wind turbines on seismic noise at monitoring stations in North Germany

Tobias Neuffer[1], Simon Kremers[1]

1 DMT GmbH & Co KG, Tobias.Neuffer@dmt-group.com

In recent years, several seismic events could be observed in the apparently aseismic region of North Germany. A seismic monitoring network was installed in the region consisting of borehole stations with sensor depths up to 200 m and surface stations. After installation of the network in 2011, an increasing number of wind turbines was established in close proximity to several stations. This study demonstrates the influence of wind turbines on seismic noise level in a frequency range of 1 - 10 Hz at the monitoring sites with correlation to wind speed. Power spectral density (PSD) functions and I95 values of waveforms from a time period of four years were calculated characterizing the noise level. The azimuthal direction of incoming Rayleigh waves at a surface station was determined to identify the direction of the noise sources. Moreover, the influence of varying noise levels at a station on the ability to automatically detect seismic events was investigated. It could be shown that higher wind speeds increase the PSD amplitudes at distinct frequencies between 1.0 and 5.0 Hz, depending on local site conditions as well as number and type of influencing wind turbines. The analysis of the perturbed wave field at the surface station showed that Rayleigh waves with back azimuths pointing to wind turbines in operation are dominating the wave field in a frequency band of 3 – 4 Hz (Fig. 1). The increased noise level in correlation to higher wind speeds at the monitoring sites deteriorates the station's recording quality inhibiting the automatic detection of small seismic events. As a result, functionality and task fulfilment of the seismic network is more and more limited by the increasing number of nearby wind turbines.

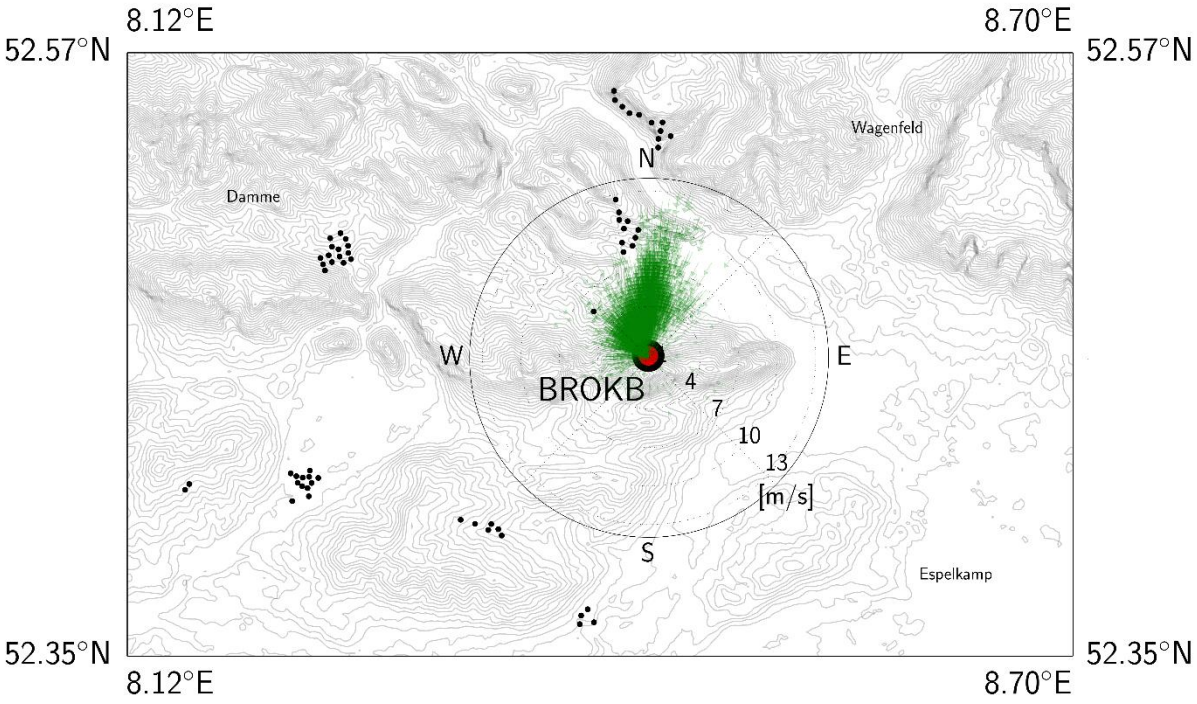

Fig. 1 The influence of wind turbines at surface station BROKB: The Rayleigh wave dominated wave field between 3 – 4 Hz allows to identify the direction of the noise sources. The polar plot shows the direction of the arriving Rayleigh waves (green arrows) as a function of wind speed. It can be clearly seen that the observed noise is generated by nearby wind turbines (black dots).

Analysis of static stress variations in the 2013 Valencia Gulf (NE Spain) seismic sequence

Lluis Salo[1,2], Tanit Frontera[2], Xavier Goula[2], Lluis Pujades[1], Alberto Ledesma[1]

1Universitat Politecnica de Catalunya, Barcelona School of Civil Engineering, Spain, lluis.salo@upc.edu; **2** Institut Cartografic i Geologic de Catalunya, Spain, tanit.frontera@icgc.cat

In this study we assess the role of static stress transfer during the earthquakes that struck the Valencia Gulf in September and October, 2013, some 20-30 km offshore, while and after gas injections in the area to develop an Underground Gas Storage (UGS) were conducted. The events built-up to reach a maximum of M_L 4.3 on October 2nd and some were felt by the nearby population.

We use the Coulomb Failure Function criterion ($\Delta CS = \Delta\tau \pm \mu'\Delta\sigma$) to quantify Coulomb stress change (ΔCS), and so determine whether failure is promoted or inhibited on mapped faults as a result of static stress change. First, source faults (slip $\neq 0$) are derived from Focal Mechanism (FM) information of the 8 strongest events in the sequence (M_L 3.5-4.3); FMs are calculated using full waveform inversion and compared with solutions shown in the available references. To assess ΔCS, we build a first-stage 3D fault model of the area both with source faults and known faults derived from geological studies, the latter acting only as receiver faults (no slip) due to FM solutions having been resolved at greater depths (Fig. 1).

Based on the studied physical mechanism, the three main findings of the study are: 1) static stress transfer is revealed as a potentially destabilizing mechanism in the sequence; 2) The East 4 structure is the one with higher probability of having been activated, should one of the mapped faults have slipped; 3) The seismic cycle concerning the Main Fault's characteristic earthquake (M_w 6.0) was not (remarkably) shortened by the experienced events.

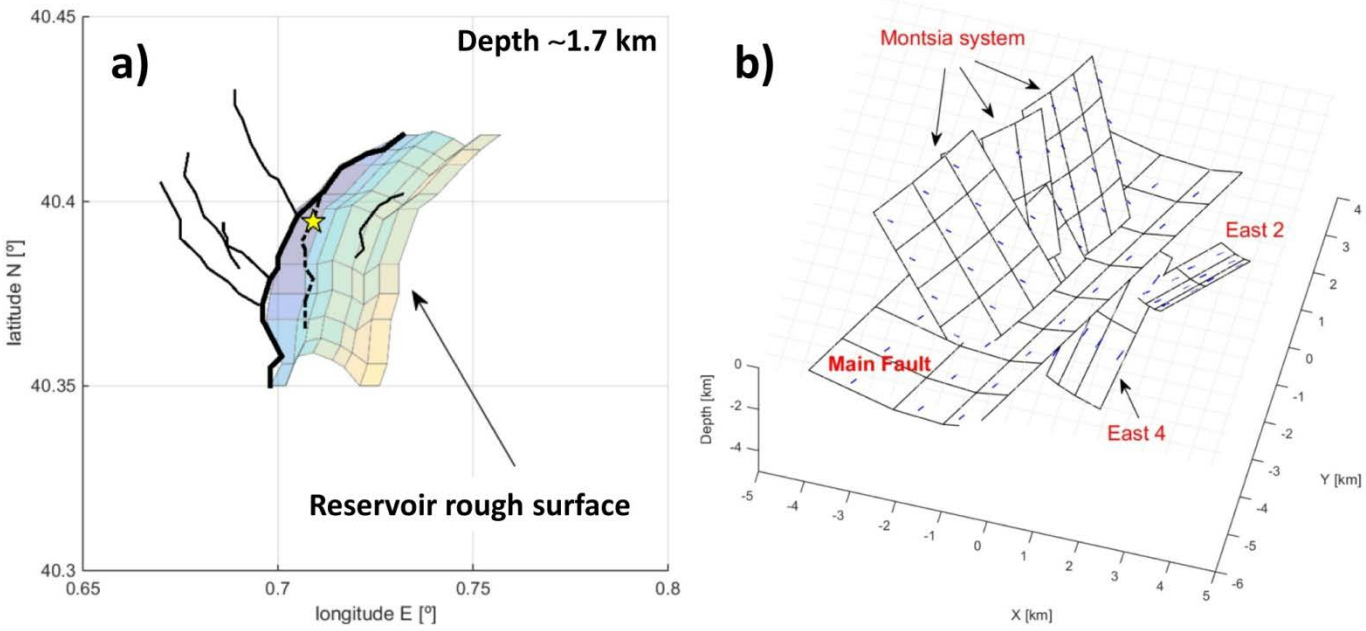

Fig. 1 a) Horizontal slice of the geometrical 3D model of known faults, near reservoir top, derived from existing references. Fault traces are shown as black lines, continuous if dipping to the west and discontinuous otherwise (East 4). The yellow star shows the UGS platform location. **b)** Fault model used in COULOMB calculations, generated using a) as an input. Just receiver (mapped faults) are shown, source faults being smaller and deeper. The Montsia system and the Main Fault reach depths near surface, while the East faults' shallowest point is about reservoir top depth.

Statistical evidence of production driven seismicity at Groningen Field

Danijela Sijacic[1], Manuel Nepveu[1], Karin van Thienen-Visser[1]

1 TNO, Energy Division, Utrecht, Netherlands, danijela.sijacic@tno.nl

Depletion of gas fields, even in a tectonically inactive area can induce earthquakes. This is the case for the Groningen gas field - the largest European gas field, located in the north of the Netherlands. Depletion of the Groningen gas field started in 1963 and has continued up to the point where now more than 75% of the gas originally in place has been produced and pressures have declined from about 300 bar to about 100 bar. Induced seismicity occurred frequently since 1991 and with time the number of events and magnitudes of events have been increasing. Increased seismic activity raised public concern which led to the government trying to understand the cause of the earthquakes and optimize production such as to minimize the risk of induced seismicity. The main question is how production is correlated with induced seismicity.

We have developed a method to assess seismic event rate, its changes and tendencies using Bayesian model comparison and Bayesian change point model. The question of interest is whether the production reduction since January 2014 has had an effect on the seismicity occurring in the Groningen field. We present evidence that changes in seismicity are closely related to changes in production. The number of events in the Groningen field in the area affected by the production change has been reduced significantly. Both statistical methods led to a conclusion that seismicity at Groningen field had a fairly constant event rate up to 2003, an increasing event rate from 2003 to 2014 and a decreasing event rate from early 2014 to now. The results of Bayesian change point analysis are summarized in Figure 1.

Furthermore, seasonality in the production and the number of events is identified. The seasonality indicates a delay ranging between 2 to 8 months between seismicity and production changes.

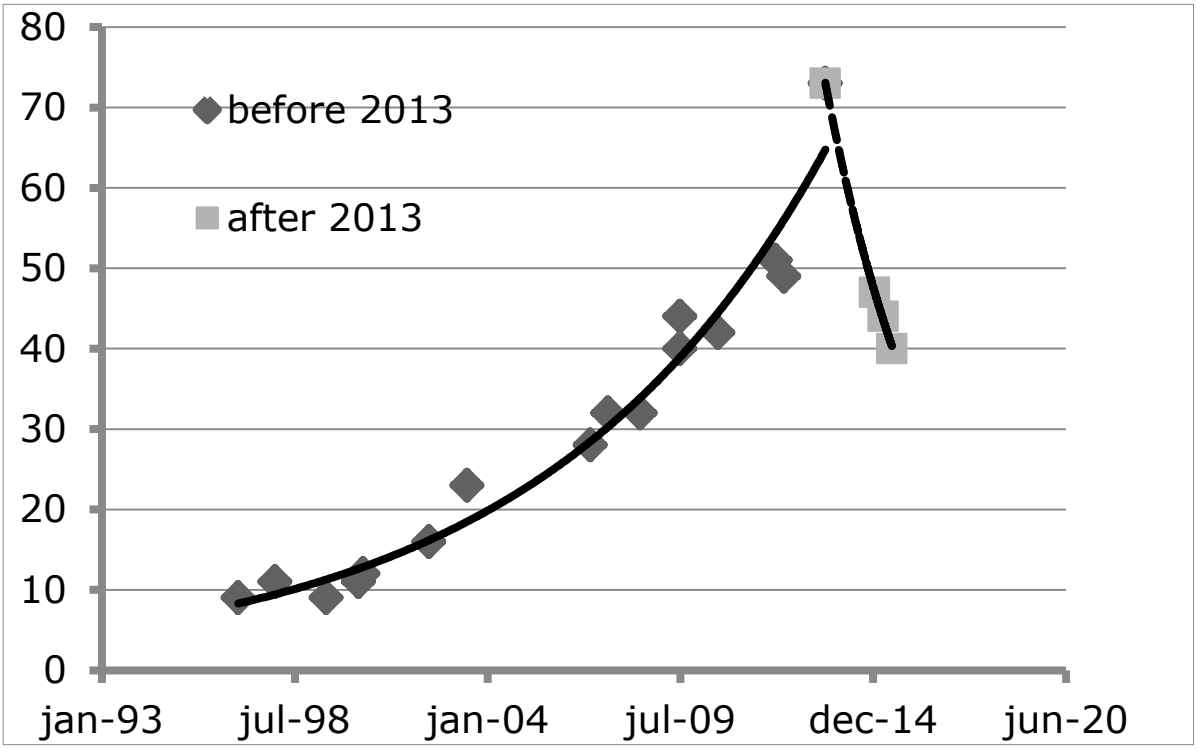

Fig. 1 Event ($M_L \geq 1.0$) rate change with time for the entire Groningen field. The solid lines are the exponential fits trough the data before and after 2013 meant as an illustration.

A Procedure to Forecast Effects of Induced Seismicity on Buildings after an Exceptionally Strong Mine Tremor

Zbigniew Zembaty[1], Piotr Bobra[1], Michał Paprotny[2], Andrzej Póda[2], Czesław Bubała[3], Juliusz Kuś[1]

1 Opole University of Technology, Faculty of Civil Engineering, Poland, z.zembaty@po.opole.pl; **2** *"Wujek"* Coal Mine, Katowice Coal Holding, Katowice, Poland;

On April 18th 2015, a rockburst of magnitude m_L=4.2 occurred in the area of the activity of "Wujek" mine in the Upper Silesia Coal Mine Basin in Poland (below the town of Katowice). The energy released was assessed as equal to 4×10^9 Joule. The rockburst resulted in a catastrophic underground failure and some damages in the buildings on the ground surface. Respective ground motion records from the local seismic network displayed maximum peak ground acceleration PGA=2.31 m/s^2 and peak ground velocity PGV=0.11m/s. The latter value exceeded the 4-5cm/s thresholds settled for the level of so called "construction damages", dangerous with respect to the safety of buildings, by special, so called *GSI* scale measuring destructiveness of underground mine activities to civil infrastructure and buildings on the ground surface.

Such the alarming level of ground vibrations raised a question of the safety of buildings during the planned, future mine exploitation. For these reasons the forecast of surface ground motion for the years 2016-2017 was updated (see figure below).

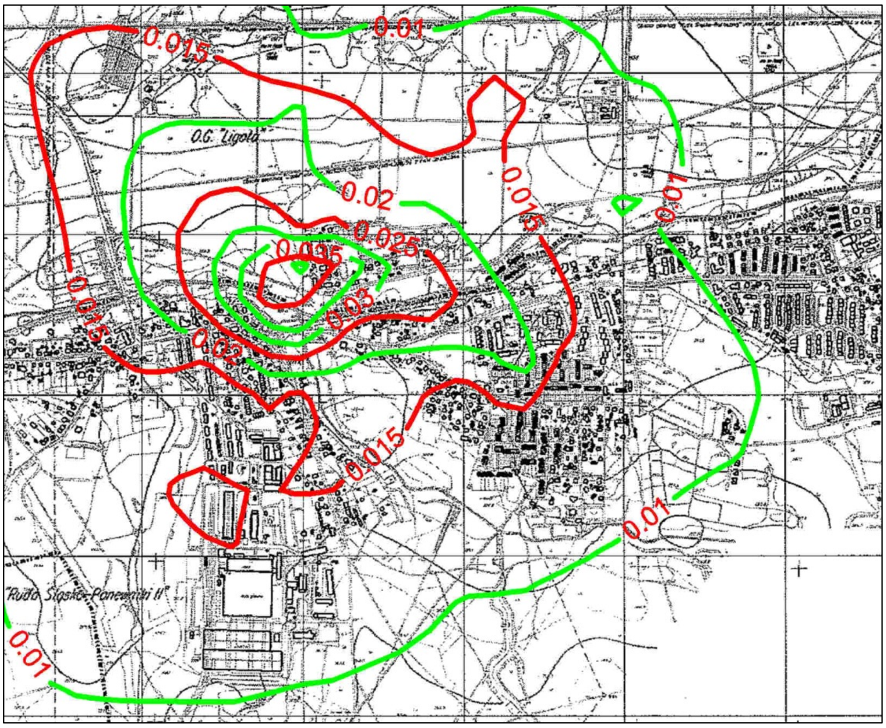

Fig. 1. Map of maxima of horizontal peak ground velocities [m/s] forecasted for the years 2016-2017 as induced in the "*Wujek"* mine exploitation surface area in Katowice, Poland

Next all the records of the rockburst of April 18th 2015 measured by the surface mine seismic network were analysed in detail, leading to yet another map showing approximate surface horizontal velocities on the ground during that event. Comparing the map of the forecasted surface velocities with the velocities already sustained by the buildings during the rockburst of April 18th 2015 made it possible to treat this event as a real-life seismic test of the buildings.

The presentation planned for the Schatzalp 2017 Workshop will show results of a detailed comparison of the mapped ground velocities from the April 18th 2016 event, damages of the building stock and the forecasted ground velocities. This way a procedure for applying ground vibration records of a strong rockburst to serve as a real-life seismic test to assess seismic resistance of building stock of an urban area under which deep mining exploitation takes place.

Abstracts Posters, Part II

Session 3 and 4

Understanding and Modeling of Induced Seismicity

Stick-slip dynamics of flow-induced seismicity on rate and state faults

Luis Cueto-Felgueroso[1], David Santillán[1], Juan Carlos Mosquera[2]

1 Technical University of Madrid. Department of Civil Engineering: Hydraulics, Energy and Environment, Spain, david.santillan@upm.es; **3** Technical University of Madrid. Department of Continuum Mechanics and Structures, Spain

Recent observations have shown that changes in pore pressure due to the injection or extraction of fluids from underground formations may induce potentially damaging earthquakes or increase the sensitivity of injection sites to remote triggering. The basic mechanism behind injection-induced seismicity is a change in effective stress, which weakens preexisting faults. The seismic potential of a given fault is related to the partitioning between seismic and aseismic slip once sliding starts to occur, and fault slip pattern emerges as a manifestation of stick–slip frictional instabilities.

We have developed a numerical framework with fault frictional contact described by the Dieterich–Ruina rate- and state-dependent constitutive law and we model rock as a poroelastic solid. We investigate the evolution of slip due to pore pressure increase in a simplified underground injection model (Fig.1-left). Our model is able to reproduce stick–slip behavior (Fig.1-right), and a variety of stick–slip patterns are identified for different constitutive parameters, ranging from stable sliding or a sequence of many small slip events, to a single, larger slip event after significant aseismic slip has occurred.

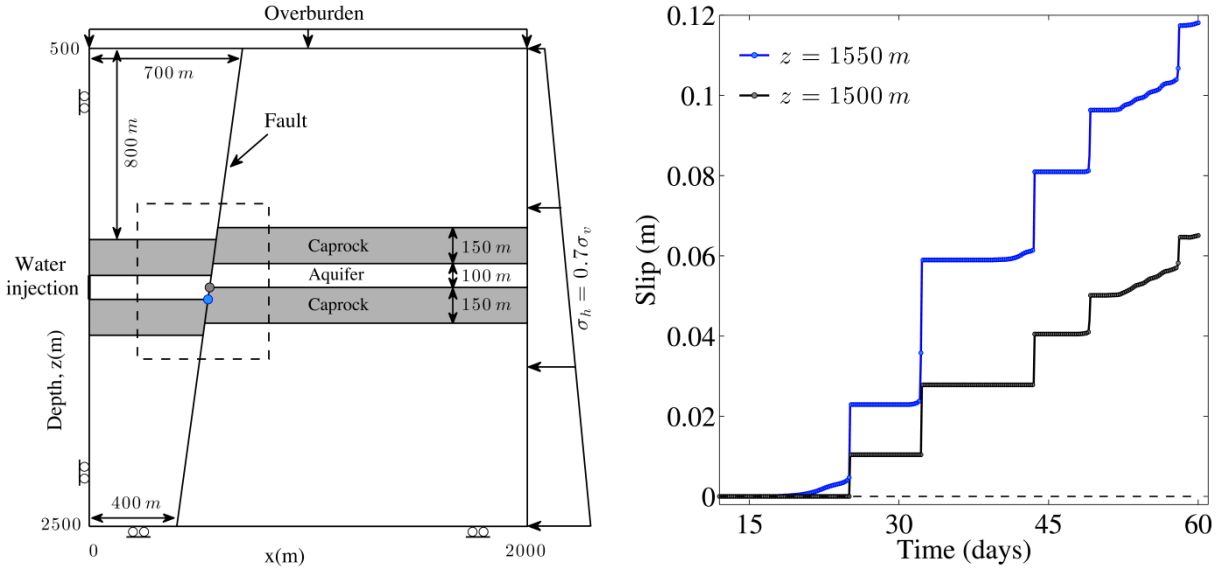

Fig. 1 Left: Schematic of the model. We simulate water injection into a confined aquifer. We model the rock as poroelastic domain. The domain is initially at lihostatic equilibrium and the fluid pressure is hydrostatic. The tectonic ratio of horizontal to vertical stresses is 0.7. We inject fluid at a constant rate **Right**: Evolution of slips at two points along the fault, located at depths of 1500 m and 1550 m (black and blue solid lines, respectively). The slip behavior shows a characteristic stick-slip pattern.

Fluid injection and re-injection in deep wells: numerical modelling and implication on induced seismicity.

Giuseppe De Natale, Claudia Troise, Renato Somma

INGV, Naples, Italy, giuseppe.denatale@ingv.it

Induced seismicity can be associated to the activity of fluid withdrawal and injection from/into the shallow crust (fracking, wastewater disposal into the deep crust, EGS technology, fluid extraction in oil fields and geothermal power plants).

It is common experience worldwide that small plants, with considerable re-injection of geothermal fluids in the same reservoir, does not show any significant induced seismicity. This work presents convincing evidence that the perturbation of geothermal systems, as due to close cycles withdrawal re-injection in the same aquifer, is negligible also in the long term, with respect to continuous withdrawal or injection only. This result is achieved by analysing the potential for induced seismicity as due to the above activities.

A set of simulations of withdrawal/injection/reinjection cycles from/into the same reservoirs, by using the numerical code TOUGH2®, is applied to conceptual models of different geothermal reservoirs, to compare the time growth of perturbed volumes obtained with withdrawal reinjection cycles to those obtained during simple withdrawal or injection, using the same flow rates.

Our results clearly show that withdrawal-reinjection is by far less critical than simple injection or withdrawal, because the perturbed volumes are remarkably smaller and remain constant over the simulated time, so minimizing the likelihood of interference with seismogenic faults.

This results have significant implications in the application to geothermal projects and in the assessment of potential risk related to fluids stimulation and induced seismicity.

New horizons in the understanding & mitigation of induced seismicity: physics, risk, communication

Arnaud Mignan[1]

1 ETH Zurich, Institute of Geophysics, Switzerland, arnaud.mignan@sed.ethz.ch

The rise in the frequency of anthropogenic earthquakes is posing economic, societal and legal challenges to geo-energy projects (e.g., Enhanced Geothermal Systems, EGS). Existing tools to assess and control such risk are insufficient. To resolve this issue, induced seismicity is studied from three fronts: (1) the physics of seismicity, both tectonic and induced, is poorly understood. We move away from the Complexity trend (bottom-up triggering, criticality) to a reductionist approach (top-down loading, non-criticality) to explain the main laws of seismicity. For the case of induced seismicity, both the linear flow rate-induced seismicity rate relationship and the parabolic induced seismicity spatial front are explained from simple geometric operations on a static stress field (Mignan, 2016). It follows that the simple statistical laws that describe induced seismicity time series (Fig. 1a) can be related to only 2 physical parameters (activation & background static stress amplitude range). (2) With a physical model that can be described algebraically, a data-driven adaptive forecasting system can be run that is computationally cheap. Decision variables can also be derived from such model to define a traffic light system (TLS) in respect to a given safety criterion (Mignan, Broccardo, Wiemer, Giardini, "*When is anthropogenic seismicity too risky*", submitted). (3) Although the security criterion can be respected (in average) with the use of a TLS, the known scattering of the activation parameter makes the future of an EGS project uncertain. Based on the EGS costs (mainly drilling), expected profits ($/kWh) and risk curves obtained from *a priori* activation values (Fig. 1b), one can decide during the planning phase if the project should go ahead or not. By communicating risk uncertainty and how the stakeholder is subjective (pessimistic or optimistic), rational decisions can be made.

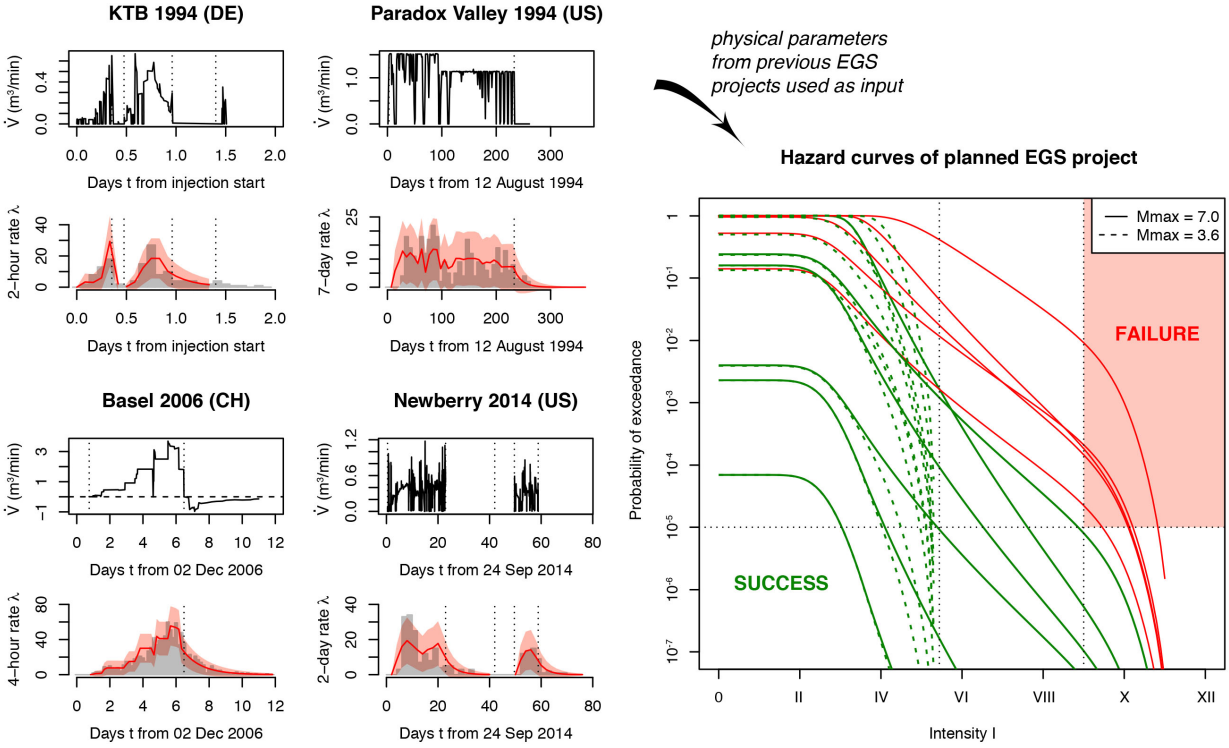

Fig. 1 (a) Induced seismicity time series (in grey) and model (in red); (b) Based on the hazard curves derived for an *a priori* induced seismicity activation level, should the planned EGS project go ahead?

References: Mignan, A. (2016), NPG, 23, 107-113, doi: 10.5194/npg-23-107-2016

Simulation of induced seismic ground motions using coupled geo-mechanical and seismic models

Bob Paap[1], Brecht Wassing[1], Dirk Kraaijpoel[1] and Loes Buijze[1]

1 TNO, the Netherlands, bob.paap@tno.nl

Geomechanical modelling packages such as FLAC[1] and DIANA[2] are well equipped to simulate the complex behavior of fault systems under changing stress fields. These packages cover a wide range of physical conditions, including large (finite) strains and non-linear constitutive relations, and can be run both in static mode for slowly evolving situations and dynamic mode for fast rupture processes. In comparison, seismic modelling packages such as SPECFEM2D[3] are limited to small (infinitesimal) strains and (poro-/an-)elastic materials, but within this limited domain run much more efficiently. By coupling geo-mechanical models to seismic wave propagation models, complex fault behavior can be simulated while the resulting seismic motions can be propagated to the far field with acceptable runtimes.

Here, we present an approach to model the seismic rupture on a fault, which intersects a producing gas reservoir, and the resulting outward propagation of seismic waves towards the surface. The modelling approach consists of three components. A 2D static numerical geo-mechanical model (FLAC[1] and DIANA[2]) is used to model the onset of fault reactivation caused by the reservoir pressure changes and the compaction of the gas reservoir. Once the nucleation of a seismic event is observed, the static model is switched to a dynamic mode, which is used to model the dynamic fault rupture process. The near fault deformation in the dynamic simulation is then transferred to SPECFEM2D by means of an equivalent force field. The wavefield is then propagated to the surface.

This approach is suited to determine the expression of specific source characteristics, resulting from, e.g., differences in fault configurations, in seismic records at varying distances from the source. From these simulations the design of seismic monitoring networks can be optimized. More detailed simulations will also allow a better interpretation of observed earthquake data and provide input to hazard and risk analyses from seismic signals at surface level, such as peak ground acceleration, frequency content, earthquake duration and amplification.

[1] Itasca. 2013. FLAC3D Fast Lagrangian Analysis of Continua in 3 Dimensions. User's guide. Itasca Consulting Group.

[2] TNO Diana, 2014. DIANA: Finite element program and User Documentation, version 9.6.

[3] J. Tromp, D. Komatitsch, and Q. Liu. Spectral-element and adjoint methods in seismology. Communications in Computational Physics, 3(1):1–32, 2008.

Modeling of earthquake interaction for induced seismicity

Antonio P. Rinaldi[1], Flaminia Catalli[2], Massimo Nespoli[3], Valentin Gischig[4], Stefan Wiemer[1]

1 Swiss Seismological Service, ETH Zurich , Switzerland, antoniopio.rinaldi@sed.ethz.ch; **2** Deutsches GeoForschung-Zentrum, GFZ – Potsdam, Germany; **3** Dipartimento di Fisica, Università di Bologna, Italy; **4** Swiss Competence Center for Energy Research, ETH Zurich , Switzerland

We explore the role of earthquake interactions during an injection induced seismic sequence. We first propose a 2D model, which considers both a transient pressure and the static stress redistribution due to event interactions as triggering mechanisms for induced seismicity. We produce more than one thousand of stochastic seismic catalogues that allow a probabilistic analysis of the problem. By calibrating the model against observations at the Enhanced Geothermal System (EGS) of Basel, Switzerland, we are able to reproduce the time behavior of the seismicity rate. In particular for Basel, we observe that considering earthquake interactions in the modelling can lead to a larger number of expected seismic events (24% more) if compared to a pressure-induced seismicity only. The increase of the rate is true particularly after the end of the injection activity, in accordance with the simultaneous increase of the Coulomb Index (CI, i.e. the percentage of events that occur in locations with positive, cumulative Coulomb static stress changes).
Then, we generalized the model for injection induced seismicity to a full 3D fluid flow and geo-mechanical-stochastic configuration, including stress transfer. We performed a sensitivity study on a generic injection case aimed at understanding the role of earthquake interaction when changing the width of the seismic cloud.
We conclude that implementing a model for estimating the static stress changes due to mutual event interactions increases significantly the understanding of the process.

Seismic and mass-movement processes stimulation modelling

Nodar Varamashvili, Tamaz Chelidze, Victor Chikhladze, Zurab Chelidze

Ivane Javakhishvili Tbilisi State University, M. Nodia Institute of Geophysics, Tbilisi, Georgia
nodar.varamashvili@tsu.ge

In this abstract, we present the results of the laboratory experiments on the mechanical initiation of mechanical instability (slip) with moisture change.

Experiments were conducted on a Burridge-Knopoff laboratory model for the system consisting of a fixed basalt plate, an upper moving platform and a single/two/three sliding basalt plate(s) (Fig.1). Plates were pulled by the upper platform. Experiments were conducted also on simple spring-slider system. In order to study the phenomena of stick-slip and mechanical stimulation under the influence of gravitational force we assembled a laboratory equipment with inclined and horizontal planes. We can impose an external periodic mechanical loading to sliding plate and at several points of fixed plate separately or jointly on both models. For modeling of stimulation of landslide with moisture changing an inclined equipment was assembled where we can change inclination angle from 0° to 80° and also the moisture of slipping body.

Stimulation and synchronization of instabilities in experimental systems were studies by recording acoustic emission, accompanying the slip events and an accelerometer was attached to each plate, which measured the x component of the acceleration. We can also measure pulling force in the spring-slider and Burridge-Knopoff experiments. In experiments Three-axial accelerometer MXR9500G/M and piezosensors were used. Experiments on the standard spring-slider system and Burridge-Knopoff system subjected to a constant pull and superimposed to it weak mechanical periodic force show that, at definite conditions, the system manifests the effect of phase synchro-nization of micro-slip events with the weak periodic excitation and triggering effect by prolonged excitation. The quality of stimulation and synchronization depends on the intensity and frequency of the applied field. With increasing external mechanical forcing reduced the waiting time before the slip (in gravitational experiments). In the landslide modeling experiments with moisture changing, we can not say that humidity increase causes decrease in the critical slip angle threshold of the experimental body. Here, as though, exists a threshold humidity when begins slip process.

We conclude that our laboratory experiments give a sound principal basis for interpretation of field data on the control of seismic and mass-movement regime by relatively weak natural or artificial perturbations.

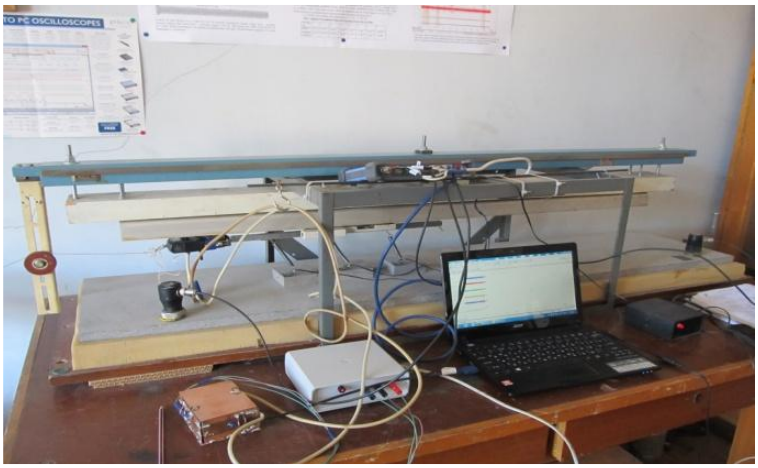

Fig.1. Burridge-Knopoff horizontal laboratory model

The impact of visco-elastic caprock on fault reactivation and fault rupture in producing gas fields

Brecht Wassing[1], Loes Buijze[1,2], Bogdan Orlic[1]

1 Netherlands Organisation for Applied Scientific Research - TNO, Princetonlaan 6, 3584 CB, Utrecht, The Netherlands, brecht.wassing@tno.nl; **2** HPT laboratory, Faculty of Geoscience, Utrecht University, Budapestlaan 4, 3584 CD, Utrecht, The Netherlands

In The Netherlands, gas is produced from over 150 onshore gas fields. In several dozen of these fields seismicity has been recorded during production. These seismic events are interpreted to be induced by pore pressure changes in the reservoir rocks, resulting in stress changes on faults within and in close vicinity of the gas reservoirs. Magnitudes of seismic events up to Mw 3.6 have been recorded in the Groningen field, and a trend of increasing seismic activity and magnitudes with ongoing production is observed. Understanding the underlying processes of the non-stationary seismicity in the Groningen field is crucial for the assessment and mitigation of seismic hazards during ongoing production in both the Groningen and smaller producing gas fields. In this study, we use a numerical geomechanical model in FLAC3D to analyze the relation between changes in reservoir pore pressures and associated reservoir and fault stress changes. We use a static geomechanical model to investigate the effects of reservoir and fault geometry, fault strength, initial reservoir (over)pressure and the presence of a visco-elastic (rocksalt) caprock on the timing of fault reactivation. Subsequently, we use a dynamic analysis in FLAC3D to analyze the nucleation of seismic events and the main characteristics of the fault rupture in terms of slip displacements, slip velocity, rupture area, event duration and stress drops. Modelling results show that reservoir and fault geometry, fault strength and the presence of the visco-elastic rocksalt influences the timing of fault reactivation and extent of fault rupture. Faults with significant offset are reactivated at an earlier stage of reservoir depletion than faults with no offset. However, related fault slip, rupture areas and stress drops are smaller as compared to faults with no offset, which are reactivated at a later stage of reservoir depletion. The presence of the rocksalt caprock further promotes fault slip and nucleation of seismic events at an early stage of depletion, whereas slip displacements, stress drops and rupture area are comparable to cases without visco-elastic caprocks.

Are we past peak pressure in Oklahoma?

Matthew Weingarten and Mark D. Zoback

Stanford University, Department of Geophysics, Stanford, CA, mweingarten@stanford.edu

In early 2016, the Oklahoma Corporation Commission (OCC) began the largest field-scale induced seismicity experiment in scientific history. Over a 10,000 km^2 area, designated the Area Of Interest (AOI), in central and northern Oklahoma, the OCC mandated a 40% reduction from 2014 injection volume for more than 600 injection wells. As of July 2016, injection levels have decreased below the mandated threshold. This mandate is aimed at reducing the likelihood of induced seismicity by reducing the reservoir pressure perturbation from injection. Several questions of importance remain: (1) where and over what timescale will reservoir pressure perturbation decrease? (2) where and over what time scale will induced seismicity rates respond?

To answer these questions we built a reservoir model which simulates past injection into the Arbuckle formation from 1997 - Nov. 2016. We then extend the reservoir model to simulate four future scenarios of AOI injection over the next ten years. The four modeled injection scenarios, are as follows: (1) assume the current reduction from 2014 levels continue over the full period, (2) injection is further reduced to pre-2008 levels, (3) injection rates return to 2014 levels by 2019, (4) all injection wells are shut-in for the entire period. To evaluate our model results, we define the term 'peak pressure' as the maximum reservoir pressure change a given point in space experiences through time. We hypothesize that once a given location is past 'peak pressure', the seismicity rate will begin to decline.

Under the current management scenario, we observe a leveling off of modeled reservoir pressure with some areas still experiencing an increase in reservoir pressure, albeit much more slowly than in past years. Scenarios 2 and 4, where injection rates are reduced further, we observe a reduction from 'peak pressure' in most of the region of interest. However, we do expect pressure diffusion to temporarily increase observed pressures at distance from managed injection wells. Sensitivity analysis simulating a range of reservoir permeabilities either lengths or shortens the delay time to reduced reservoir pressure at distance. Scenario 3, which gradually returns injection volumes to 2014 levels by 2019, exceeds peak pressure in all areas of the AOI by 2020, even in high-permeability scenarios, suggesting a return to past injection levels may yield a return to increased seismicity rates.

Fluid-Induced Seismicity – Comparison of Rate - and State - and Critical Pressure Theory

Friedemann Wenzel[1]

1 KIT Geophysical Institute, Germany, friedemann.wenzel@kit.edu

Induced seismicity as generated by the injection of fluid in a homogeneous, porous medium with faults with variable proximity to rupture conditions is simulated using rate- and state-dependent frictional fault theory (RST) of Dieterich (1994) and the critical pressure theory (CPT) developed by Shapiro (2015). In CPT the seismicity is proportional to the pressure rate but limited by the Kaiser Effect. There is no time delay between a change in pressure rate and change in seismicity. RST is more complex and includes a time delay between a pressure change and the seismicity. This is best seen by looking at the initial application of RST for modelling aftershocks. If the shear stress is changed instantaneously by a main shock the seismicity does not appear immediately in the area around the main fault where the stress change is large enough but evolves with time resulting in an Omori-type temporal distribution of seismicity. A step-wise change of pressure behaves in a similar way. Comparing both modelling approaches numerically at fixed location this delay can be significant. However, it is small where the seismicity is high and larger where it becomes small. The evolution of the total seismicity in the medium where fluid is injected with time is thus very similar with both modelling approaches so that RST and CPT provide very similar results (Fig. 1). This applies also for the case of pressure shut-in. The

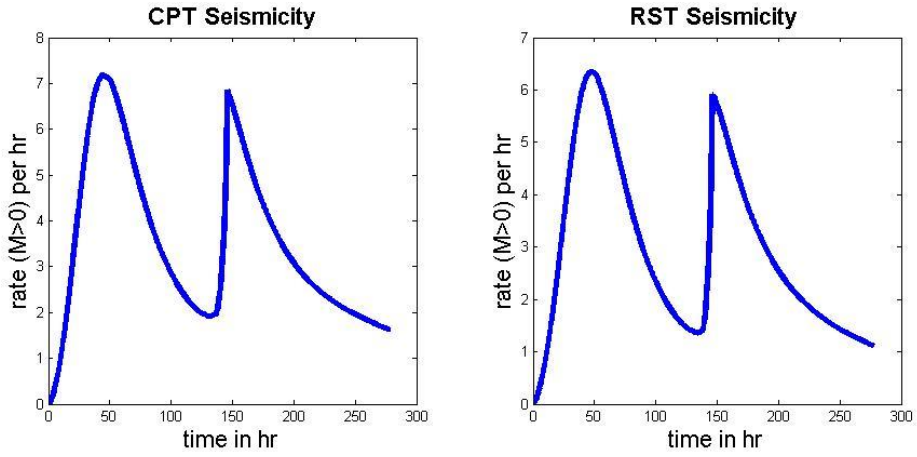

Fig. 1 Comparison between the CPT and RST results for total seismicity of a two-cycle injection with diffusivity D=0.1 m2/s and lower trigger threshold of 1 kPa after integration over the entire volume of fluid infiltration.

'free parameters' of CPT and RST can be specified in a way that both methods provide similar solutions. Moreover, the evolution of seismicity in RST is described by a Ricatti Equation, which allows for an analytic solution. The features of both theories after pressure shut-in are of particular importance as this time is important for the maximum magnitudes that can emerge. The post-shut-in seismicity is controlled by the diffusion constant of the pressure and the lower cut-off pressure below which no seismicity can be triggered. This applies to both theories and do not constitute a major difference. I show that, within reasonable approximations, RST coincides with CPT so that the numerical findings for particular cases are general features of RST.

Dieterich J (1994) A Constitutive Law for the Rate of Earthquake Production and its Application to Earthquake Clustering, J. Geophys. Res., vol. 99(B2), 2601-2618
Shapiro SA (2015) Fluid-Induced Seismicity, Cambridge University Press, p.75

On the physics-based processes behind production-induced seismicity in natural gas fields

Dominik Zbinden[1], Antonio Pio Rinaldi[1], Luca Urpi[1], Stefan Wiemer[1]

1 ETH Zurich, Swiss Seismological Service, Switzerland, dominik.zbinden@sed.ethz.ch

Induced seismicity due to natural gas production is observed at different sites around the world. Common understanding is that the pressure drop caused by gas production leads to compaction, which affects the stress field in the reservoir and the surrounding rock formations, hence reactivating pre-existing faults and induce earthquakes. Previous studies have often assumed that pressure changes in the reservoir compartments and intersecting fault zones are equal, while neglecting multi-phase fluid flow.

In this study, we show that disregarding fluid flow involved in natural gas extraction activities is often inappropriate. We use a fully coupled multiphase fluid flow and geomechanics simulator, which accounts for stress-dependent permeability and linear poroelasticity, to better determine the conditions leading to fault reactivation. In our model setup, gas is produced from a porous reservoir, cut in two compartments that are offset by a normal fault, and overlain by impermeable caprock.

Results show that fluid flow plays a major role pertaining to pore pressure and stress evolution within the fault. Hydro-mechanical processes include rotation of the principal stresses due to reservoir compaction, as well as poroelastic effects caused by the pressure drop in the adjacent reservoir. Fault strength is significantly reduced due to fluid flow into the fault zone from the neighbouring reservoir compartment and other formations. We also analyze the case of production in both compartments, and results show that simultaneous production does not prevent the fault to be reactivated, but the magnitude of the induced event is smaller.

Finally, we analyze scenarios for minimizing seismicity after a period of production, such as (i) well shut-in and (ii) gas re-injection. Results show that, in the case of well shut-in, a highly stressed fault zone can still be reactivated several decades after production stop, although in average the shut-in result in reduction of seismicity. In the case of gas re-injection, fault reactivation can be avoided if gas is injected directly into the compartment under depletion. However, accounting for continuous production at a given reservoir and gas re-injection at a neighbouring compartment does not stop the fault from being reactivated.

Abstracts Posters, Part II

Session 5

Scaled Experiments

Microseismic Observations in a Series of Hydraulic Fracture Experiments on Barre Granite

Bing Q. Li[1], Bruno M. Goncalves da Silva[12], Herbert H. Einstein[1]

1 MIT Dept. of Civil and Environmental Engineering, USA. bingqli@mit.edu **2** New Jersey Institute of Technology Department of Civil Engineering, USA

The work consists of a series of laboratory experiments in which 3" x 6" x 1" specimens of Barre granite with varying orientations of (one or two) pre-cut notches (see fig 1) were subjected to a constant vertical load of 0 or 5 MPa. The specimens were then loaded to failure with water pressure applied to the inside of the notches to produce hydraulically induced fractures. The cracking process was observed with high resolution and high speed photography, as well as acoustic emissions through an array of eight piezoceramic sensors with 200 kHz resonant frequency sampled at 5 MHz. The photos were used as visual tools to determine the extent of microcracking and cracking, and the AE were captured throughout the experiment.

It was found that, in general, damage and AE only occurred when the water pressure approached its peak value, and that the occurrence rate of AE increase dramatically towards crack initiation. Source location showed that the damage largely occurred where the cracks eventually propagated; however there were a number of instances where AE also occurred where the rock showed significant "white patching" i.e. microcracking but the crack did not propagate through this area. Moment tensor inversion showed that many of the AE events contained significant double couple components, even in areas where visually the crack appears to initiate in tension. Analysis was also performed to determine the extent to which events occurring in close succession were related to each other in location and source characteristics.

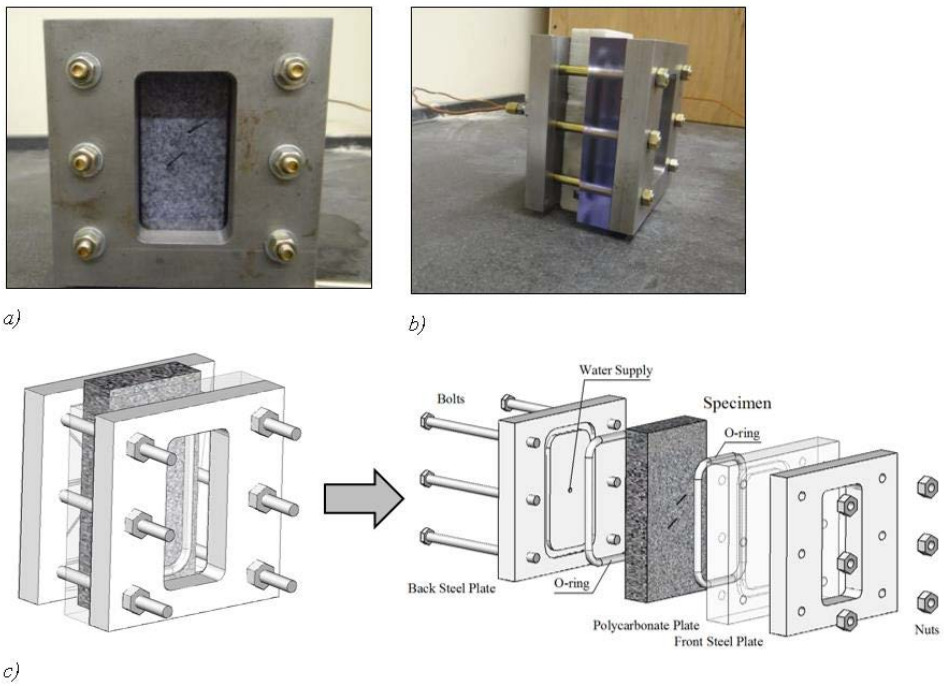

Fig. 1 Experimental Setup. Top figure shows photos of setup, bottom figure the schematic.

The effect of fluid injection on an experimental fault and its role on frictional stability and earthquake triggering

Marco M. Scuderi[1], Cristiano Collettini[1] and Chris Marone[3]

1 La Sapienza University of Rome, Italy marco.scuderi@uniroma1.it, **2** Penn State University, USA

Fluid overpressure is one of the primary mechanisms for triggering tectonic fault slip and human-induced seismicity. This mechanism is appealing because fluids lubricate the fault and reduce the effective normal stress that holds the fault in place. However, current models of earthquake nucleation imply that stable sliding is favored by the increase of pore fluid pressure, because the resulting decrease in effective stress tends to increase the friction stability parameter K=k/kc and thus promote stable sliding. Despite this apparent dilemma, there are few existing studies of the role of fluid pressure on frictional stability under controlled, laboratory conditions. Here, we describe laboratory experiments, conducted in the double direct shear configuration in a true-triaxial machine on carbonates and shale fault gouge, to: 1) evaluate the rate- and state- friction parameters and 2) study fault creep evolution as the pore fluid pressure is increased from hydrostatic to near lithostatic values. We show that the friction rate parameter (a-b) evolves from slightly velocity strengthening to velocity neutral and the critical slip distance, Dc, decreases from about 100 to 20 µm as pore fluid pressure is increased. Similarly, fault creep is slow (i.e 0.001µm/s) under hydrostatic boundary conditions and accelerates as pore fluid pressure approaches lithostatic values, where we observe episodic accelerations/decelerations that in some cases evolve to small dynamic events. These events are accompanied with an increase in fault porosity and permeability. Upon fault failure, fault slip velocity is controlled by fault zone mineralogy and permeability, with carbonates that showed fault failure at dynamic slip velocities (i.e. ~2mm/s), while shale failed by accelerated, but slow, shear slip (i.e. ~250 µm/s). Our data suggest that fluid overpressure can increase aseismic creep with the development of local frictional instability and dynamic rupture even for faults that are characterized by a velocity strengthening behavior, which indeed should favor aseismic creep. We show that fault rheology and fault stability change with fluid pressure, which suggests that a comprehensive characterization of these parameters is important for better assessing the role of fluid pressure in natural and human induced earthquakes.

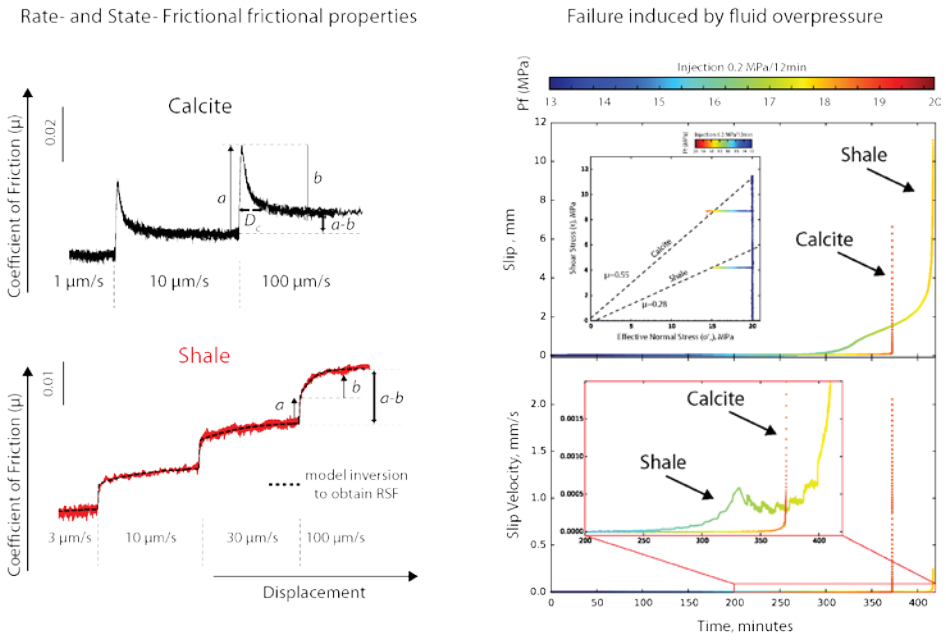

Fig. 1 Left hand panel shows the velocity dependence of friction for calcite and shale gouges characterized by a velocity strengthening behavior. Right hand side shows fault failure caused by fluid overpressure. To note that calcite gouge is characterized by dynamic slip velocity upon failure (i.e. peak slip velocity of 2mm/s) while shale gouge shows slow but accelerated fault slip (i.e. fault failure at 250 µm/s)

Micro-seismic monitoring during hydraulic-shearing experiments at the Grimsel Test Site

Linus Villiger[1], Valentin Gischig[2], Joseph Doetsch[2], Nathan Dutler[3], Hannes Krietsch[2] Florian Amann[2], Stefan Wiemer[1]

1 Swiss Seismological Service (SED), ETH Zurich, Switzerland **2** Swiss Competence Center for Energy Research – Supply of Electricity (SCCER-SoE), ETH Zürich, Switzerland **3** Center for Hydrogeology and Geothermics (CHYN), University of Neuchâtel, Switzerland

The In-situ Stimulation and Circulation (ISC) experiment at the Grimsel Test Site (GTS) is an ongoing inter-disciplinary project to study the pressure, temperature and stress changes in the rock mass due to hydraulic stimulation. In early 2017, the project enters the second phase, which includes the main stimulation experiment. It involves the high-pressure fluid injections into a fault zone along which slip will be induced (i.e. hydraulic-shearing). The experiment series was established to support research related to deep geothermal energy which should play a significant role in the Swiss energy mix by 2050 (Swiss Energy Strategy 2050).

In addition to comprehensive geological analysis and geophysical characterization, the first phase of the project included drilling of two 45 m deep injection boreholes (Fig. 1, light blue) drilled trough the targeted shear zones. Six suitable sections of 1 to 6 m length distributed over the two injection boreholes were identified for stimulation. During the experiment hydraulic processes, mechanical processes and induced micro-seismicity will be monitored with an unprecedented multi-sensor monitoring system.

The micro-seismic monitoring network consists of 14 acoustic emission sensors (bandwidth: 1 – 100 kHz, highest sensitivity at 70 kHz) placed in the surrounding tunnels (Fig.1, green cones, HS01-14). Eight acoustic emission sensors of the same type are distributed over four monitoring boreholes which run in parallel to the S3 shear zone (Fig. 1, green cones on pink lines), which will be stimulated. To allow an estimation of the magnitude of the recorded seismic events the uncalibrated piezo-sensors are complemented with calibrated accelerometers (bandwidth: up to 25 kHz, Fig.1 red cones) at five sensor positions. In addition to passive recordings, seismic sources in boreholes as well as hammer hits in the surrounding tunnels will be used for surveying transient seismic velocity changes throughout the experiment.

The hydraulic shearing experiment will be conducted beginning of February 2017. The analysis of the micro-seismic data should in a first step lead to the location of events. The combination of the various sub datasets should then shed light on stimulation processes such as fluid/fracture propagation and many more. First results will be presented at the 2017 Schatzalp Workshop.

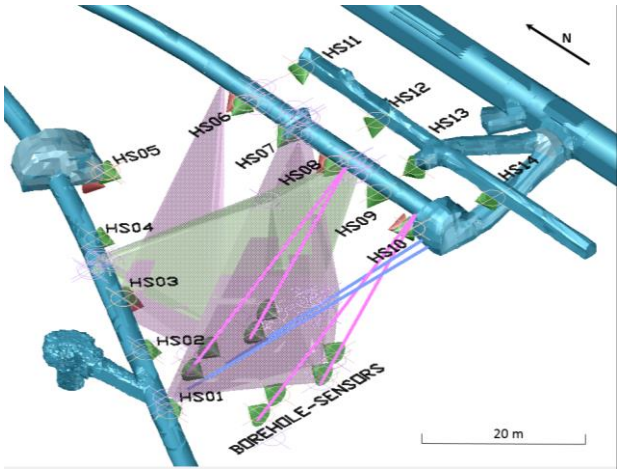

Fig. 1 Overview of the micro-seismic network at the Grimsel underground laboratory. Blue indicates the existing tunnels. Blue and pink colored lines represent the injection and monitoring boreholes. The shaded planes mark the sub vertical shear zone S1 (purple) striking North-East South-West and the sub vertical shear zone S3 (green) striking East-West.

Abstracts Posters, Part II

Session 6 and 7

Monitoring and Analysis of Induced Seismicity

Earthquake source-type variations at the Salton Sea geothermal field, California

Stephan Bentz[1], Patricia Martínez-Garzón[1], Grzegorz Kwiatek[1], Marco Bohnhoff[1,2], Joerg Renner[3]

1 GFZ Potsdam German Research Centre for Geosciences, Section 4.2: Geomechanics and Rheology, Germany, bentz@gfz-potsdam.de; **2** Free University Berlin, Institute of Geological Sciences, Germany; **3** Ruhr-University Bochum, Institute of Geology, Mineralogy and Geophysics, Germany

Over the last decade a large number of induced earthquakes have raised the public awareness for operations involving fluid injection into the subsurface, such as the exploitation of geothermal reservoirs and unconventional hydrocarbon reservoirs. Understanding the source mechanisms of triggered and/or induced earthquakes can help mitigating risks associated with injection activities and optimizing monitoring processes. Full moment tensor (FMT) inversion has become a central tool for characterization of faulting associated with earthquakes. However, the analysis of small (e.g. M_w < 3.5) events by full waveform approaches to FMT inversion is often hindered by poor signal-to-noise ratio in low frequency bands. In this study, we investigate the source mechanisms of 100 earthquakes at the Salton Sea geothermal field, with magnitudes ranging from 2.2 to 5.1, using combined data from a local network of shallow boreholes containing short period instruments, and regional broadband stations. We employ two FMT inversion techniques using full waveforms and P-wave first motions and compare their performance. Results show that for the lower half of the considered magnitude range the classical FMT inversion using waveforms is unable to reproduce the observed seismograms to a detail sufficient for successful FMT estimations. Therefore, we focus here on the FMT inversion from P-wave first motion amplitudes. Results are refined using the relative FMT inversion technique hybridMT to account for poorly known path and site effects. We find that the majority of shallow earthquakes contain significant non-double-couple (NDC) components, indicating complex, non-shear rupture processes. Events located near active injection wells show positive NDC components, representing tensile opening, whereas more distant earthquakes exhibit smaller NDC components (see Figure 1). Deep earthquakes -possibly unrelated to the reservoir formation- are found to be almost pure shear failures. The prominent NDC components near the wells may be related to large pore pressure changes and thermal contrasts between rock matrix and injected fluid, which should decay as distance from the well increases, resulting in more common shear ruptures. This observation highlights the effect of fluid injection on the source characteristics of induced seismicity. These features become only visible after including local sensors in the analysis. It is recommended that in the future field operators use this method to track long-term reservoir development and stimulation, as well as to automatically assess and predict associated seismic hazards.

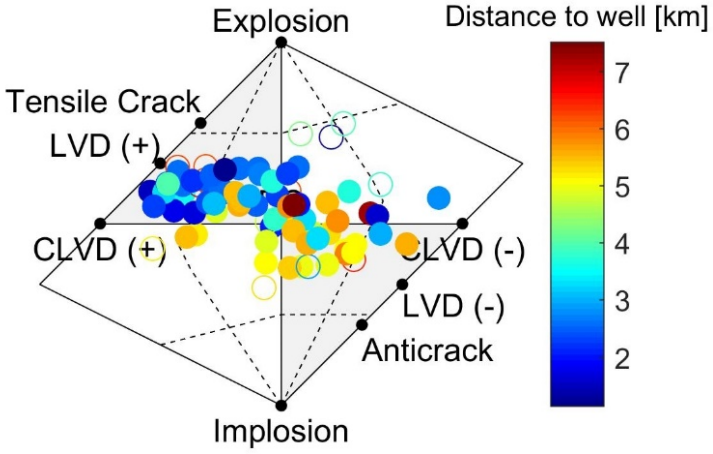

Figure 1: Hudson source-type representation of the full moment tensor solution, based on P-wave first motion polarities and amplitudes, color coded by the epicentral distance to the nearest injection well. Hollow points indicate events, where the RMS error of the amplitude exceeded our threshold.

Detecting and locating acoustic emissions from hydraulic fracturing experiments at Äspö Hard Rock Laboratory (Sweden)

José Ángel López Comino [1], Simone Cesca [1], Sebastian Heimann [1], Francesco Grigoli [2], Claus Milkereit [1],Torsten Dahm [1], Arno Zang [1]

1 GFZ German Research Centre for Geosciences, Potsdam, Germany, Simone Cesca, cesca@gfz-potsdam.de; **2** ETH Zurich, Swiss Seismological Service, Switzerland

An in situ hydraulic fracturing underground experiment (Nova project 54-14-1) was performed at the Äspö Hard Rock Laboratory (Sweden), aiming at optimizing geothermal heat exchange in crystalline rock mass. The basic idea of the experiment was to compare hydraulic fracturing growth and induced seismicity under controlled conditions in a horizontal borehole 30 meter long for different fluid-injection schemes (continuous, progressive, pulse injection). A near field network with 11 acoustic emission (AE) sensors was installed. The piezo-electric sensors have their highest sensitive in the frequency range 1 to 100 kHz, but sampling rates were extended to 1 MHz. Recently developed automated full waveform detection and location algorithms are applied and we present the results obtained during the conventional, continuous water-injection experiment HF2 (Hydraulic Fracture 2).

The earthquake detector is based on the stacking of characteristic functions. It follows a delay-and-stack approach, where the likelihood of the hypocenter location in a pre-selected seismogenic volume is mapped by assessing the coherence of the P onset times at different stations. Smooth characteristic function calculated from normalized amplitude envelopes allows reducing the spatial and temporal sampling. This improves the computational performance of the algorithm and allows its application to high-sampling data as a detector. Most detection is concentrated during the fluid injection, at the time of the fracturing and each refracturing stages. A low detector threshold is chosen, in order not to loose weaker events. This approach also increases the number of false detections. Therefore, the dataset has been revised manually, and detected events classified in terms of true AE events related to the fracturing process, electronic noise related to 50 Hz overtones, long period and other signals. Electronic noise is found temporally associated with the fluid injection stages. Its occurrence hinders the search of fracturing events, requiring a posteriori classification. Anthropogenic noise, long period and other signals are also detected throughout the whole experiment. For such cases, the values of amplitude of the characteristic function are usually low, so that these events could be easily removed by increasing the detection threshold.

The location of the AE events is further refined using a more accurate waveform stacking method which uses both P and S phases. The proposed method is fully automatic and only requires a few control parameters, which can be chosen following a trial and error approach on a small subset of the largest events. A 3D grid is generated around the hydraulic fracturing volume and we retrieve a multidimensional matrix, whose absolute maximum corresponds to the spatial coordinates of the seismic event. The relative location accuracy is improved using a master event approach. Relative magnitudes are finally estimated upon the decay of the maximal recorded amplitude from the AE location. The resulting catalogue is composed of more than 4000 AEs. Their hypocenters are spatially clustered in a planar region, resembling the main fracture plane; its orientation and size are estimated from the spatial distribution of AEs.

Advanced Real-time Monitoring for Induced Seismicity

John Clinton[1], Francesco Grigoli[2], Maren Boese[2], Tobias Diehl[2], Toni Kraft[2], Marcus Hermann[2], Philipp Kaestli[2], Luca Scarabello[2], Stefan Wiemer[2]

1 Swiss Seismological Service, ETH Zurich, Switzerland, jclinton@sed.ethz.ch; **2** Swiss Seismological Service, ETH Zurich, Switzerland

It is common practice to operate temporary dense seismic networks during background monitoring and stimulation phases of geothermal projects where induced seismicity can be expected. We propose a comprehensive approach to automatic monitoring of induced seismicity sequences, extending a standard regional seismic network infrastructure to the denser local network configuration. The main advantages of using existing an operational seismic network infrastructure is we can 1) use existing well-established and continually exercised procedures to manage data and metadata and create catalogues; and 2) effectively combine the existing background network with the new densified network. Simply applying standard network monitoring tools at regional level to induced seismicity sequences is not sufficient – without significant configuration optimisation and indeed building new tools, it is not possible build sufficiently complete catalogues and to accurately characterize all events – for robust sequences with very short inter-event spacing, many events can be missed, and it is challenging to accurately locate and quantify seismicity at magnitudes well below the traditional resolution of regional networks.

We outline an approach where we integrate multiple new features tailored to induced seismicity within a routine monitoring approach using a standard automatic software framework, *SeisComP3*. We improve detection capability and absolute location tools, and compliment the event catalogue in close to real-time using cross correlation to lower the magnitude of detection and relative locations and relative magnitudes to better understand emerging seismicity patterns. Results from this infrastructure can significantly improve real-time hazard assessment for the induced seismicity community.

Evaluation of Microseismic Array Performances (EMAP): Case Study of a Deep Metal Mine Monitoring Network

Francesca De Santis[1,2], Isabelle Contrucci[1], Armand Lizeur[1], Alice Tonnellier[1], EmanuelaMatrullo[3], Pascal Bernard[4], Anders Nyström[5], ShahramMozaffari[5]

1 INERIS, France, francesca.de-santis@univ-lorraine.fr; **2** GeoRessources-Université de Lorraine, Mines Nancy, France; **3** EOST, France; **4** IPGP, France; **5** Boliden, Sweden

Underground mines can experience certain levels of microseismic activity as a consequence of stress perturbations and rock damages due to mining excavations. The understanding of the complex interaction between state of stress modifications and the generation of induced seismicity is a fundamental purpose in order to control the rate of seismicity and guarantee mine workers safety. In this context, microseismic monitoring in active mines has become a worldwide consolidated tool for observing and analyzing mining-induced seismicity. The performance of seismic networks, in terms of events detectability and location accuracy, is, thus, one of the basic concerns. However, a good performance of seismic networks is often hard to achieve, especially in the complex environment of active mines characterized by very low magnitude seismic events and where network geometries are limited by available galleries and mine production plans.

In this work we present a simple methodology for the evaluation of microseismic array performances (EMAP). For a given network geometry in a monitored volume, EMAP determines: (i) the minimum events magnitude that can be detected and located and (ii) the distribution of predicted location errors for a specific magnitude. Given a velocity model and the attenuation relationship, for several virtual seismic sources regularly located within the monitored volume, EMAP estimates synthetic amplitudes, wave arrival times and polarization angles at each seismic probe. Based on the background noise at stations, signal-to-noise ratios (S/N) are computed per each couple source-receiver. The magnitude of completeness is, then, determined comparing the S/N ratios with imposed threshold for detection and location, respectively. In addition, for the estimation of expected location errors, initial synthetic values of arrival times and polarization directions are perturbed with errors, which follow a Gaussian distribution. Performing several simulations per each grid point, location errors are then given by the average value of the difference between the synthetic locations and the ones determined after input data alteration.

We applied EMAP algorithm to the underground seismic network of the deep metal mine of Garpenberg (Sweden), which is equipped with both one-component and three-component seismometers, over a monitored area of 64×10^6 m^3. Considering an empirical attenuation law for amplitudes, an homogeneous velocity model and determining the noise level at stations from real records, we tested the algorithm for different geometries of the monitoring network. Detectability performances were evaluated in the local magnitude range $0 \leq M_L \leq -4.5$, while location errors were determined for a M_L of -2. The detectability performances are in agreement with magnitudes of real microseismic events normally recorded and located in the site. Results showed smaller location errors in the central area of the seismic network, which is around 1200 meters below ground surface, where source points are more constrained. Geometrical effects in detection and location performances are observed and caused by the heterogeneous locations of the stations due to exploitation constrains that prevent a complete optimization of the network. As expected, performances are improved, both in terms of events detectability and location accuracy, for network configurations when increasing the number of seismic stations.

These tests showed that EMAP works properly not only for the performance evaluation of existing arrays, but also for defining efficient network geometries that may significantly reduce initial location errors in complex sites. Besides the application to local underground arrays our methodology can be also suitable for regional earthquake monitoring networks.

Automated microseismic event detection and location algorithms: Picking vs Waveform based methods

Francesco Grigoli[1], Maren Böse[1], Luca Scarabello[1], Tobias Diehl[1] , Stefan Wiemer[1] and John F. Clinton[1]

1 ETH Zurich, Swiss Seismological Service (SED), Switzerland, francesco.grigoli@sed.ethz.ch

Microseismic monitoring is extensively employed in different underground industrial activities related to the production of energy, such as hydrocarbon production and natural gas storage, geothermal energy exploitation or mining. Since these activities can potentially generate induced seismicity, they require the deployment of dedicated microseismic monitoring networks. If well designed, these monitoring systems allow the detection of very weak earthquakes, even in the presence of strong seismic background noise. Improved detection performance, however, will generate extremely large seismic event catalogues and, for this reason, noise tolerant and fully automated data analysis procedures must be established. Furthermore, microseismic sequences are often characterized by multiple events with short inter-event times or overlapping events; in this case, correct phase identification and event association are challenging, and errors can lead to missed detections and/or reduced location resolution. To overcome these problems, various waveform-based methods for the simultaneous detection and location of microseismicity have been proposed during the last years. These methods exploit the coherence of the waveforms recorded at different stations and do not require any automated picking procedure. Although the adoption of such approaches led to recent promising results, an extensive comparison with sophisticated pick-based detection and location methods is still lacking. In this work we aim to fill this gap by a systematic comparison of the performance of one waveform-based method (LOKI, Grigoli et al. 2013) and two pick-based detection and location methods (SCAUTOLOC and SCANLOC) implemented in the SeisComP3 software package. SCANLOC is a relative new approach used to detect and to locate local and regional earthquakes. The method is based on a cluster search algorithm to associate detections to one or many potential earthquake sources. While the cluster search itself is based on P-phases only, in a second step S-phases are also associated and used for locating the earthquake. Once a seismic event is identified, its location is refined using the NONLINLOC code (Lomax et al. 2000) and a more detailed velocity model. We compare the performance of LOKI and SCANLOC with a standard automated pick-detection and location procedure, using the SeisComP3 SCAUTOLOC module. We analyze the performance of the three methodologies for a synthetic dataset as well as for the first hour of continuous waveform data, including the Ml 3.5 St. Gallen earthquake, recorded by a dedicated microseismic network deployed in that area. For the second dataset we compare our detection and location results with a more complete catalogue based on waveform template matching and with a manual revised catalogue.

References:

Grigoli et al. 2013: Automated Seismic Event Location by Travel-Time Stacking: An Application to Mining Induced Seismicity, Seismological Research Letters

Lomax et al. 2000: Probabilistic earthquake location in 3D and layered models: Introduction of a Metropolis-Gibbs method and comparison with linear locations, in Advances in Seismic Event Location

Reservoir properties and wastewater induced seismicity at the Val d'Agri oilfield (Italy) shown by 3-D passive seismic tomography

Luigi Improta[1], Samer Bagh[1], Pasquale De Gori[2], Luisa Valoroso[2], Marina Pastori[2], Davide Piccinini[3], Mario Anselmi[1], Mauro Buttinelli[1] and Claudio Chiarabba[2]

1 INGV Department of Seismology and Tectonophysics, Rome, Italy, luigi.improta@ingv.it; **2** INGV-CNT, Rome Italy; **3** INGV Department of Pisa, Pisa, Italy

The oilfield of Val d'Agri in southern Italy is the largest in onshore Europe. Oil and associated gas are extracted at 2-3 km depth from a high-productivity reservoir consisting of fractured, low-porosity thrust-related limestone anticlines of the Apulia Carbonate Platform (ACP). Co-produced wastewater has been injecting by a high-rate well that induced swarm microseismicity (ML ≤ 2.2) since the initiation of disposal activity in 2006.

We performed a high-spatial resolution tomography to investigate the reservoir structure and properties and to precisely locate and track natural and induced seismicity. We used nearly 1200 natural and induced earthquakes (ML≤3.2) recorded at up to 60 permanent and temporary seismic stations. Vp and Vp/Vs images, which agreed with subsurface data, provide valuable insights into lithological changes, fracture density and pore fluid pressure in the Apulian hydrocarbon and aqueous carbonate reservoirs. Relevant findings are: (i) a zone of low Vp, high Vp/Vs under the injection well that represents a fluid saturated fault zone ruptured by the swarm-like seismicity; (ii) high Vp/Vs in correspondence of culminations of the ACP that represent saturated, liquid-bearing zones of the hydrocarbon or aqueous reservoirs; (iii) a region of very-low Vp and low Vp/Vs in the southern sector of the oilfield that we ascribed to a highly fractured and depleted zone characterized by significant hydrocarbon withdrawal, and (iv) very-high Vp zones that mark the transition from limestone to dolomitic rocks of the ACP.

Reservoir properties (fracture density and pore fluid pressure) and inherited structures formed during Pliocene compression play a primary role on the occurrence of natural and induced microseismicity that concentrates at 2-5 km depth in the ACP. We propose a comprehensive picture of the injection-linked swarm seismicity obtained by integrating reservoir-scale tomographic images with high-precision hypocentral locations, subsurface information, stress data and injection curves. The driving mechanism for inducing slip events is the channeling of pore pressure perturbations through a high permeable fault zone hosted by the fractured and saturated injection reservoir. The ruptured zone relates to a Pliocene reverse fault that is optimally oriented in the current SW-NE extensional stress field. Pore pressure build up reactivated with normal mechanisms small faults that have diameters lower than 150 m and slip less than a few mm. The ruptured zone measures 2 km along strike and 4 km along dip and is restricted vertically by low permeability and ductile formations.

At a general scale, our study underlines the benefits of using high-spatial resolution passive seismic tomography for characterizing hydrocarbon reservoirs and investigating the driving mechanisms of wastewater induced seismicity.

Scaling of seismic response to reservoir impoundment

Abror Karimov[1] Jean-Robert Grasso[1]

1 ISterre,Osug, université de Grenoble-Alpes, France, jean-robert.grasso@univ-grenoble-alpes.fr;

We analyze the seismicity patterns in the vicinity of the top 30 largest French reservoirs. Because a comprehensive seismic catalogue (SisHex, Mc>2.5 1962-2009) is only available since 1962, we select reservoirs with 1960-1995 impoundment dates in order to analyze the seismicity in a 20 yrs time window after the reservoir impoundment. Because most of the impoundments were achieved in the late 60's, we were unable to test seismicity changes after-before reservoir filling. Accordingly we aim to detect seismicity patterns around reservoirs that will help to classify seismicity as related to reservoir impoundment or as related to tectonics seismicity. For distance range we use both 10, 30, 50 km and 1L, 3L, 10L distances from the reservoir. Similarly to earthquake interaction analysis, we test (L), the reservoir length, (the equivalent of mainshock fault length), as the characteristic dimension that drives the stress change pattern induced by the reservoir impoundment. Such a working hypothesis corresponds to test how the reservoir size possibly impacts on the reservoir triggering power and on the M_{max} value of reservoir induced seismicity.
For mainshock-aftershock interactions, the size of the impacted area/volume (the triggering zone) is mapped by static stress perturbations in the mainshock near field. This later is estimated to be in the 1L-3L range for aftershock triggering. One must note there is a lack, for now, of consensus on the a-priori distance to be selected to relate a given earthquake to a given reservoir impoundment. Accordingly, we test the triggering pattern around reservoir in the continental France using both 10, 30, 50 km and 1L, 3L, 10L distances from the reservoir. The reference, for tectonic seismicity background (as a far field seismicity) we used, is the seismicity within 10L and 50 km distances from the reservoir. For all the reservoirs we analyzed the triggering patterns by (i) the impacted earth crust volume, (ii) the role of reservoir size parameters (volume, surface, length, depth) and (iii) the earthquake patterns (M_{max}, Numbers)
We define reservoir induced seismicity as earthquake sequence that occurs within 1L or 10 km distances from the reservoir lake. It allows to tests which parameters of the reservoir size drive or do impact the seismicity patterns (triggering, M_{max}, number, time and distance) and how the normalized distance hypothesis (reservoir length) may help to clarify triggered seismicity patterns. We assume 1L, 10 km distance as robust near field reservoir effect, and 10L, 50 km as far field null effect of reservoir stress changes on seismicity.
We find that 15% of the reservoirs, (6 reservoir dams), trigger seismicity within 1L, 20 yrs space time window, 9 triggers within 10km distances. For 65% (23 reservoirs) of triggering within 30km, there are 40% (13) of triggering within 3L distance. 100% of triggers are recovered for both 10L and 50km distances. The reservoirs that trigger in the near field are larger as estimated by length values than the non-triggering others, both for triggering in 1L and 10km. The 2.5-4.7 M_{max} values do not correlate with reservoir parameters. In an attempt to extract thresholds for triggering from reservoir parameters, Length-Volume pairs isolate more than 80% (5/6) of 1L triggering, with one false alarm. For the Km distance analysis, Length-Volume thresholds only succeed to extract 30% of 10km distance triggering. Note that using a single length threshold allows for 5/6 (80%) triggers in 1L with 2 false alarms. To achieve such a 80% (7/9) success rate for triggers using the 10 km distance we record 14 false alarms. It supports to be more difficult to define efficient thresholds for triggering, using absolute rather than normalized distance triggering.
On the 6 lake reservoirs we identified as triggering in 1L distance, 4 case studies correspond to previously referenced RIS cases. For the Serre-Poncon reservoir, we suspect the small M_{max}=2.8 is the main reason for not referencing this case study as RIS case. Except for the one case that cumulates low values for volume and surface and depth and length values, each of the five dams that trigger within 1L distance are ranked in the top 3 French reservoir for at least one of the reservoir parameter values.

Probabilistic assessment of seismic catalogue completeness with application to the Groningen Field

Dirk Kraaijpoel[1]

[1]TNO, The Netherlands, dirk.kraaijpoel@tno.nl

Seismic networks are usually designed to have a certain level of completeness in terms of magnitudes. This means that within a certain area of interest, all seismic events with a magnitude greater than some magnitude-of-completeness (Mcn, a design parameter for the network) should be guaranteed to be detected. In practice, the performance of a network will vary in time and space due to factors such as varying noise conditions, operational issues, and the particular spatial configuration of both network stations and rock/soil conditions. The probability of detecting an event with a specific magnitude will therefore vary in both time and space. Assuming a significant seismicity rate, many events lower than Mcn will be detected. In fact, the greater part of the seismic catalogue may consist of events below Mcn. Also, if the network was well designed, the actual magnitude-of-completeness of the observed catalogue (Mcc) may be well below the design value Mcn.

This contribution proposes a probabilistic method to assess the completeness of a seismic catalogue Mcc using the detection (hit/miss) data obtained with the operating network. Rather than a distinct detection threshold, the method uses a detection probability function that it is calibrated to the available data. The combination of the detection probabilities for all stations provides a detection probability map for the entire network. In a probabilistic treatment the concept of a precise magnitude-of-completeness ceases to exist and should be replaced with a definition such as the one used in Figure 1. Alternatively, rather than by means of a threshold magnitude Mcc, the completeness of a catalogue may be described by means of a fraction as a function of magnitude. This is a very useful description for further analysis and forecasting of seismic catalogues.

The proposed method is illustrated with a case study on the historic induced seismicity catalogue of the Groningen Field, see also Figure 1.

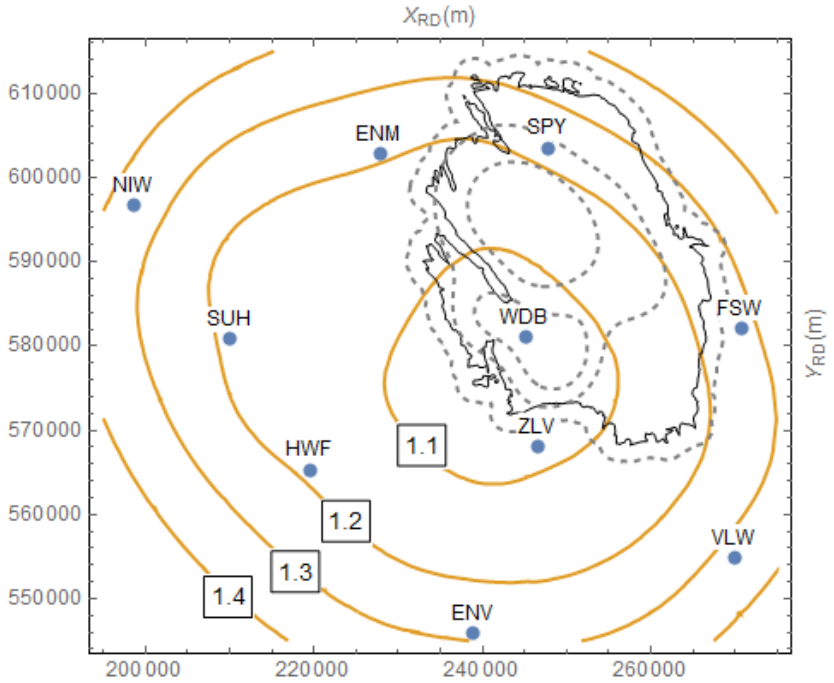

Fig. 1 Magnitude of completeness contours for the Groningen borehole network in the period 2010-2014, based on a probabilistic model for event detection. Magnitude of completeness in this Figure is defined to be the lowest magnitude that has a 95% probability of being detected in 3 or more of the borehole stations (ENM,SPY,NIW,SUH,WDB,FSW,ZLV,HWF,VLW,ENV). Solid black line: field contour; dashed grey lines: seismic zones according the KNMI seismic hazard model.

Induced Seismicity at the geothermal project Schlattingen, CH.

Toni Kraft[1], Tobias Diehl[1], Thessa Tormann[1], Marcus Herrmann[1] & Bernd Frieg[2]

1 Swiss Seismological Service, ETH Zurich, Switzerland, kraft@sed.ethz.ch; **2** Nagra, Wettingen, Switzerland

The geothermal project in Schlattingen was privately initiated by a vegetable farmer in 2007 aiming to reduce the heating costs for his greenhouses. A first vertical borehole (SLA-1) was drilled to a depth of 1508 m (TVD) into the crystalline basement by Jan. 2012. After an intense testing and well-logging campaign, the well was back-cemented to a level of 1185 m (TVD) and the selected target aquifer in the Upper Muschelkalk chemically stimulated in Oct. 2012. A long-term pumping test confirmed a successful increase of the transmissivity in the aquifer by one order of magnitude and yielded flow rates of about 6 l/s and water temperatures around 62 °C. After an evaluation and planning period, a second deviated well (SLA-2b) with a 735 m long sub-vertical section was drilled into the Muschelkalk aquifer. Massive mud losses which occurred when the deepest part of the well was drilled between 19-24. Apr., 2013, were confirmed to be related to a high-permeable fault zone with fracture apertures up to 1 cm in the subsequent well logging program. Acid stimulations of the open-hole section in May 2013 and February 2015 only slightly increased the pre-stimulation flowrates to 8 l/s, since most of the injected fluids (deluded dichloridic acid) may have gone into the high-permeable fracture zone in the deepest wellbore section. Geothermal greenhouse heating started in test operation in December 2016.

The Swiss Seismological Service (SED) monitored the end of the drilling phase of SLA-2b and the two acid stimulations in May 2013 and February 2015 using a local surface network. Between April and July 2013 a borehole seismometer was installed in SLA-1 at a depth of 1185 m (TVD) only 0.3 to 1.0 km away from the subvertical section in the Upper Muschelkalk aquifer. More than 400 microearthquakes of magnitude between ML0.4 and ML-2.5 were detected using the recently implemented template matching technique of the SED (see abstract of Herrmann et al.). About 70 of these events could be located using the surface network. The single-event locations aline in a NW-SE direction in agreement with the orientation of major fault systems in the region.

In our paper we report on relative relocations and statistical analysis of the induced sequences and discuss the results in the light of the hydraulic activities performed at the well. Our analyses document the first well-monitored case of drilling induced seismicity in Europe.

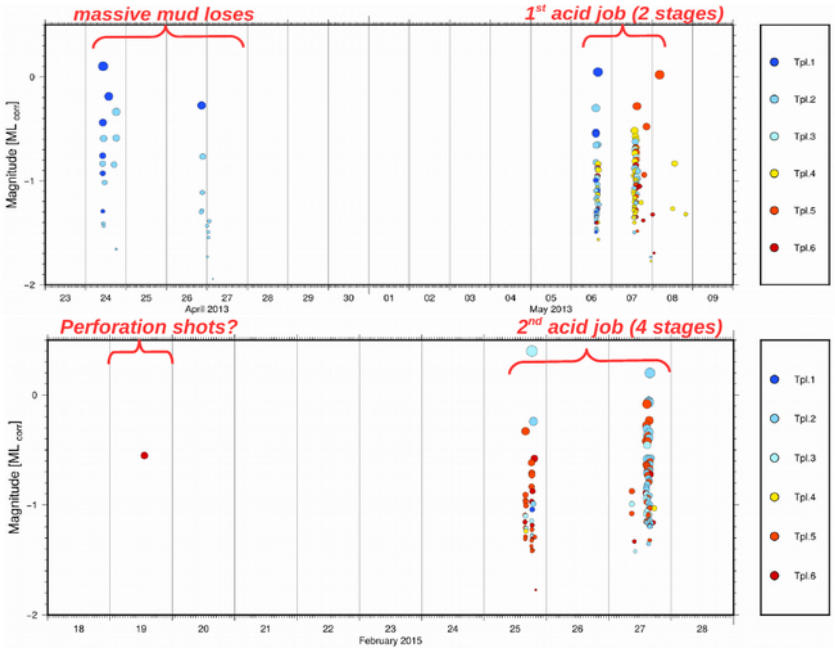

Fig. 1 Timeline of the induced microearthquakes during drilling and 1st acid stimulation in 2013 (top), and after perforation shots and 2nd acid stimulation in 2015 (bottom). Detections were obtained by template matching at a surface station (QSLA3) in 2.5km distance. Colors represent the 6 templates used.

Local event tomography in the Kiirunavaara iron ore mine, Sweden

Björn Lund[1], Karin Berglund[1], Ari Tryggvason[1], Savka Dineva[2], Linda Jonsson[3]

1 Uppsala University, Uppsala Sweden, bjorn.lund@geo.uu.se; **2** Luleå Technical University, Luleå, Sweden; **3** LKAB, Kiruna, Sweden

The Kiirunavaara mine in northernmost Sweden is one of the largest underground iron ore mines in the world. The ore body is a magnetite sheet of 4 km length, with an average thickness of 80 m, which dips approximately 55° to the east. The mine has been in operation since the 1890s and went from open pit to underground mining in the 1950s. In 2007-2008, when mining reached a depth of approximately 670 m, the mine became seismically active. Current mining production is at a depth of 785 – 855 m. The mining method is sub-level caving and the production in recent years is approximately 28 million tonnes of ore per year.

The mine currently has a seismic monitoring system of 204 geophones, a mixture of uni- and tri-axial, which during 2015 recorded on average approximately 1,000 local seismic events per day. The events are of various origins such as shear slip on fractures, non-shear events, and blasts, with magnitude estimates up to 2.5. The events occur mostly in the part of the mine where mining activities are most intense, but also in the slowly deforming hanging wall.

In this study we use data from approximately 1.2 million mining induced events which occurred between May 2013 and January 2016 in the southcentral part of the mine. A subset of events with at least 7 phases, less than 180° azimuthal gap and at least 6 geophones above and below is selected for tomography. We use manually picked P- and S-waves in the tomography and we require that both phases are present as we found that events from the routine automatic processing need screening for anomalous P- versus S-travel times, indicating occasional erroneous phase associations. For the tomography we use the 3D local earthquake tomography code PStomo_eq (Tryggvason et al., 2002), which we adjusted to suite the mining scale. The study volume is 1.2 x 1.8 x 1.8 km and the velocity grid size is 10x10x10 meter. The Vp/Vs ratio is fixed at 1.77 in the first iterations but then allowed to vary freely.

Checkerboard tests indicate that the resolution vary from approximately 40 m in the central areas to 80 m further out, in agreement with numerical estimates of Fresnel zone sizes. The tomographic images show clearly defined regions of high and low velocities. Low velocity zones are associated with mapped clay zones and areas of mined out ore, and also with the near-ore tunnel infrastructure in the foot-wall. We also see how the low S-velocity anomaly continues to depth below the current mining levels, following the inferred direction of the ore. The tomography shows higher P- and S-velocities in the foot-wall away from the areas of mine infrastructure.

We relocate all 1.2 million events in the new 3D velocity model. The relocation significantly enhances the clarity of the event distribution in space and we can much more easily identify seismically active structures. One example of this is the clarity with which deformation of the ore-passes is correlated with the intensity and distribution of relocated seismic events. The relocations also show more structures in areas of the mine where rock stability is a significant problem.

The large number of events makes it possible to do detailed studies of the temporal evolution of stability in the mine. We present preliminary results of time-lapse tomography in an area where a few events of magnitude 2+ occurred in September 2015.

Constraining location depth of induced seismicity in the complex 3D velocity structure of the Groningen gas field

Volker Oye, Ben Dando, Sonja Greve, S. Peter Näsholm, Andreas Wüstefeld, Daniela Kühn

NORSAR, Kjeller, Gunnar Randers vei 15, Norway, volker@norsar.no

The Groningen field in the Northeast of the Netherlands is Europe's largest gas field, which started production in 1963. In recent years, the amount of induced microseismicity felt by the local population has increased and is raising public concern. In order to estimate seismic hazard and risk, the seismicity needs to be located adequately such that events can be related to faults identified in active seismic data, and to distinguish between events within the reservoir and above/below the reservoir. The seismic velocity structure at the Groningen field is very complex, with large impedance contrasts, faults and multiple thin salt layers. This complexity is recognized in observations of real data, both at the near surface (using a dense borehole network at 50-200 m depth) and in deep boreholes deployed with geophones in and above the reservoir.

Arrival times of different seismic phases are generally difficult to interpret on the seismograms from the deep borehole receivers, because of the variety of reflected, refracted and converted phases, which are partly superimposed with direct phases as they arrive almost simultaneously. To overcome this challenge, we have computed synthetic seismic waveforms using the SW4 3D viscoelastic Finite Difference (FD) wave equation solver which is accurate to the 4th order in space and time. To obtain realistic and comparable synthetic seismic waveforms, we used a central frequency of 50 Hz, sampled the model with 1.2 m spacing in 3D, and applied the most commonly observed normal faulting source mechanism. We then investigated movies of the spatial divergence and curl of the synthetic seismic wavefield to understand the moveouts and amplitude behaviour of the different seismic phases, depending on depth and distance to the borehole sensors. However, to locate seismic events based on phase picking, we still require phase arrival travel-time tables, and as such we investigated 3D Eikonal travel times and 3D raytracing travel-times based on the wavefront construction method, depending on different degrees of model smoothing, and how confident arrival times match with our FD computations. Finally, we conducted waveform cross-correlation analysis and clustering of a 500 event catalogue dataset as well as relative event locations within clusters.

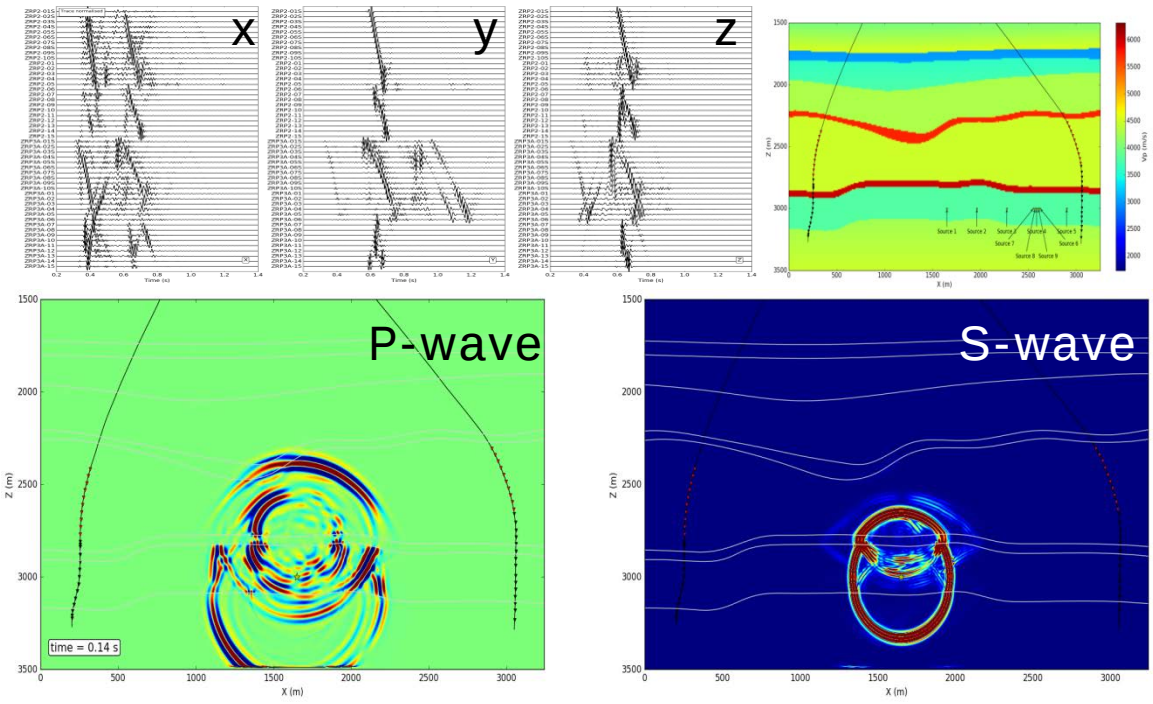

Fig. 1 A snapshot of 3D FD wavefield computed for a normal faulting magnitude 1 microseismic event in the Groningen gas reservoir, centered between two observation wells. Top panels: the x, y, and z synthetic seismograms computed for the sensors shown in the rightmost panel map. Bottom left: the spatial divergence which is related to the P wavefield component. Bottom right: the curl which is related to the S component.

Current State of the Groningen Seismic Network

Elmer Ruigrok, Jesper Spetzler, Bernard Dost, Gert-Jan van den Hazel, Jordi Domingo Ballesta and Läslo Evers

1 R&D Seismology and Acoustics, Royal Netherlands Meteorological Institute, De Bilt, The Netherlands, elmer.ruigrok@knmi.nl

The Groningen gas field is a massive natural gas accumulation in the north-east of the Netherlands. Decades of production have led to significant compaction of the reservoir rock. The (differential) compaction reactivates existing faults leading to induced seismicity.

Detailed geologic information is publicly available for the north of the Netherlands, from 3D seismics and an extensive network of logged and cored boreholes. Moreover, there is comprehensive subsidence monitoring program in place. Since the beginning of 2015, these data are augmented by seismic observations from more than 300 geophones and 85 accelerometers. Continuous seismic data is publicly available for the last year. Event data is available from the start of the nineties.

Seismicity in the Groningen area is monitored primarily with an array of borehole stations. In the nineties a network of 8 boreholes was deployed. Since 2015, this network has been expanded with 70 new boreholes. Each new borehole consists of an accelerometer at the surface and four downhole geophones with a vertical spacing of 50 m (Fig. 1). With the new network in place, Groningen likely has become the best instrumented place to study induced seismicity by a depleting gas reservoir and the associated seismic hazard.

We give an overview of the current state of the seismic network and ongoing efforts to improve data quality and access. Amongst others, we discuss data availability, seismic noise, sensor orientations and sensor placement. Also, we outline the deployment of additional infill arrays. Furthermore, we discuss recent developments in data processing.

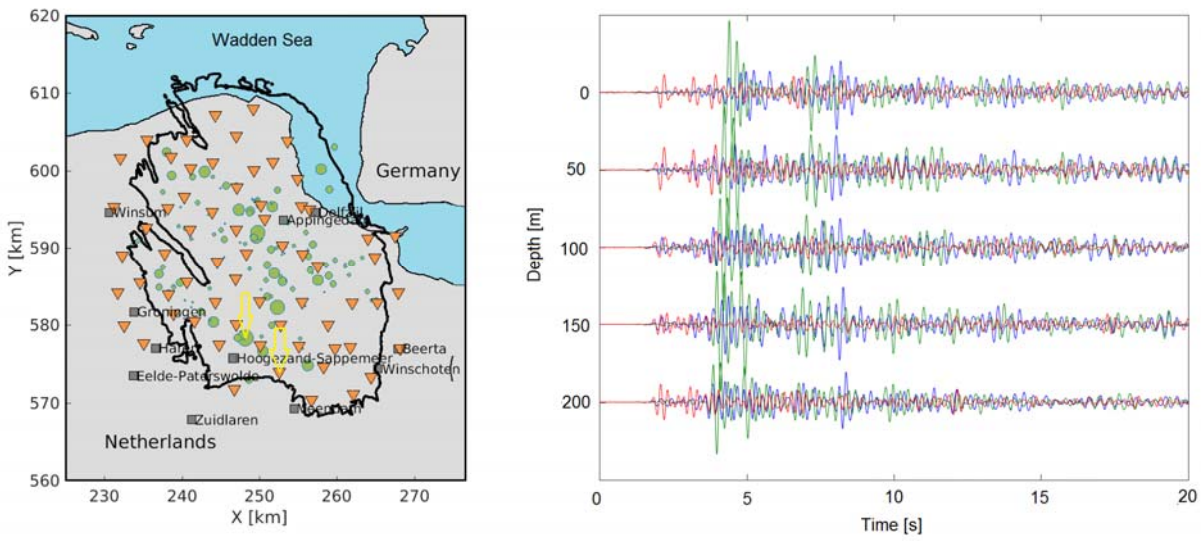

Fig. 1 *(left) map of the Groningen area with the outline of the Groningen gas field (black line), the Groningen shallow borehole network (orange triangles) and 2016 seismicity (green rounds). One station and one earthquake are highlighted with yellow arrows. Dutch RD grid coordinates are used. (right) 3-component recordings at 5 depth levels of the highlighted station (G55) and highlighted event (Froombosch, 25 Feb. 2016, M=2.4). Red, blue and green denote the vertical, radial and transverse particle-velocity recordings, respectively.*

pyNetOpt3D – A Python API for Monitoring Network Optimization

Tobias Megies[1], Toni Kraft[2]

1 LMU Munich, Germany, tobias.megies@lmu.de; **2** ETH Zurich, Switzerland, toni.kraft@sed.ethz.ch

Monitoring networks are often still set up following simple rules of thumb, for example as a simple circular array in case of a confined seismogenic volume. However, in more complex monitoring scenarios, e.g. when designing a monitoring network for seismicity spread over a large area or in the case of several closely spaced seismogenic regions (e.g. several geothermal doublets), such simple design principles can not be applied. Furthermore, background noise characteristics and thus detection capabilities usually are spatially strongly heterogeneous and therefore the quality of a monitoring network is not only controlled by plain source-receiver geometry. Monitoring network layouts should therefore be justified by quantitative means of network optimization.

Monitoring network design and evaluation at the Swiss Seismological Service (SED) is conducted using a set of C codes (named 'NetOpt3D') based on work by Hardt and Scherbaum (GJI, 1994) and further developed by Kraft et.al. (GJI, 2013). NetOpt3D finds D-optimal designs using a simulated annealing approach. It handles 3D-velocity and attenuation models, accounts for existing stations and the expected SNR of bodywaves at existing and new stations. A model of man-made seismic noise (Kraft 2016) is used to estimate the noise level at sites without test measurements. The SED is currently implementing the capability for array optimization - specifici for borehole instrumentation used in hydo-frac monitoring into NetOpt3D.

In its current form, NetOpt3D is lacking in usability, and it is also rather time consuming to set up new optimization problems. Currently, input files (for velocity models, synthetic catalogs, etc.) have to be set up manually in fixed ASCII formats used by the C programs and a large number of helper programs (mostly Linux shell scripts) are used for preparational steps (e.g. to set up equidistant station grids) and for analyzing and plotting optimization output.

To improve this situation, we have developed a consistent and easy to use Python API 'pyNetOpt3D' that internally uses the aforementioned C code base but hides all unwieldy steps (input file setup, parsing results, etc.) from the user. With the newly developed API it will be possible to steer a complete optimization run using only a single Python program that makes use of the newly developed API. We will also enhance reproducibility by providing easy serialization of a full optimization problem, including all input data (velocity/attenuation models, synthetic event catalog, existing station distributions, etc.), optimization parameters (raytracer parameters, simulated annealing parameters, etc.) as well as all optimization output (optimum network layout, intermediate results of iterative inversion, location uncertainty maps, etc.) into a single file. It will therefore be possible to conveniently load a performed optimization again at a later point in time (or by a colleague) to review the optimization by plotting results again or to perform a modified optimization. A graphical user interface for pyNetOpt3D is under development.

In this paper we demonstrate the newly developed Python API pyNetOpt3D at the example of the design and evaluation of optimal monitoring networks for five hydrothermal doublets in the Munich area.

Hardt, M., & Scherbaum, F. (1994). The design of optimum networks for aftershock recordings. *Geophysical Journal International*, *117*(3), 716-726.

Kraft, T., Mignan, A., & Giardini, D. (2013). Optimization of a large-scale microseismic monitoring network in northern Switzerland. *Geophysical Journal International*, *195*(1), 474-490.

Kraft, T., A high-resolution and calibrated model of man-made seismic noise for Europe, 76. DGG annual meeting, Münster, 16. March 2016

Abstracts Posters, Part II

Session 8

Risk Governance, Societal Acceptance, and License to Operate

Induced seismicity by hydrofracking and wastewater disposal: the re/insurance perspective

Sarah Barrett[1], Iain Bailey[1], Michael Diggin[1], Simona Esposito[1]

1 Swiss Re, Switzerland, Simona.Esposito@swissre.com

Since 2008, a significant increase in seismicity has been observed in several parts of the United States, most particularly in the state of Oklahoma. A consensus of scientific opinion now connects this increase to oil and gas operations, specifically the disposal of wastewater. This induced seismicity present an emerging risk of which the insurance industry is taking note.

The increased number of induced earthquakes brings several concerns for insurers and reinsurers. For example, risk models that are used to predict future earthquake losses based on a long-term hazard perspective are no longer accurate; vulnerability of the building stock in these regions is poorly understood; many people affected are unaware that standard insurance policies do not cover them against earthquake damage; if an earthquake is deemed to have been induced by human activity, it is not clear as to who will be liable for damages and how that could be proved. A large induced earthquake will lead to complexity and confusion in determining how to compensate damaged parties, or whether they are even covered. Some insurers and reinsurers have a potential for accumulation of loss via property and casualty (liability) lines of business that is very difficult to quantify.

In this study we focus on three aspects of induced earthquakes that are relevant for the insurance industry. First, the scientific basis for a connection between the hydro-fracking industry boom and increased earthquake activity, especially in Oklahoma. We focus on the difficulties of establishing if an individual earthquake is induced, triggered or natural, which complicates the issue of liability.

Second, we evaluate a portfolio representing residential and commercial buildings in Oklahoma to quantify the current risk landscape and the increased potential for loss. Results from our in-house earthquake loss model after updating earthquake activity rate to a level observed in recent years, shows that the probability of a USD 100 million-loss event increases approximately 30 times.

Third, we discuss key issues for insurers and reinsurers, such as liability precedents, the low penetration of earthquake insurance, and the potential impact of regulation in the oil and gas industry. Finally, we present suggestions as to how re/insurance industry can take a proactive approach in terms of a more meaningful product for such a unique type of earthquake risk.

A Hierarchical Bayesian Model for Controlling Induced Seismicity Associated with Geothermal Exploration

Marco Broccardo[1], Arnaud Mignan[1], Stefan Wiemer[1]

1 Swiss Competence Center for Energy Research supply of Electricity, ETH Zürich, bromarco@ethz.ch;

A key component of the risk governance framework for induced seismicity arising from geothermal exploration is the definition of a set of risk mitigation strategies. Among the possible strategies, Traffic Light Systems (TLS) are frequently used to mitigate induced seismicity risk by modifying the fluid injection profile. Shortly, a TLS defines one decision variable (event magnitude, peak ground acceleration, etc.) and a series of safety thresholds above which injection should be modified or eventually stopped. The first part of this study presents a model-driven TLS in which the thresholds are quantitatively assessed in order to meet prescribed safety targets. In particular, we use the moment magnitude as decision variable, while we use two distinct safety criteria to quantify the magnitude threshold. One safety criterion is defined based on the Instantaneous Individual Risk, *IIR*, (defined as the probability that an average unprotected person, present at a certain location, is killed due to a given hazardous event) while the other criterion is based on the yearly Individual Risk, *IR*, (defined as the *annual* probability that an average unprotected person, *permanently* present at a certain location, is killed due to *any* hazardous event). Figure 1 shows the mapping between *IIR* and Moment Magnitude for a given location.

In the second part of the study the stimulation project is interpreted as a dynamic feedback loop system where the input (rate of fluid injection) is modified based on the risk arising from the output of the system (earthquake rate). The statistical model is based on a Non-Homogeneous Poisson Process (NHPP), where the time varying seismic rate is defined by a parametric piecewise function (injection/post injection). In particular, in this study we consider the parameter of the the piecewise function as random variables by defining a Hierarchical Bayesian TLS (HBTLS). Briefly stated, a hierarchical Bayesian model utilizes multistage prior distributions of the model parameters. A major strength of the Bayesian approach is that it allows uncertainties and information about parameters to be encoded into a joint prior distribution of the model parameters. Moreover, it allows the computation of posterior predictive distribution of the model parameters as soon as the project is started and information becomes available. Markov Chain Monte Carlo based on GIBBS sampling is used for determining the joint posterior distribution of the model parameters and to update the rate earthquake model and the arising risk.

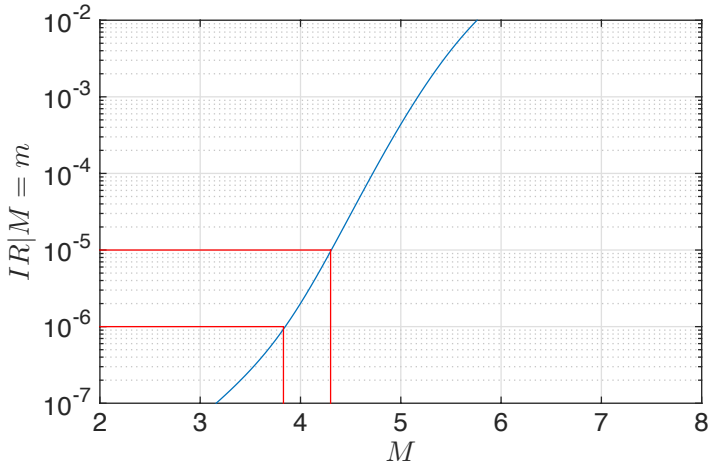

Fig. 1 Definition of Moment Magnitude thresholds for different safety criteria

Quantifying risk due to induced seismicity in Oklahoma and Kansas

Deborah Kane[1], Jochen Woessner[2], Marleen Nyst[1]

1 Risk Management Solutions Inc., Newark, CA, USA; **2** Risk Management Solutions Inc, Zurich, Switzerland, jochen.woessner@rms.com

In 2016, the USGS published a hazard forecast including contributions from induced seismicity in the central and eastern United States (2016 One-Year Seismic Hazard Forecast for the Central and Eastern United States from Induced and Natural Earthquakes, USGS OFR 2016–1035). The forecast defines regions of induced seismicity based on published peer-reviewed research, and models the resulting seismic hazard in these regions using a different set of temporal windows, spatial smoothing kernels, and maximum magnitudes than those used in the USGS National Seismic Hazard Maps (Documentation for the 2014 Update of the United States National Seismic Hazard Maps, USGS OFR 2014–1091).

We present a probabilistic earthquake risk model for Oklahoma and Kansas constructed from a stochastic event set, ground motion modeling, building response modeling, and a financial loss model. We investigate the impact of induced seismicity on the subsequent earthquake risk by applying the smoothed rates from the 2016 induced seismicity forecast to the event set and comparing with the risk using the smoothed rates from the 2014 USGS National Seismic Hazard Maps. Risk metrics for comparison include simple scenario calculations where regional damage and loss are modeled for a single earthquake, average annual loss calculations representing an annualized expected loss level (used by insurers to set their annual premium rates), and complete loss exceedance probability curves (used by insurers to address solvency and manage their portfolio risk).

Communicating induced seismicity of deep geothermal energy and shale gas: low-probability high-consequence events and uncertainty

Theresa Knoblauch[1,2], Michael Stauffacher[1], Evelina Trutnevyte[1]

1 D-USYS Transdisciplinarity Lab, Department of Environmental Science (D-USYS) ETH Zurich, Switzerland
2 theresa.knoblauch@usys.ethz.ch

Harnessing sub-surface energy, such as deep geothermal energy (DGE) or shale gas, entails the risk of induced seismicity. This risk includes low-probability high-consequence (LPHC) events. The affected public might be interested in learning about such LPHC events before and throughout siting DGE or shale gas projects. Also, good-practice induced seismicity guidelines for DGE recommend to communicate LPHC events, where appropriate. For designing respective risk communication, the scientific literature lacks empirical evidence of how the public reacts to different written risk communication formats about such LPHC events and to related uncertainty or expert confidence. This poster presents findings from an online experiment (N=590) that empirically tested the public's responses to risk communication about induced seismicity, presented for DGE and shale gas. Three formats of written risk communication were tested: qualitative, quantitative and risk comparison. Respondents found the latter two the easiest to understand, the most exact, and liked them the most. Adding uncertainty and expert confidence statements made the risk communication less clear, less easy to understand and increased concern. Above all, the technology for which risks are communicated mattered strongly: respondents in the shale gas condition found the identical risk communication less trustworthy and more concerning than in the DGE conditions. They also liked the risk communication overall less. For practitioners in DGE or shale gas projects, the study shows that the public would appreciate efforts in describing LPHC risks with numbers and risk comparisons. However, there seems to be a trade-off between aiming for transparency by disclosing uncertainty and limited expert confidence, and thereby decreasing clarity and increasing concern in the view of the public.

Imprint

Local Organizing Committee

Stefan Wiemer (Director SED)
Toni Kraft (Senior Seismologist SED)
Anja Tamburini (Communications Specialist SED)

Workshop Website

www.seismo.ethz.ch/schatzalp

Sponsors

Schweizerische Eidgenossenschaft
Confédération suisse
Confederazione Svizzera
Confederaziun svizra

Bundesamt für Energie BFE
Office fédéral de l'énergie OFEN
Ufficio federale dell'energia UFE

energieschweiz
Unser Engagement: unsere Zukunft.

SCCER SoE
SWISS COMPETENCE CENTER for ENERGY RESEARCH
SUPPLY of ELECTRICITY

DESTRESS

CH
GEO
BEST